CSNI REPORT 101

EGG-NTAP-6276

April 1983

INTERNATIONAL STANDARD PROBLEM 13
(LOFT EXPERIMENT L2-5)

PRELIMINARY COMPARISON REPORT

J. D. Burtt
S. A. Crowton

Idaho National Engineering Laboratory
Operated by the U.S. Department of Energy

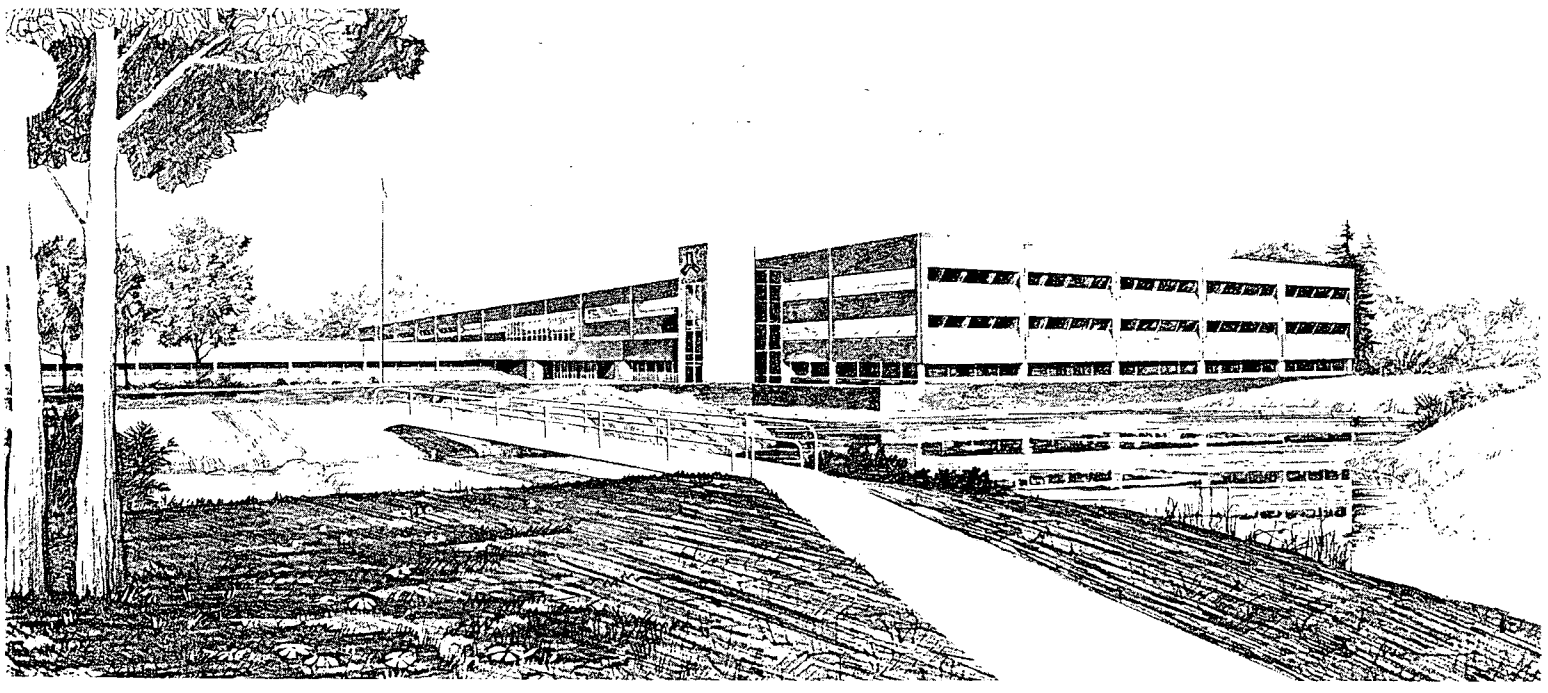

This is an informal report intended for use as a preliminary or working document

Prepared for the
U.S. NUCLEAR REGULATORY COMMISSION
Under DOE Contract No. DE-AC07-76ID01570
FIN No. A6047

EG&G Idaho

EGG-NTAP-6276

INTERNATIONAL STANDARD PROBLEM 13

(LOFT Experiment L2-5)

PRELIMINARY COMPARISON REPORT

J. D. Burtt
S. A. Crowton

Published April 1983

EG&G Idaho, Inc.
Idaho Falls, Idaho 83415

Prepared for the
U.S. Nuclear Regulatory Commission
Washington, D.C. 20555
Under DOE Contract No. DE-AC07-76ID01570
FIN No. A6047

ABSTRACT

LOFT Experiment L2-5 was designated International Standard Problem 13 by the Organization for Economic Cooperation and Development. Comparisons between measurements from Experiment L2-5 were made with calculations from 11 international participants using five different computer codes. LOFT Experiment L2-5 simulated a double ended guillotine cold leg rupture of a primary coolant loop of a large pressurized water reactor, coupled with a loss of offsite power.

SUMMARY

The Organization for Economic Cooperation and Development designated Loss-of-Fluid Test (LOFT) Experiment L2-5 as International Standard Problem 13. Calculations were submitted by 11 participants using five computer codes. Eight calculations were preceded by model submittals and qualified as blind calculations. The four remaining calculations were classified as open submittals. Comparisons were made between participant calculations and measurements from Experiment L2-5.

Experiment L2-5 simulated a double ended offset shear guillotine cold leg rupture in a large pressurized water reactor. A loss of offsite power was also simulated with a reactor coolant pump trip and an emergency core coolant system injection delay.

The participants calculated the hydraulic response of L2-5 adequately, except where there were obvious modeling problems. Densities were calculated adequately in the sections where condensation did not occur. Break flows were generally over predicted. Clad temperature heatups were calculated adequately but quench times for cladding was predicted less well.

CONTENTS

FIGURES

TABLES

1. INTRODUCTION

Experiment L2-5, conducted in the Loss-of-Fluid Test (LOFT) was identified by the Organization for Economic Cooperation and Development (OECD) as International Standard Problem 13 (ISP-13). This report documents the comparisons between participant computer code calculations and measured results from LOFT Experiment L2-5. The results from Experiment L2-5 are documented in Reference 1.

LOFT Experiment L2-5 simulated a double ended, off-set shear, guillotine cold leg rupture. The reactor coolant pumps were tripped and decoupled from their flywheels within 1 s after break initiation, simulating a loss of offsite power. Consistent with this loss of power, the high and low pressure emergency core coolant injection systems were delayed. The system description and initial conditions are presented in Section 2.

The purpose of this preliminary report is to present direct comparisons between the calculated parameters and LOFT L2-5 data. It is beyond the scope of this report to assess and analyze the reasons for discrepancies that occurred. A more detailed discussion of the comparisons will be included in the final comparison report after all the participants' comments have been received. The models used by the participants are summarized in Section 3. The eight blind calculations are compared with measurements and discussed in Section 4. Section 5 presents the comparison between measurements and results from the four open calculations. Section 6 contains the conclusions and recommendations drawn from the comparisons. Appendix A provides a nodalization diagram for each submittal.

2. LOFT EXPERIMENT L2-5 DESCRIPTION

Experiment L2-5 was conducted on June 16, 1982 in the LOFT facility. The LOFT facility is located at the Idaho National Engineering Laboratory (INEL) and was operated for the United States Nuclear Regulatory Commission by the Department of Energy at the time of the experiment. This section describes the LOFT facility and presents the initial test conditions.

2.1 System Description

The LOFT system configuration for Experiment L2-5 is shown in Figure 1. The major components of the LOFT system are: a reactor vessel including a core with 1300 unpressurized nuclear fuel rods with an active length of 1.67 m; an intact loop with a pressurizer, steam generator, two pumps arranged in parallel, and piping connected to the break plane orifice; a broken loop with a simulated pump, simulated steam generator, two break plane orifices, two quick opening blowdown valves (QOBVs), and two isolation valves; an emergency core coolant system consisting of two accumulators, a high pressure injection system and a low pressure injection system; and a blowdown suppression system consisting of a header and suppression tank. The details of the LOFT system and instrumentation are presented in Reference 2.

2.2 Test Conditions

After operating the reactor at 36.0 MW for 40 effective full power hours to build up a fisson decay product inventory, Experiment L2-5 was initiated by opening the two QOBVs, in the broken loop hot and cold legs. The primary coolant pumps were tripped by the operators at 0.94 ± 0.01 s. The pumps were not connected to their flywheels during the coastdown. High pressure injection and low pressure injection were delayed to 24 s and 37 s, respectively, to simulate the delay expected for a PWR emergency diesel to begun delivering power (in response to a loss of site power).

2.3 Initial Conditions

A summary of the measured system conditions immediately prior to Experiment L2-5 initiation is shown in Table 1. The mass flow rate in the intact loop was 192.4 ± 7.8 kg/s. The intact loop hot leg pressure was 14.94 ± .06 MPa. The intact loop hot leg temperature was 589.7 ± 1.6 K. The initial core power was 36. ± 1.2 MW with a maximum linear heat generation rate of 40.1 ± 3.0 kW/m.

TABLE 1. INITIAL CONDITIONS FOR LOFT EXPERIMENT L2-5

Parameter	Measured Value
Primary Coolant System	
Mass flow (kg/s)	192.4 ± 7.8
Hot leg pressure (MPa)	14.94 ± 0.06
Cold leg temperature (K)	556.6 ± 4.0
Hot leg temperature (K)	589.7 ± 1.6
Boron concentration (ppm)	668.0 ± 15
Reactor Vessel	
Power level (MW)	36.0 ± 1.2
Maximum linear heat generation rate (kW/m)	40.1 ± 3.0
Control rod position (above full-in position (m)	1.376 ± 0.01
Pressurizer	
Steam volume (m^3)	0.32 ± 0.02
Liquid volume (m^3)	0.61 ± 0.02
Liquid temperature (K)	615.0 ± 3
Liquid level (m)	1.14 ± 0.03
Broken Loop	
Cold leg temperature near reactor vessel (K)	554.3 ± 4.2
Hot leg temperature near reactor vessel (K)	561.9 ± 4.3
Steam Generator Secondary Side	
Liquid temperature (K)	547.1 ± 0.8
Pressure (MPa)	5.85 ± 0.06
Mass flow (kg/s)	19.1 ± 0.4

3. SUMMARY OF PARTICIPANT MODELS

Calculations were received from 11 participants of which eight were preceded by model submittals to qualify as blind calculations. Table 2 lists the participants and the identifier used for each participant in this report. Five different computer codes were used in the calculations. RELAP4/MOD6 was used in seven of the calculations and RELAP5 used in two analyses. Codes other than RELAP4 are identified as such on each comparison plot. Nodalization diagrams for each participant are contained in Appendix A. The following discussion briefly summarizes the model of each participant.

3.1 Gesellschaft fur Reaktorsicherheit (GRS)

GRS used the DRUFAN 02 computer code to perform the blind calculation. The thermal hydraulic models in DRUFAN 02 are based on the solution for conservation of liquid mass, vapor mass, overall energy, and overall momentum. Determination of the critical flow at the break was made using a one dimensional nonequilibrium model which uses the geometry of the break path. The GRS calculation was terminated at 28.76 s after break initiation.

3.2 Japan Atomic Energy Research Institute (JAR)

The JAERI Division of Nuclear Safety Evaluation used an improved version of RELAP4/MOD6 for their blind calculation. Most of the major modifications to the code were developed for small break analyses, so the code used in the ISP-13 calculation was essentially equal to the original RELAP4/MOD6 code. Critical flow was calculated using Henry-Fauske/HEM with a discharge coefficient of 0.85 for both the subcooled and saturated region. The calculation was terminated 50 s after initiation of the break.

TABLE 2. SUMMARY OF ISP-13 PARTICIPANTS

Organization	Participant	Code	ID
Gesellschaft fur Reaktorsicherheit mbh Forschungsgeland (West Germany)	F. Steinhoff W. Winkler	DRUFAN 02	GRS
Japan Atomic Energy Research Institute	F. Tanabe K. Yoshida	RELAP4/MOD6	JAR
Japan Atomic Energy Research Institute	M. Akimoto M. Hirano	THYDE-P1	JAT
Central Electricity Research Laboratories (United Kingdom)	A. H. Schriven	RELAP4/MOD6	CERL
Studsvik Energiteknik AB (Sweden)	O. Sandervag	RELAP5/MOD1	STUD
Eidgenossisches Institute fur Reaktorforschung (Switzerland)	S. Guntay	RELAP4/MOD6	EIR
Los Alamos National Laboratory (USA)	T. Knight	TRAC-PD2	LANL
ENEL-CRTN (Italy)	L. Bella F. Donatini	RELAP4/MOD6	ENEL
Dipartimento di Construzioni Miccaniche e Nucleari (Italy)	M. Mazzini	RELAP4/MOD6	DCMN
Commissariat A l'Energie Atomique (France)	R. Pochard Y. Macheteau	RELAP4/MOD6	CEA
Technical Research Centre of Finland	H. Holmstrom V. Yrjola	RELAP5/MOD1, cycle 19	VTT

3.3 Japan Atomic Energy Research Institute (JAT)

The Nuclear Safety Code Development Laboratory at JAERI performed their blind calculation with THYDE-P1. The critical flow model used the modified Zaloudek and Moody correlations in the calculation with a Moody discharge coefficient of 0.6. Only the average core channel was modeled with THYDE-P1; no hot channel analysis was performed. The calculation was terminated 69.84 s after the initiation of the break.

3.4 Central Electricity Research Laboratories (CERL)

The CERL blind calculation was performed with RELAP4/MOD6. Critical flow was calculated using Henry-Fauske/HEM with a multiplier of 0.875 and a transition quality of 0.025. Separate hot pins and reflood models were used in conjunction with the average core blowdown model. The calculation was terminated 37 s after break initiation.

3.5 Studsvik Energiteknik AB (STUD)

Sweden's blind submittal of ISP-13 was performed using RELAP5/MOD1, Cycle 14. The RELAP5 critical flow model was used with a discharge coefficient of 0.87. The calculation was terminated 55 s after the break initiation.

3.6 Eidgenossisches Institut fur Reaktorforschung (EIR)

EIR performed both a blind and an open calculation for ISP-13 using RELAP4/MOD6. For the blind calculation only a single core volume was used; in the open calculation, two parallel, multivolume core channels were modeled. Except for the core, the blind and open models were identical. Critical flow was calculated using Henry-Fauske/HEM, with multipliers of 0.8 and 0.848 respectively. The blowdown portions of the calculations were terminated at 44 s, while separate reflood calculations were run out to 100 s.

3.7 Los Alamos National Laboratory (LANL)

The open calculation of ISP-13 submitted by LANL was performed using the TRAC-PD2/MOD1 computer code. TRAC-PD2 features a three dimensional treatment of the reactor vessel, two phase nonequilibrium hydrodynamic models and flow regime-dependent constitutive equations. The code does not contain a critical flow model; break flow was calculated using break geometry and normal field equations in the code. The LANL calculation was terminated 100 s after break initiation.

3.8 ENEL-CRTN

The ENEL blind calculation was performed with RELAP4/MOD6. The model used two parallel, multivolume core channels, representing the average and hot channels. Henry-Fauske/HEM was used to calculate critical flow, with multipliers of 0.865 and 0.7 for subcooled and saturated flow respectively. The long term calculation was terminated at 160 s after break initiation. Due to problems with the output tape, only the short term plots (0-30s) were available for the comparisons in this report.

3.9 Dipartimento di Construzioni Meccaniche e Nucleari (DCMN)

DCMN performed an open calculation of ISP-13 using RELAP4/MOD6. Critical flow was modeled with Henry-Fauske/HEM with discharge coefficients of 0.84. Transition quality was set at 0.003. The MOD6 heat transfer package (HTS2) was used in the calculation. The calculation was terminated 30 s after break initiation.

3.10 Commissariat A l'Energie Atomique (CEA)

The CEA blind submittal was performed using RELAP4/MOD6. Henry-Fauske/HEM was used to model critical flow, with discharge coefficients of 1.0 and a transition quality of .0025. The calculation was terminated 56 s after break initiation.

3.11 Technical Research Center of Finland (VTT)

The VTT open calculation was performed using RELAP5/MOD1, Cycle 19. Updates to the FIDRAG subroutine, which calculates the drag between fluid phases, were added. A discharge coefficient of 0.84 was applied to the RELAP5 critical flow model. The calculation was terminated 60 s after the break was initiated.

4. SUMMARY OF BLIND RESULTS

Eight ISP-13 submittals were designated blind calculations. This designation was given to those participants who submitted the models to be used in the calculation prior to the performance of experiment L2-5. The comparison of these calculations with measured data is presented in the following sections.

4.1 Sequence of Events

The measured and calculated sequence of events for L2-5 are summarized in Table 3. The experiment was initiated by opening the two QOBVs. The primary coolant pumps were turned off and the primary coolant system depressurized to saturation, both by 1 s. The cladding temperatures in the central fuel assembly departed from saturation within 2 s. Accumulator injection began at 16.8 s. The maximum cladding temperature of 1077 K (1479°F) was reached at 28.5 s, just prior to the completion of lower plenum refill. High pressure injection (HPI) initiated at 23.9 s; low pressure injection began at 37.3 s.

Most of the blind calculated sequence of events were in accord with data. The calculated end of subcooled blowdown ranged from 0.05 s (STUD, CEA) to 0.09 s (JAR). Reactor scram ranged from 0.0 s (EIR) to 0.25 s (STUD). Cladding temperatures began to deviate from saturation between 0.51 s (STUD) and 1.42 s (EIR). Both Japanese submittals tripped the reactor coolant pumps early, at the time of the break. The participants calculated pressurizer voiding between 5.0 s (ENEL) and 17 s (CEA), compared to the 15.4 s seen in the data. Accumulator initiation ranged from 12.8 (STUD) to 19.3 s (ENEL). The time of maximum peak clad temperatures calculated by the participants deviated significantly from data, ranging between 10 s CGRS and 50 s (ENEL). Only CERL's calculation reached a peak within 5 s of data at 24.0 s but their peak clad temperature of 1155 K (1600°F) was significantly higher.

TABLE 3. MEASURED AND CALCULATED SEQUENCE OF EVENTS FOR LOFT EXPERIMENT L2-5

Event	L2-5	JAR	CERL	EIR	ENEL	GRS	JAT	STUD	CEA	LANL	EIR	DCMN	VTT
L2-5 initiated	0.0	0.0	0.0	--a	--	0.0	0.	0.0	0.	0.0	0.0	0.0	0.0
Subcooled blowdown ended	0.043	0.09	0.056	0-.1	--	0.07	--	0.05	.05	--	0.-.1	--	.06
Reactor scrammed	0.24	0.11	0.24	0.0	.1	0.097	--	0.251	.24	.24	0.0	.241	.1
Clad temperatures deviate from saturation	0.91	1.15	0.8	1.42	--	0.67	--	0.51	--	1.0	1.42	.9	.5
RCP trip	0.94	0.0	0.94	1.0	.9	1.0	0.0	0.951	.94	.24	1.0	.941	.94
Subcooled break flow end	3.4	3.04	4.1	--	3.3	3.3	--	4.0	--	4.0	--	3.5	4.0
PZR emptied	15.4	14.4	10.2	--	5.0	12.1	--	15.0	17.	16.5(95%) 28.0(99%)	8.0	15.3	15.0
Accumulator initiated	16.8	17.36	16.8	13.8	19.3	16.02	17.0	12.85	15.2	17.75	15-16	16.6	16.3
HPI initiated	23.9	24.8	24.0	22.0	23.9	24.05	22.25	23.91	24.4	23.9	22.0	23.91	24.0
Maximum PC temperature reached	28.47	48.8	24.0	--	50.0	10.0	--	12.85	--	50.0	38.0	--	5.2
LPI initiated	37.32	35.0	37.0	--	37.3	--	34.75	37.31	36.3	37.32	35.0	--	37.2

a. -- = not calculated.

4.2 Pressure

The comparison between calculated pressurizer pressure and data is presented in Figure 1. JAR and CEA calculated a pressurizer depressurization slower than that seen in the experiment, while all other participants calculated a faster depressurization with STUD's calculated rate being the most severe. ENEL's calculation apparently included the isolation of the pressurizer component at 5.0 s.

Comparisons of pressure for the intact loop cold leg, broken loop hot leg, broken loop cold leg, and upper plenum are shown in Figures 2 through 5, respectively. Generally all participants, except ENEL, calculated pressure histories below that actually observed in the data. ENEL's calculation was consistently high out to 30 s. STUD again had the lowest pressures over all. The CEA calculation displayed some interesting discrepancies. Their calculation of cold leg pressures, both broken loop and intact loop were extremely close to data. However, the broken loop hot leg pressure calculated by Mssrs. Pochard and Macheteau showed an initial 5 MPa (725 psi) pressure drop below that of all the other participants. In the upper plenum, the CEA pressure history was decidedly higher than the rest of the calculations. Analyzing the reasons for this pressure discrepancy is beyond the scope of this preliminary report.

Comparison of the steam generator secondary pressure (Figure 6) was complicated by the range of initial conditions used in the calculations. STUD, GRS, and CEA all underpredicted the equilibrium pressure in the generator. JAR's initial pressure was much higher than data, but stabilized out only slighty high. JAT's and CERL's equilibrium pressure exceeded data substantially. EIR's calculation predicted the secondary pressure response quite well.

4.3 Fluid Temperatures

Calculated upper plenum temperatures when compared to data in Figure 7 showed the saturation temperatures corresponding to the respective pressure

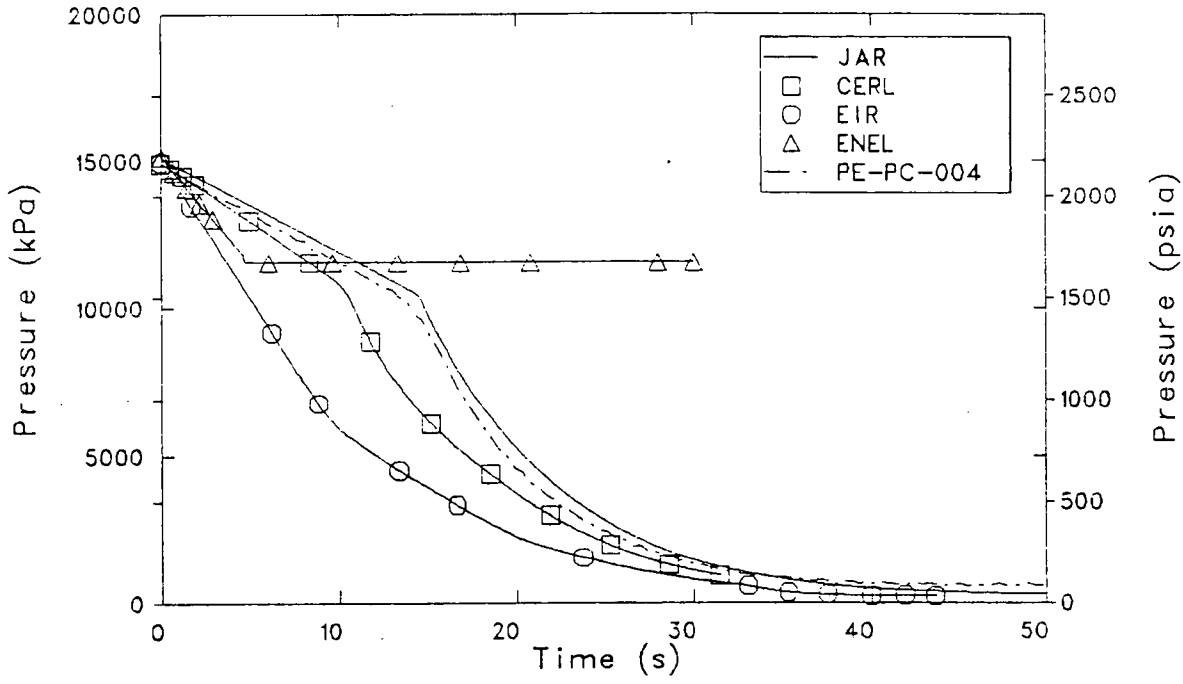

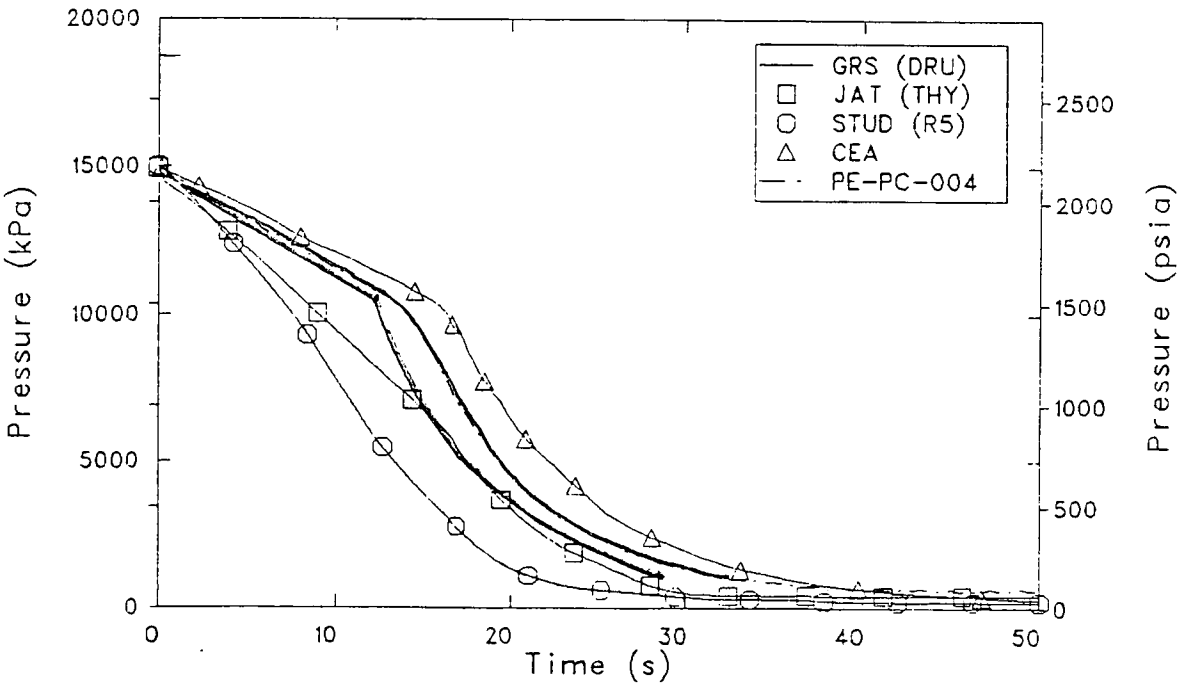

Figure 1. Comparison of measured and calculated pressurizer pressure for the blind calculations.

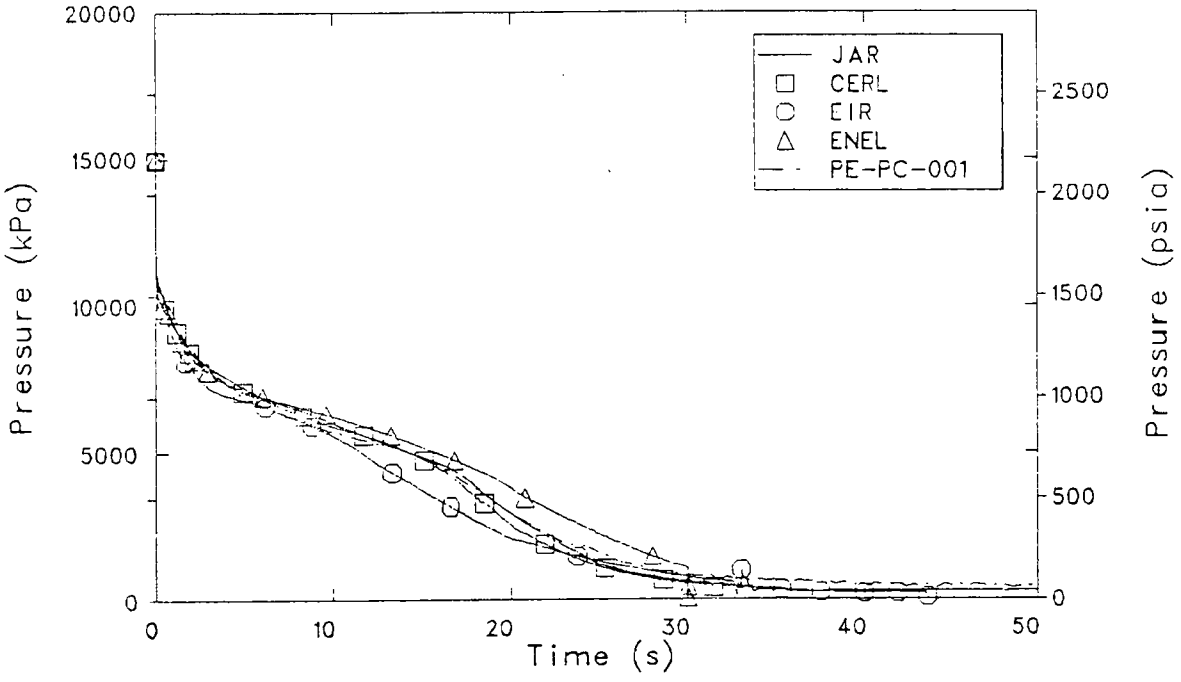

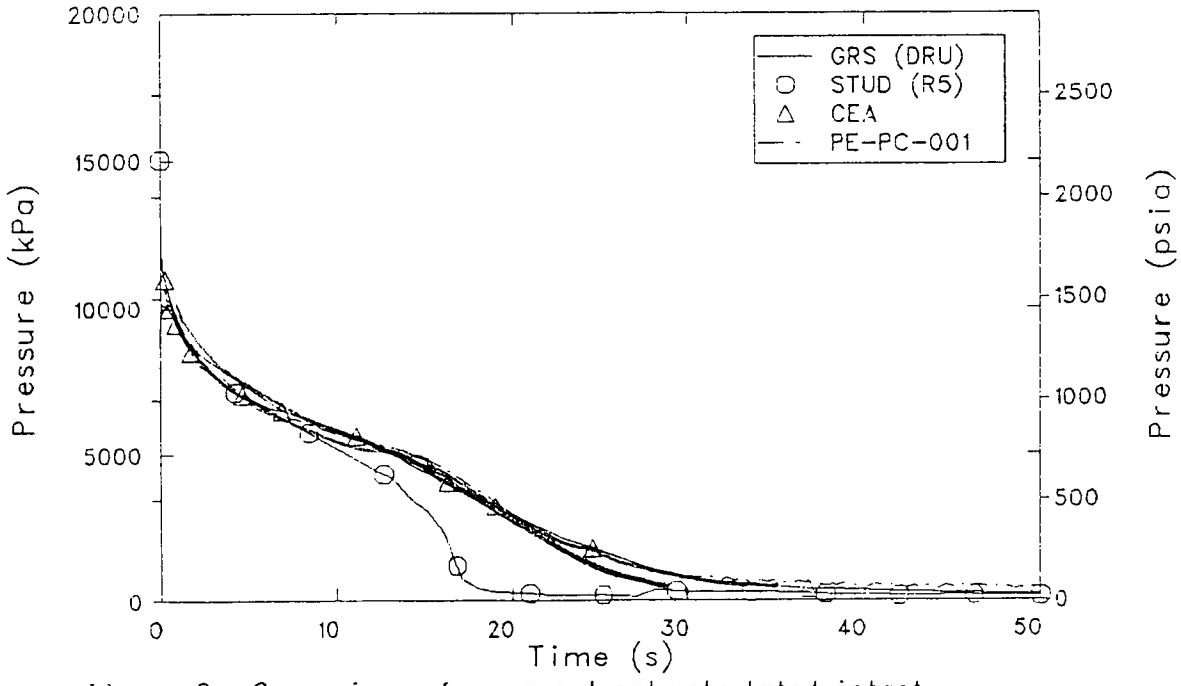

Figure 2. Comparison of measured and calculated intact loop cold leg pressure for the blind calculations.

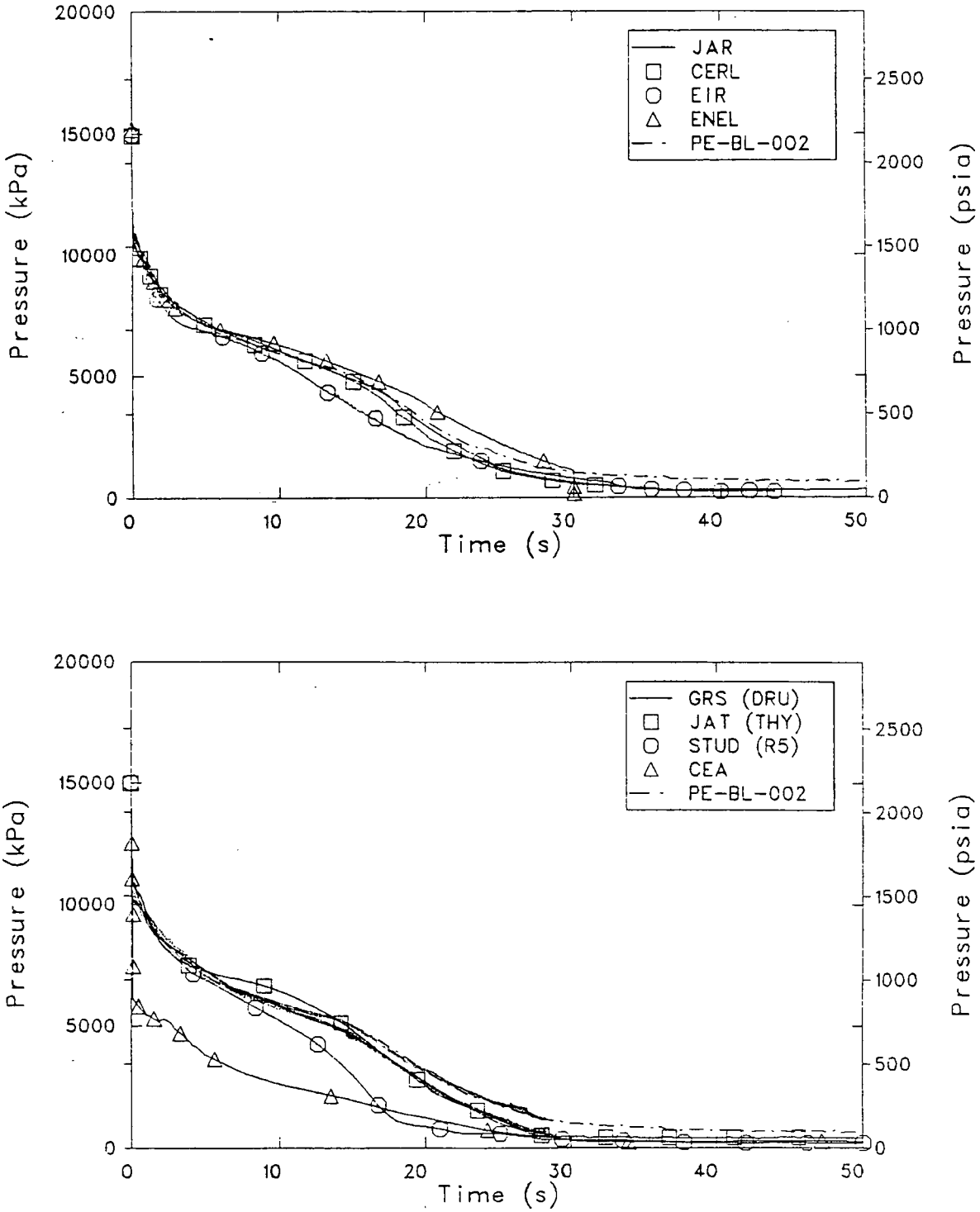

Figure 3. Comparison of measured and calculated broken loop hot leg pressure for the blind calculations.

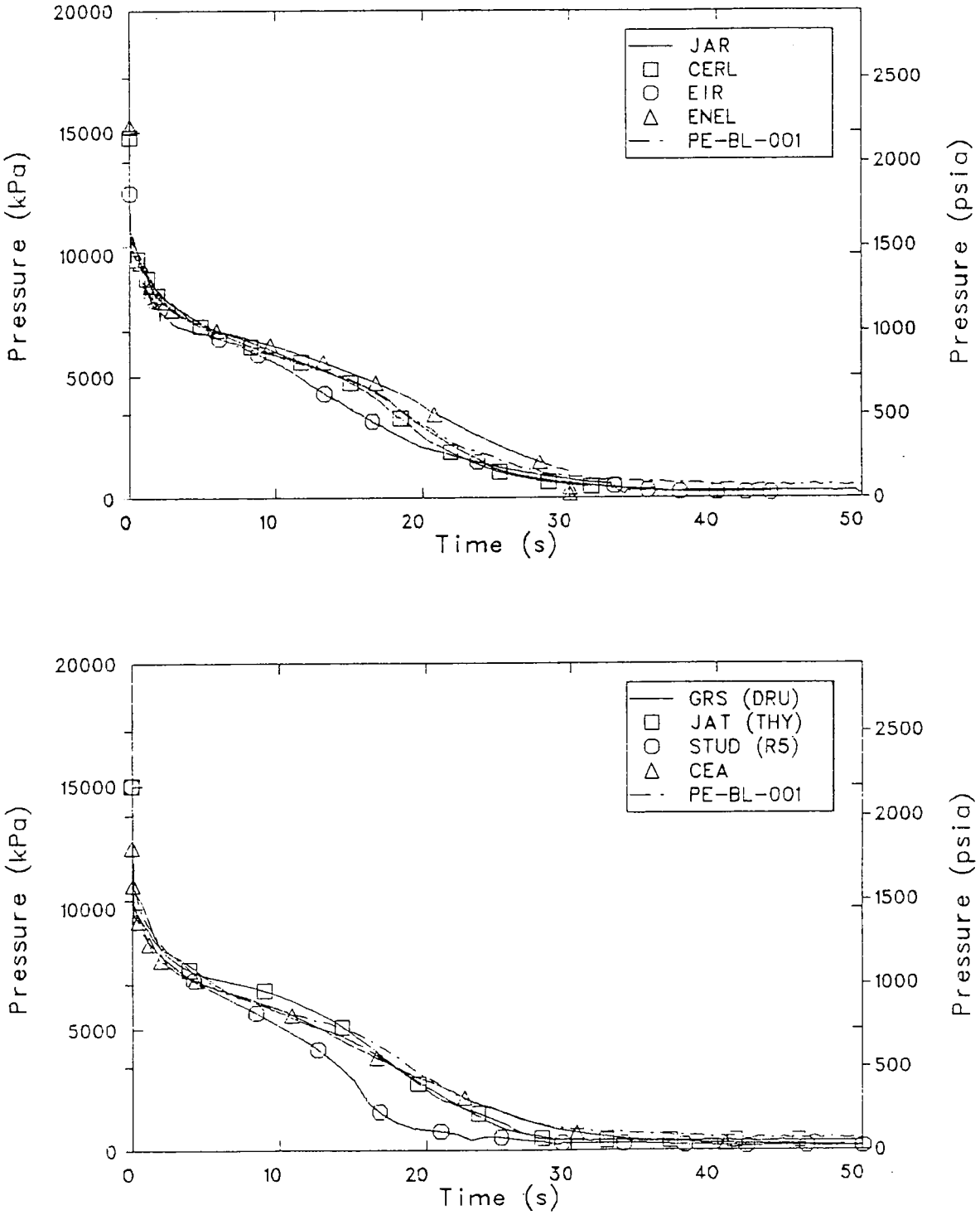

Figure 4. Comparison of measured and calculated broken loop cold leg pressure for the blind calculations.

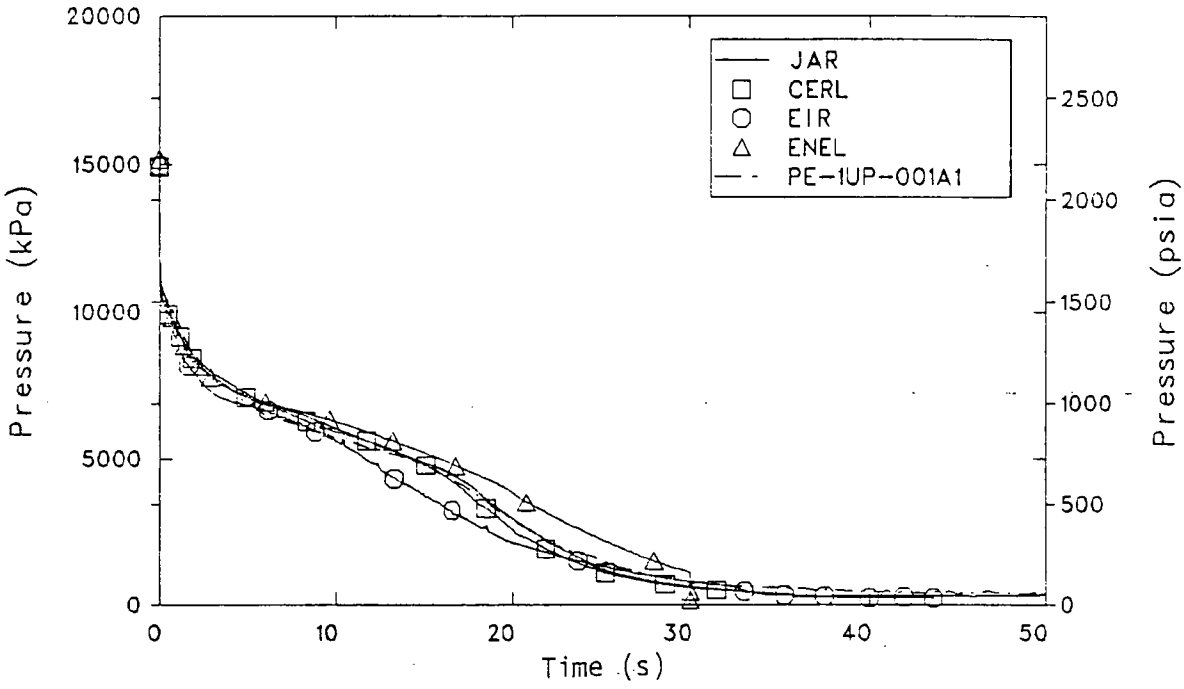

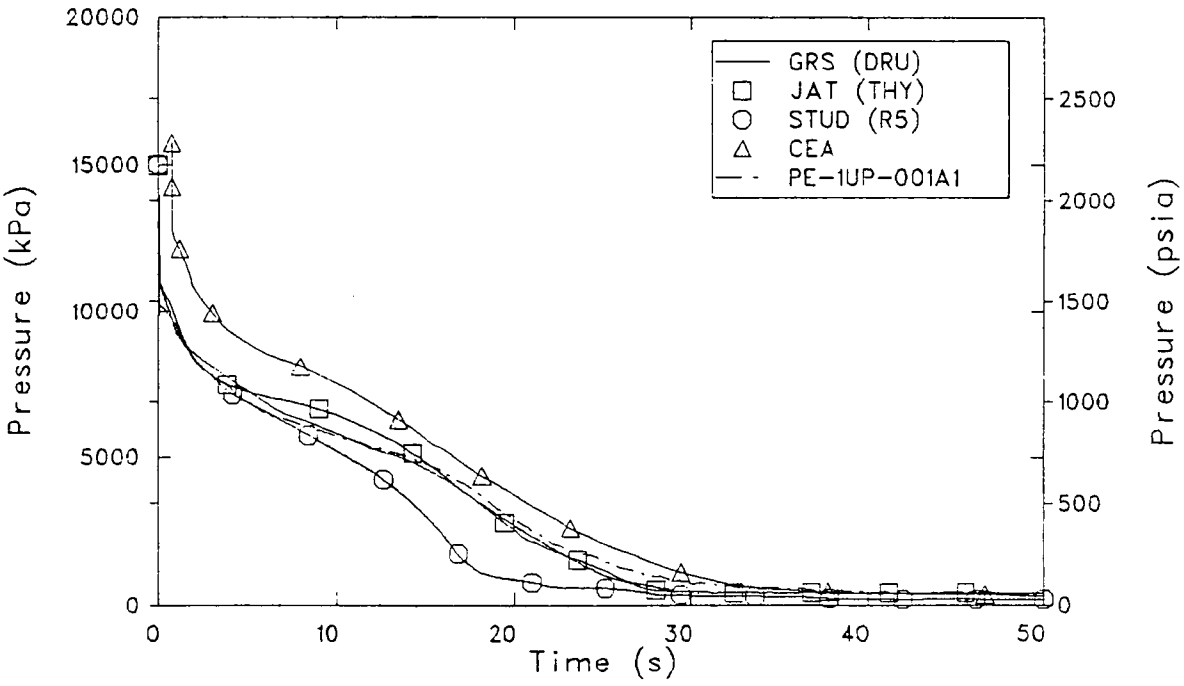

Figure 5. Comparison of measured and calculated upper plenum pressure for the blind calculctions.

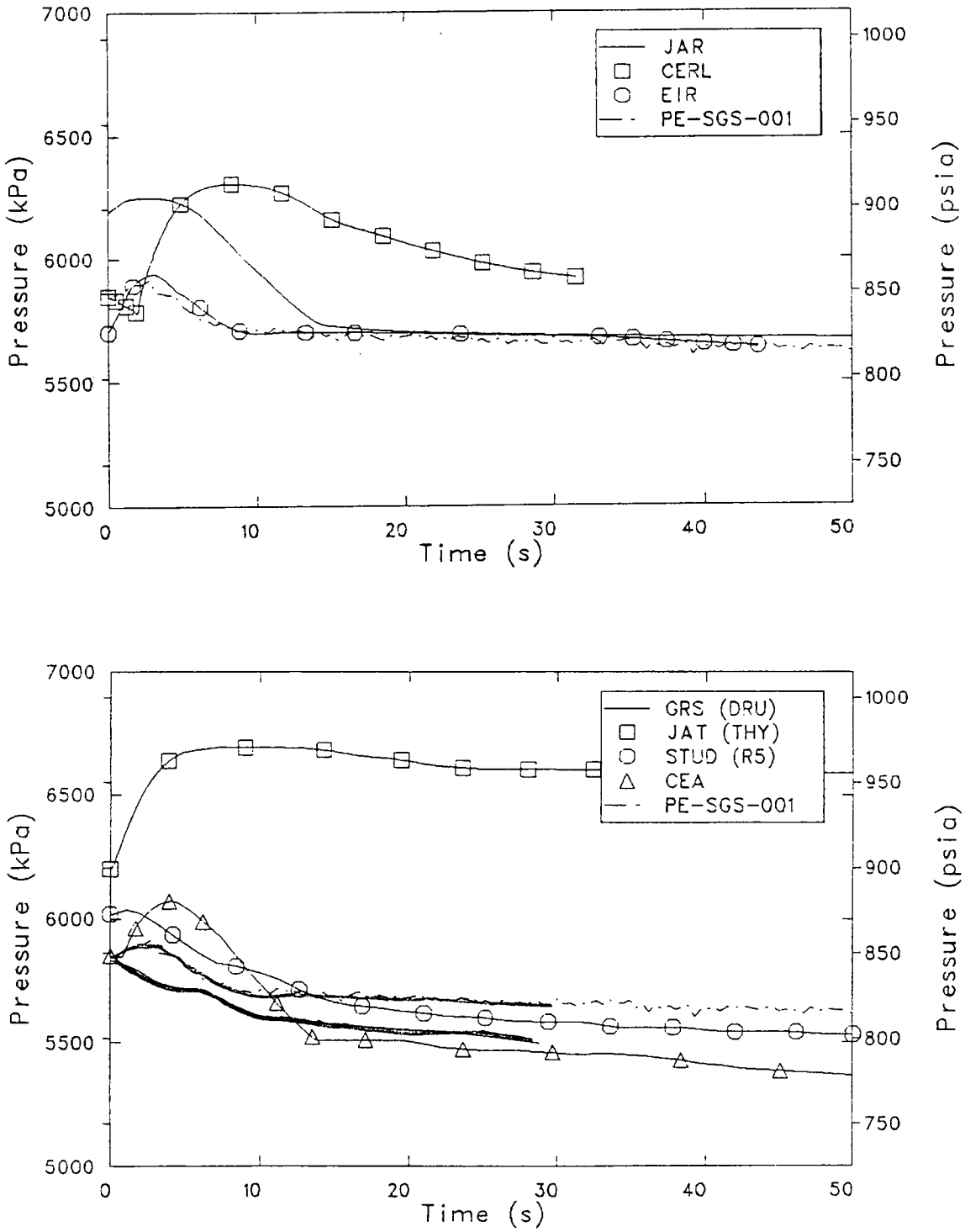

Figure 6. Comparison of measured and calculated steam generator secondary pressure for the blind calculations.

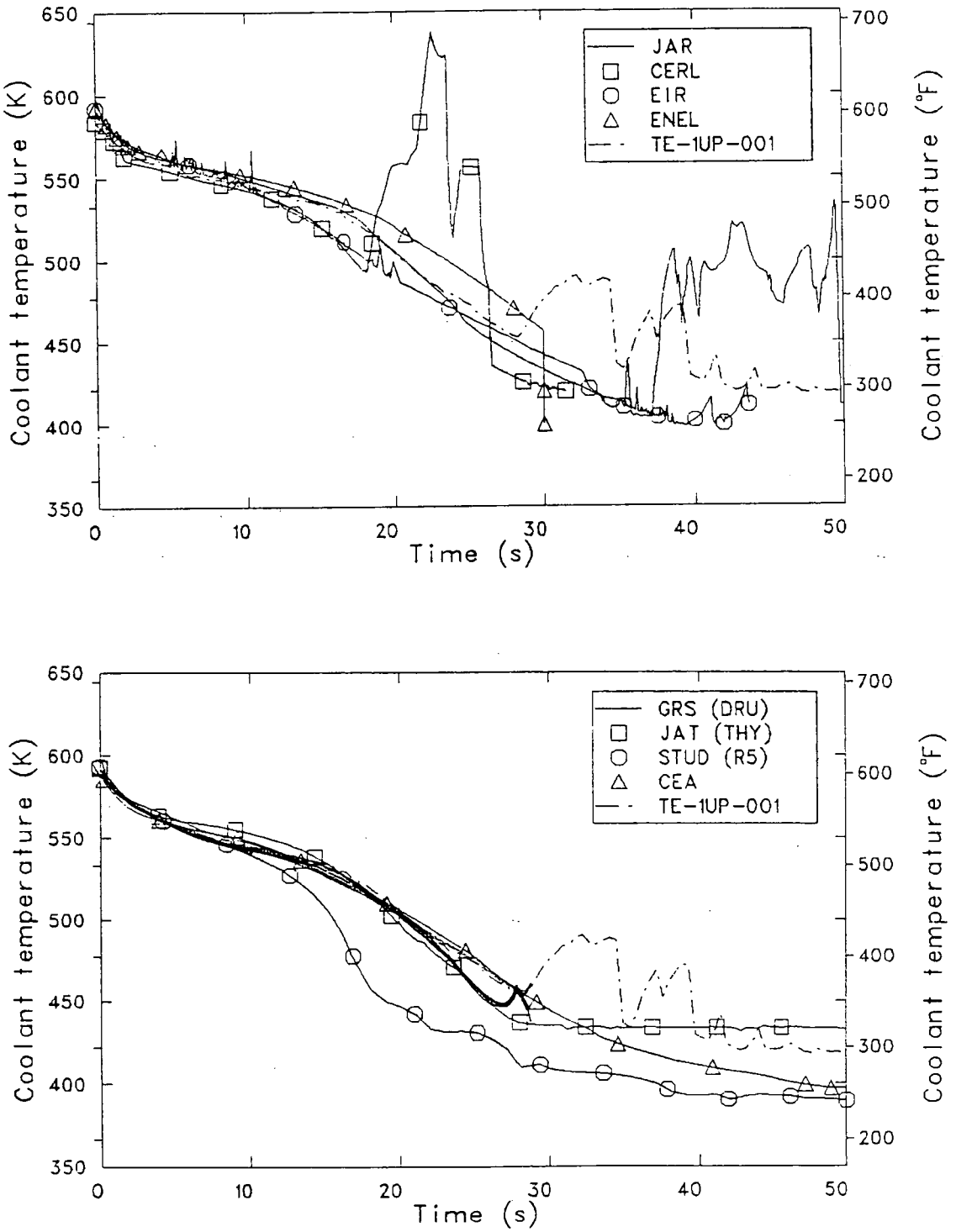

Figure 7. Comparison of measured and calculated upper plenum fluid temperature for the blind calculations.

histories. Ony ENEL and CEA fluid temperatures were consistently above data. Superheated fluid appeared in the data around 28 s. Several of the participants registered superheat at various times, ranging from 20 s (CERL) to 37 s (JAR). ENEL showed no superheat on the data plots, but their report plots show superheat beginning around 40 s. JAT, STUD and CEA showed no superheat at all in their upper plenum temperature histories.

Figure 8 compared calculated lower plenum temperatures with data, again showing the saturation temperature correspondence discussed above. JAR's RELAP4 calculation showed considerable superheat in the lower plenum starting at 27 s and quenches at 39 s. The JAT THYDE-P1 analysis registered an abrupt 68 K (124°F) drop in their temperature at 42 s, the only participant to calculate subcooling in the lower plenum.

In the intact loop cold leg temperature comparisons, seen in Figure 9, there was considerable variance in the fluid temperatures. None of the participants calculated the oscillatory behavior seen in the test. Most calculated some subcooling with GRS and JAT being the most pronounced, dropping to 310 K (100°F) at 20 s (GRS) and 31 s (JAT). The temperature drop in GRS, ENEL, and CERL appeared to correspond to the initiation of accumulator flow. There was no immediately available explanation for the drops seen by STUD and JAT.

Comparison of measured and calculated intact loop hot leg temperatures is presented in Figure 10. The LOFT experiment experienced some superheating in the hot leg around 28 s. Superheat was calculated by CERL (23 s), JAR (38 s) and JAT (34 s). None of the other participants calculated this superheating in the intact loop hot leg.

Pressurizer average temperature, shown in Figure 11 was underpredicted by all participants. This does not include the isolated pressurizer model used by ENEL.

The steam generator secondary temperatures, presented in Figure 12, reflect the various initial conditions used by the participants. In general the blind calculations, with the exception of JAT, remained above the equilibrium L2-5 temperature.

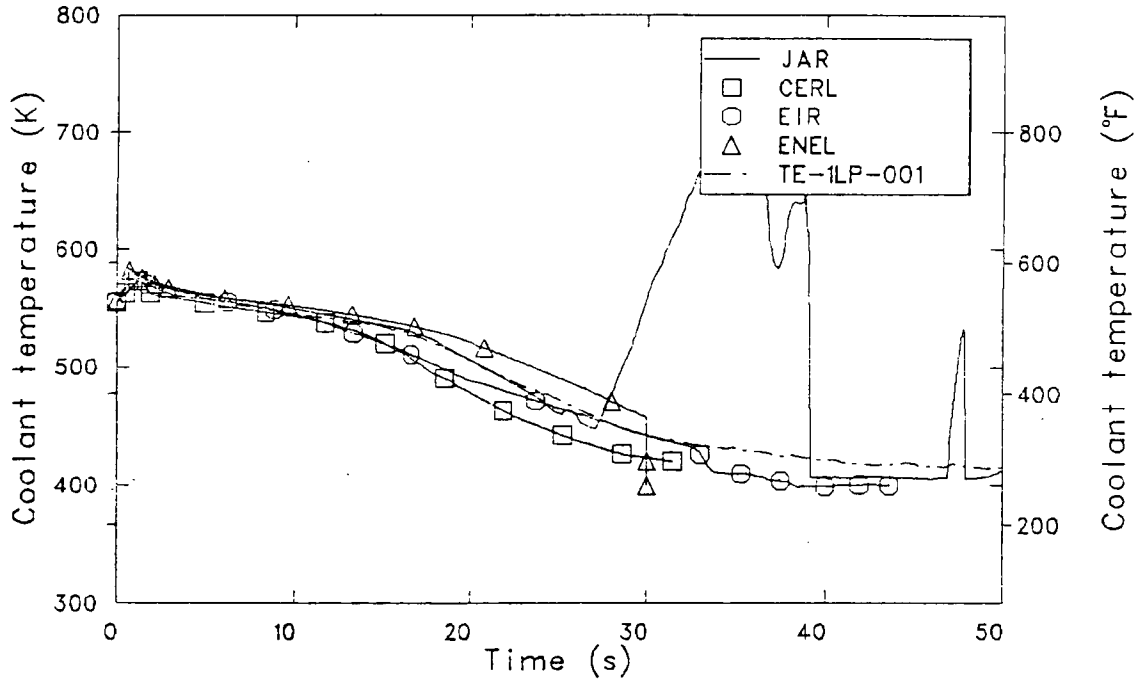

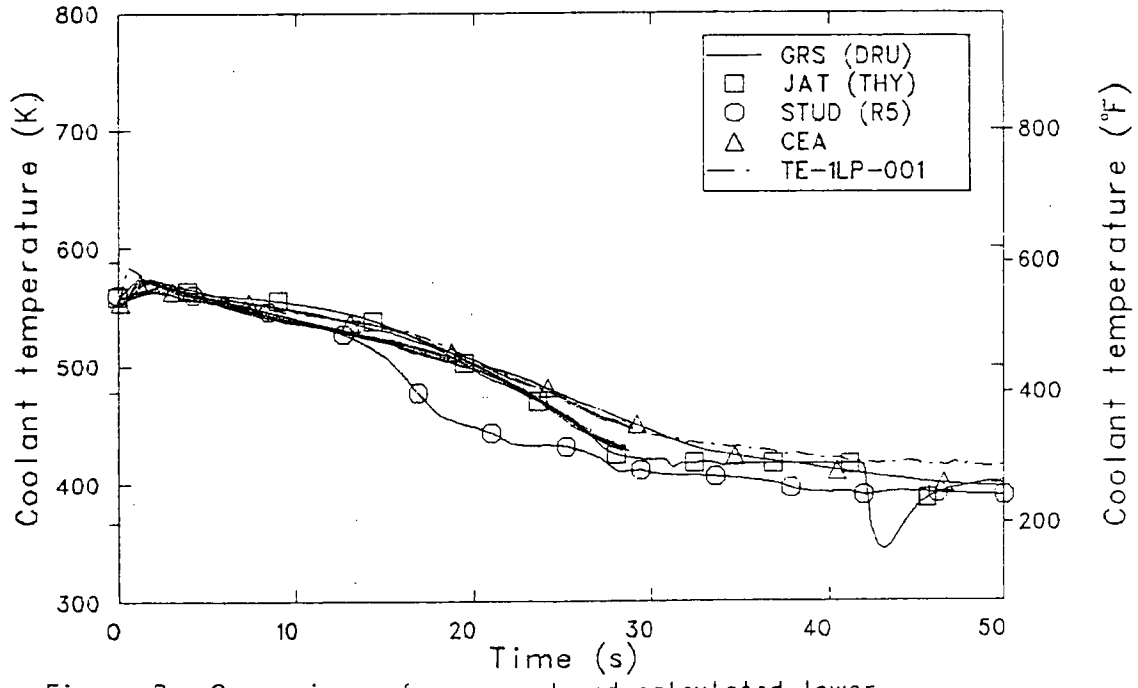

Figure 8. Comparison of measured and calculated lower plenum fluid temperature for the blind calculations.

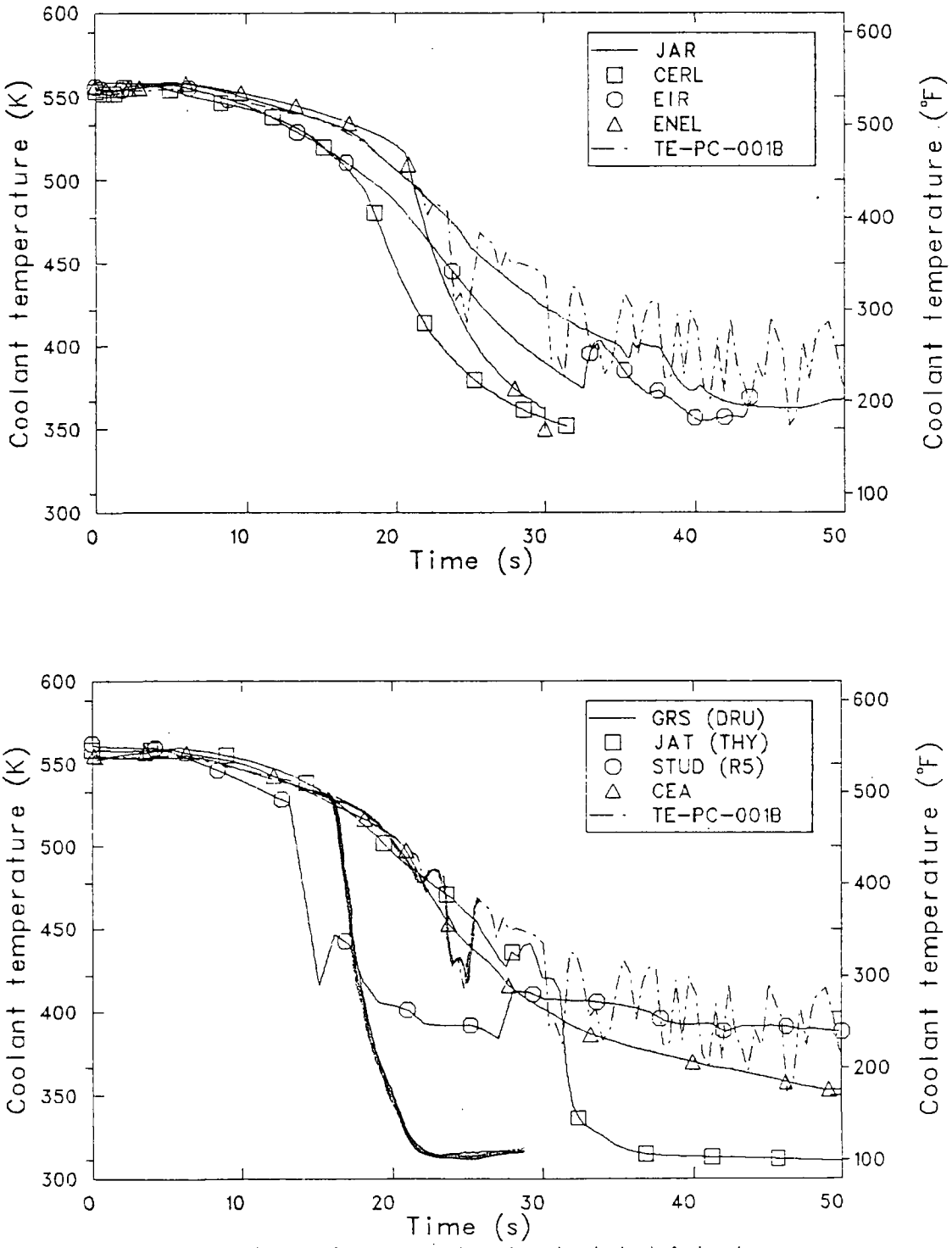

Figure 9. Comparison of measured and calculated intact loop cold leg temperature for the blind calculations.

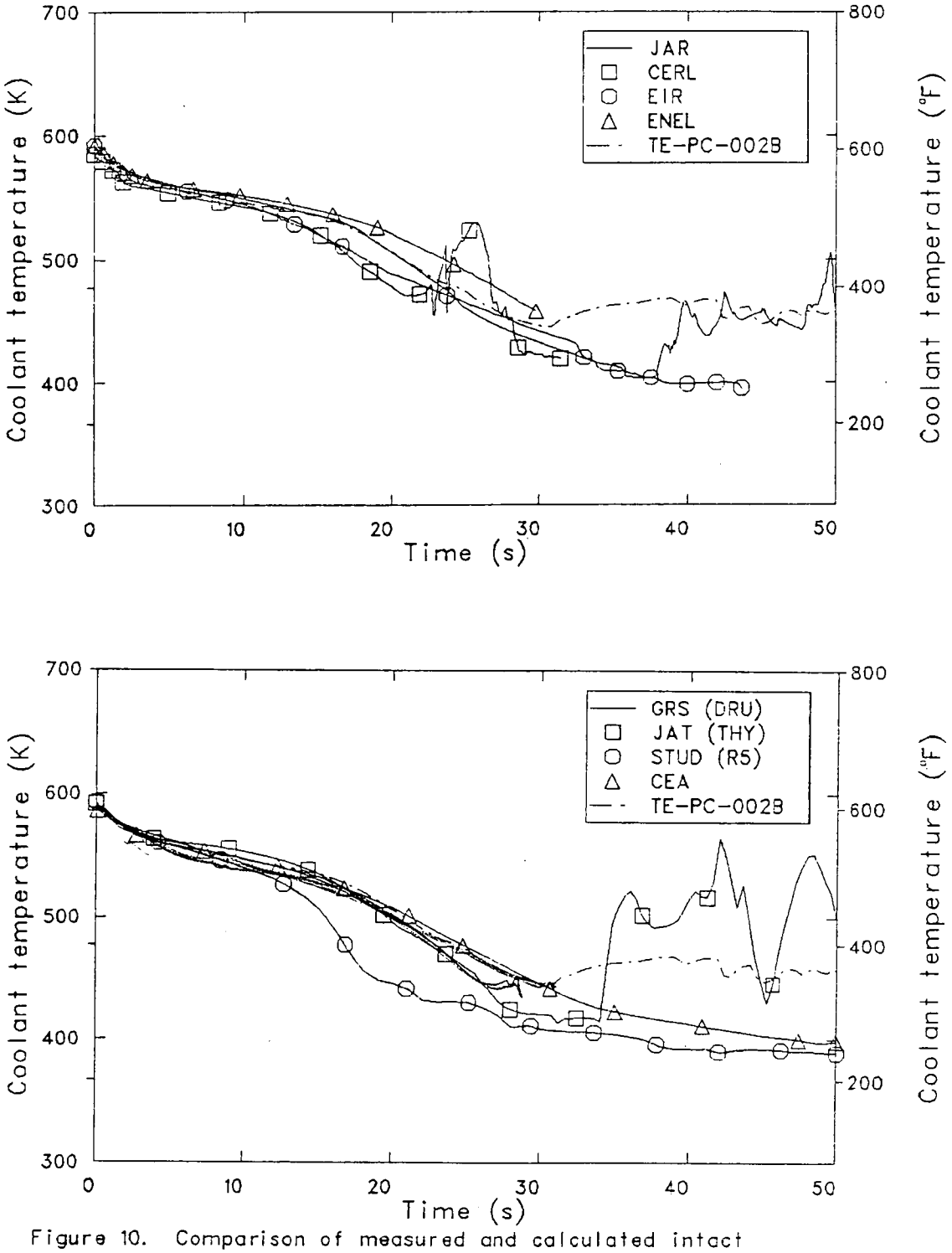

Figure 10. Comparison of measured and calculated intact loop hot leg temperature for the blind calculations.

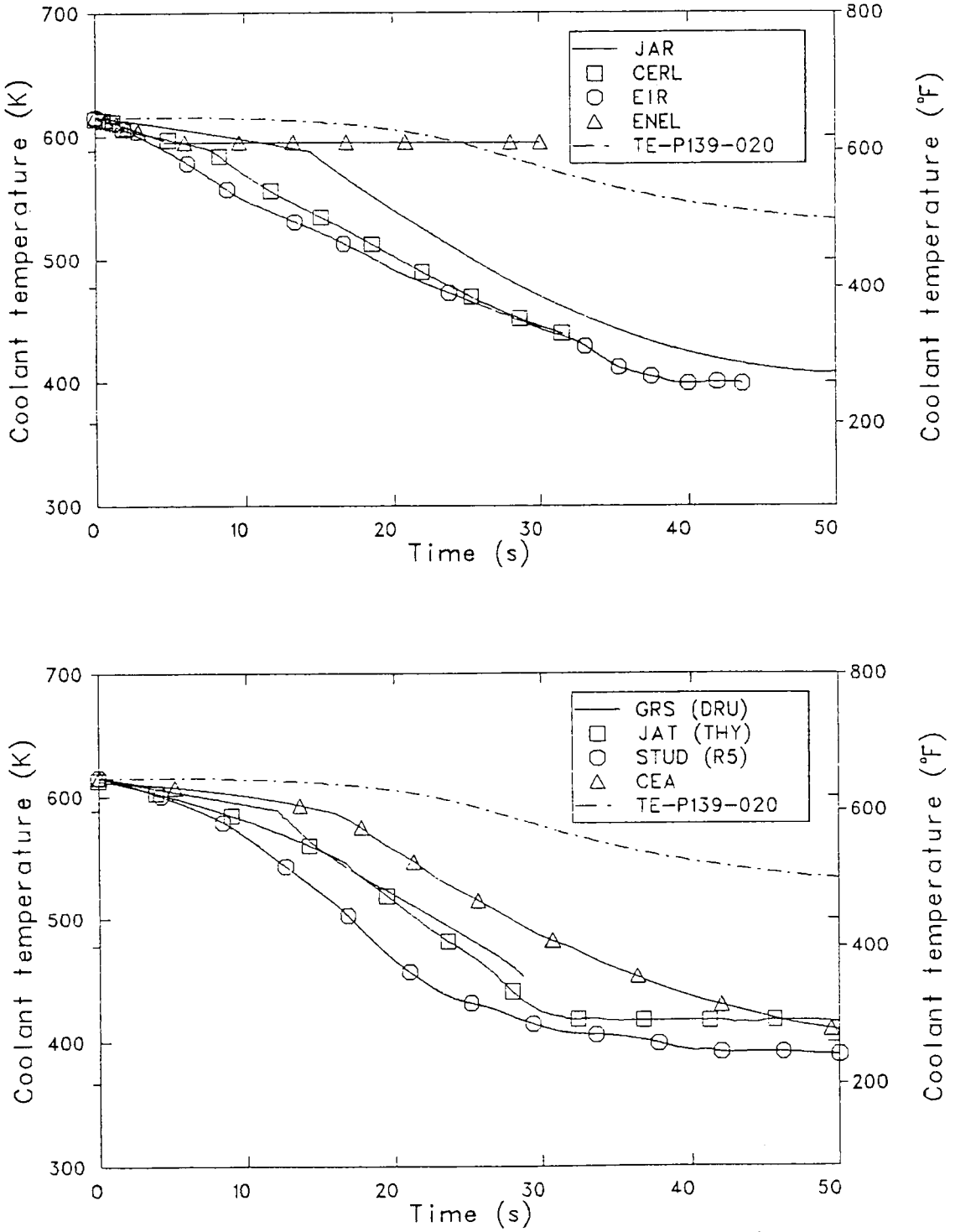

Figure 11. Comparison of measured and calculated pressurizer temperature for the blind calculations.

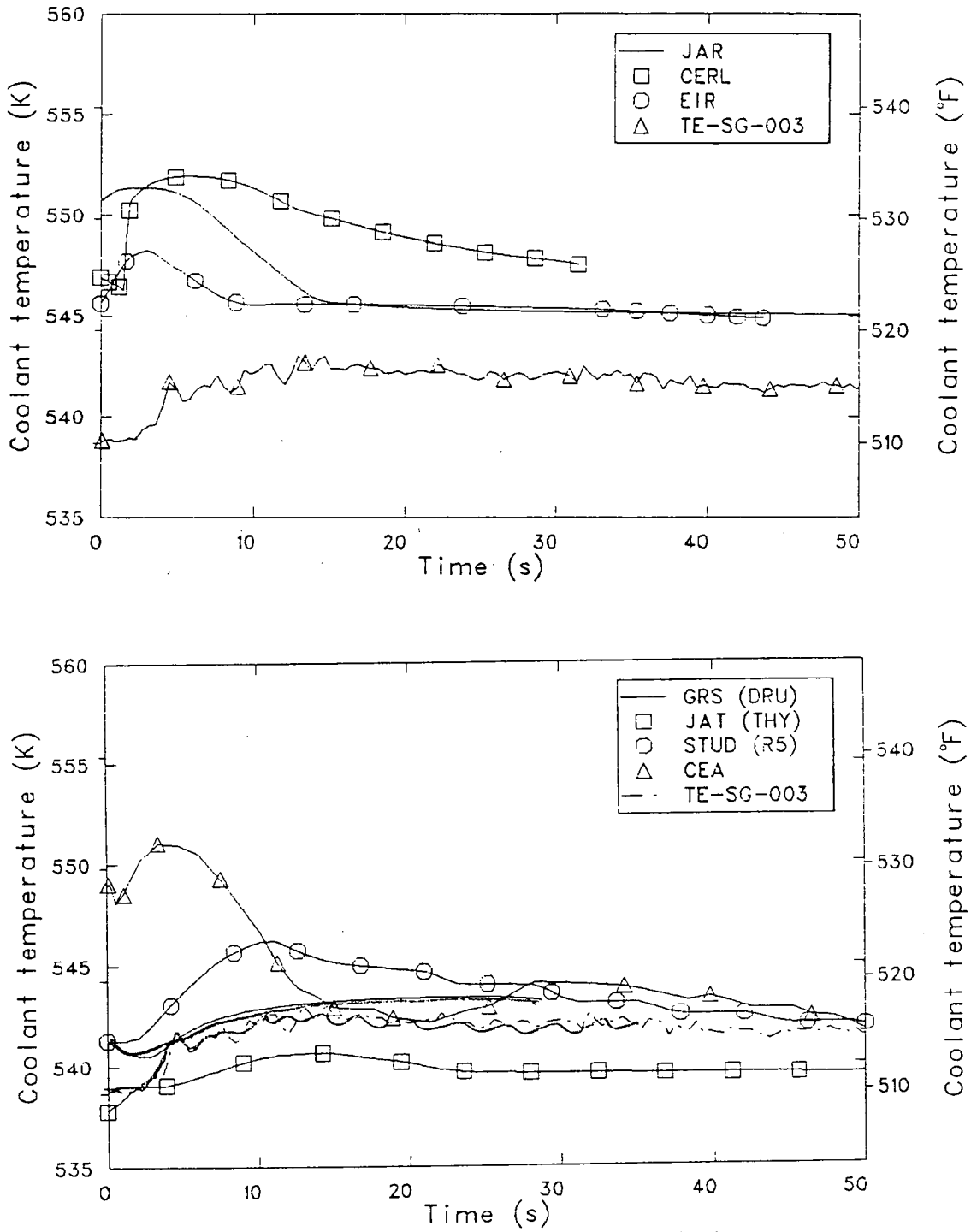

Figure 12. Comparison of measured and calculated steam generator secondary temperature for the blind calculations.

4.4 Fluid Density

The comparison between the calculated average volume density and the measured density in the intact loop cold leg showed significant differences as presented in Figure 13. Five calculations (CERL, EIR, ENEL, JAR, JAT) resulted in an initial voiding of the cold leg, followed by a complete refill. This refill time ranged from CERL's 16 s to JAT's 31 s. This refill was considerably different from the oscillations seen in the data. STUD calculated a single slug of liquid from 13 s, to 17 s, then voided completely. The remaining submittals simply voided the cold leg. The problem could be connected to the average density calculation and the difficulty the codes have calculating the effects of subcooled ECC injection.

There was better agreement between the average intact loop hot leg densities and the data taken in L2-5 as shown in Figure 14. By 30 s, all participants calculated a voided hot leg. JAT and ENEL calculated significantly higher density between 5 and 20 s than other submittals.

In the broken loop, both cold leg and hot leg shown in Figure 15 and 16 respectively, there was again considerable difference in the comparisons with the measured density and with the participants calculations themselves. All of blind calculations, with the exception of CERL, predicted a slower voiding in both legs during the first 10 s. In the hot leg, all participants's submittals showed a voided pipe after 20 s. In the cold leg, slug flow, seen in the data, was evident in the ENEL and CERL calculations. STUD, JAT, and EIR calculated major refills of the cold leg pipe starting at times ranging from 16 s (STUD) to 35 s (EIR). Both STUD's and JAT's analyses showed the cold leg pipe emptying again between 35 s and 42 s. EIR's calculation was terminated before the cold leg emptied.

4.5 Mass Flow

A comparison of the calculated core inlet flow, presented in Figure 17, shows the characteristic reversed core flow signature of a major cold leg break. All participants, except JAT, calculated approximately the

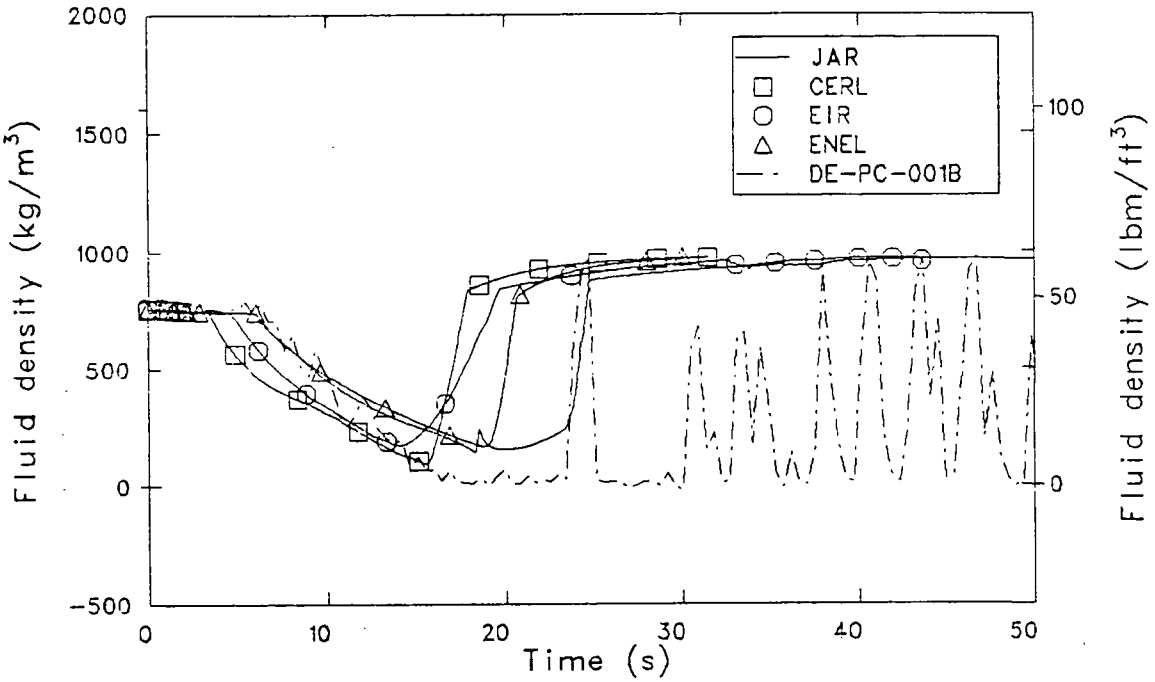

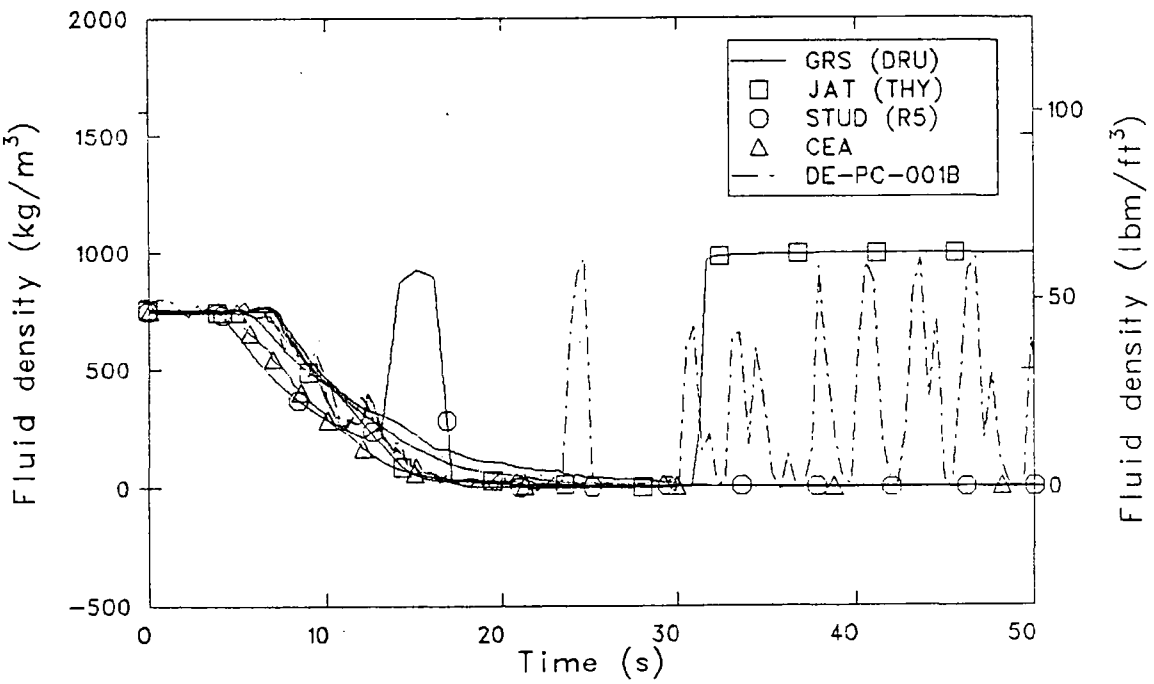

Figure 13. Comparison of measured and calculated intact loop cold leg density for the blind calculations.

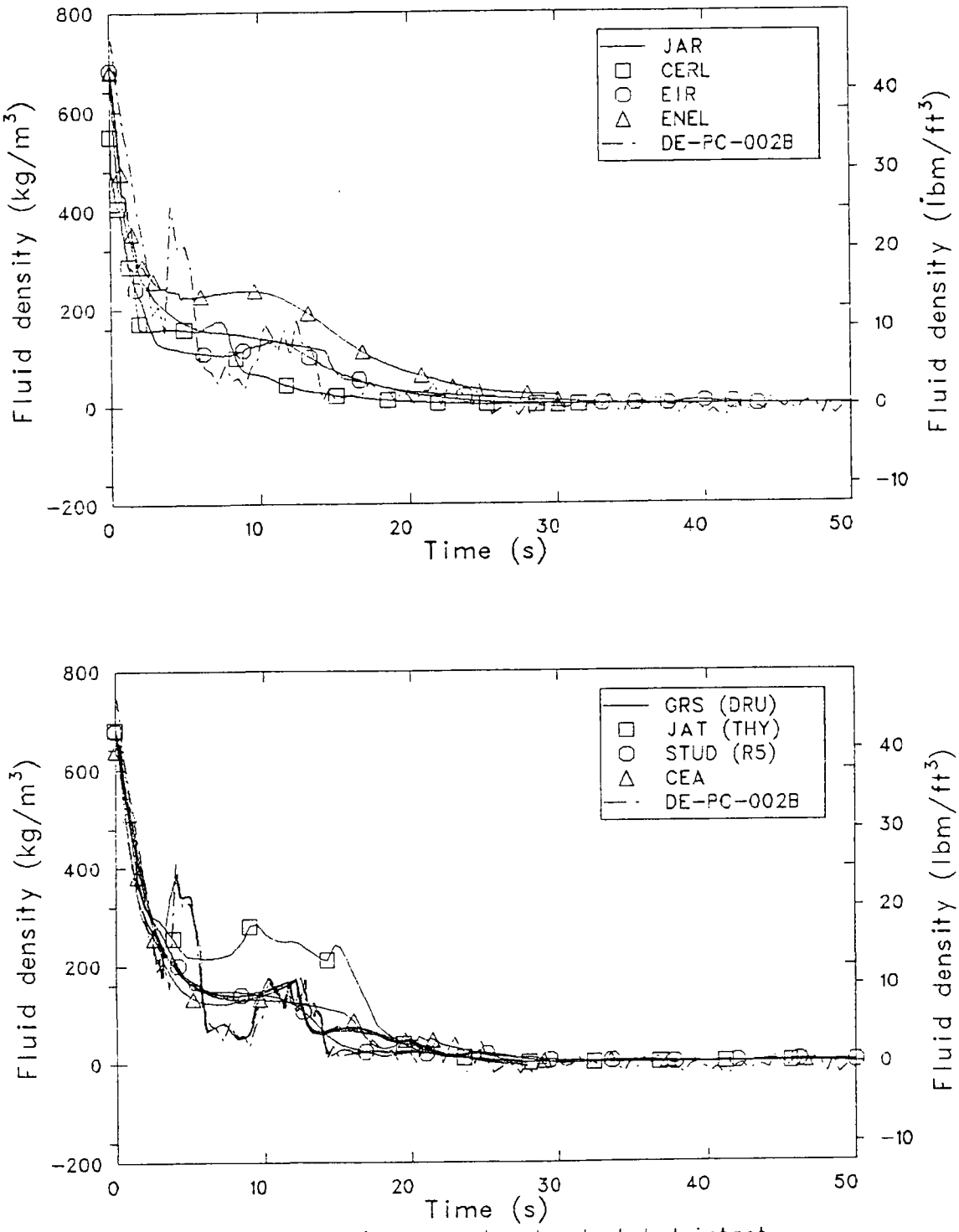

Figure 14. Comparison of measured and calculated intact loop hot leg density for the blind calculations.

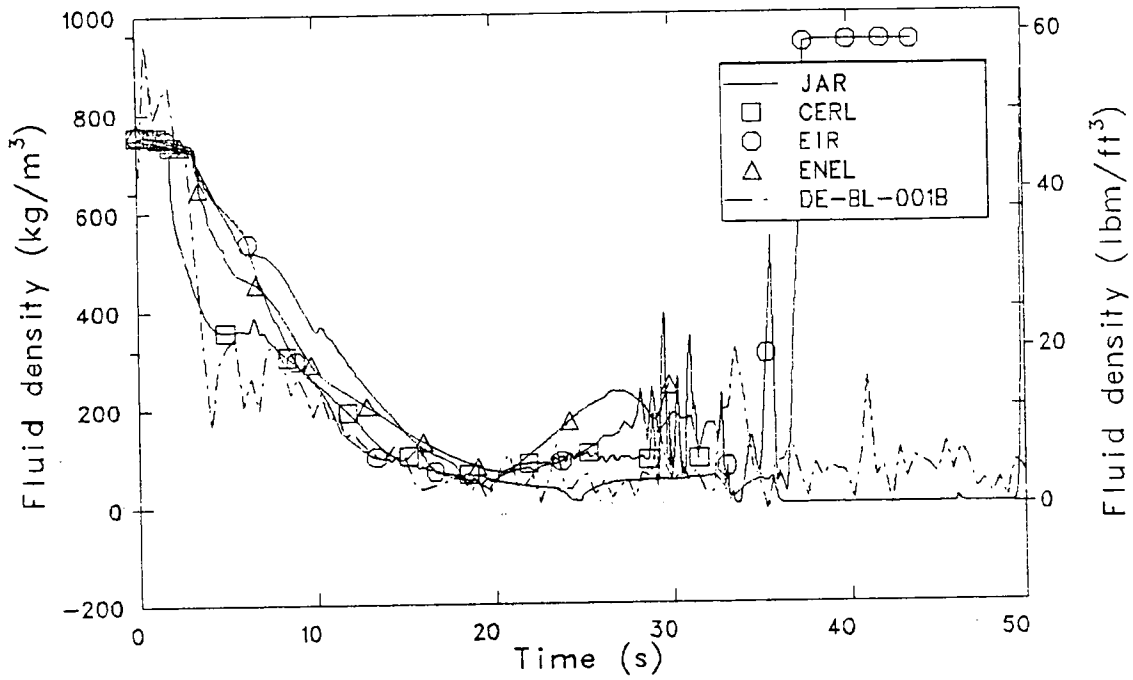

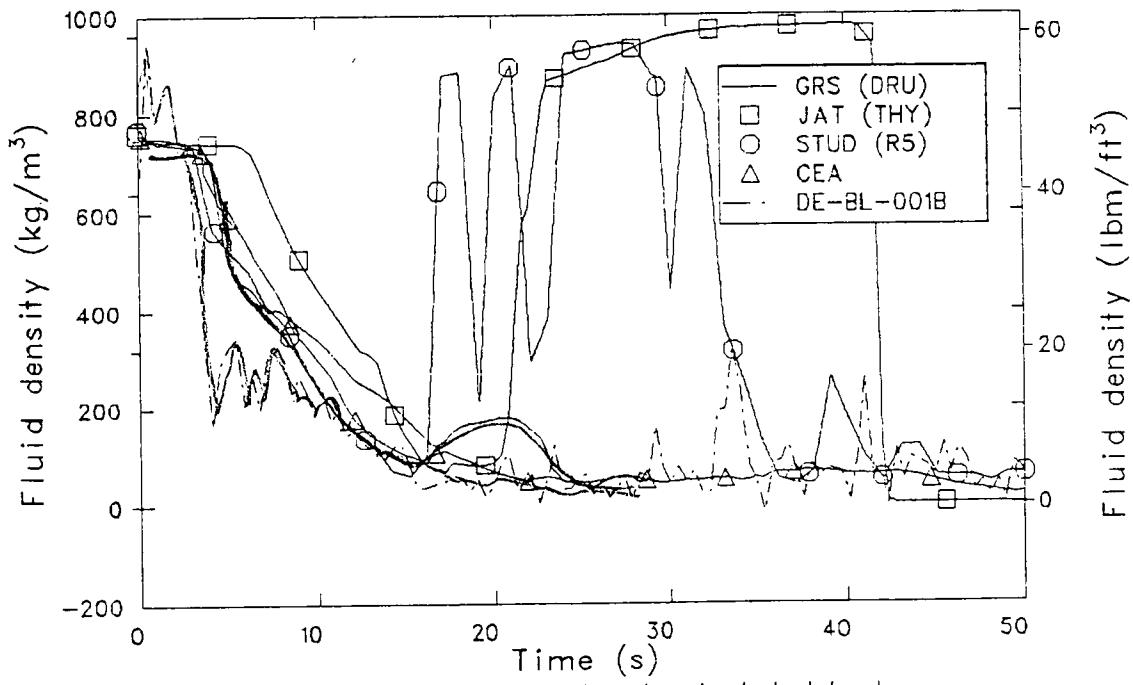

Figure 15. Comparison of measured and calculated broken loop cold leg density for the blind calculations.

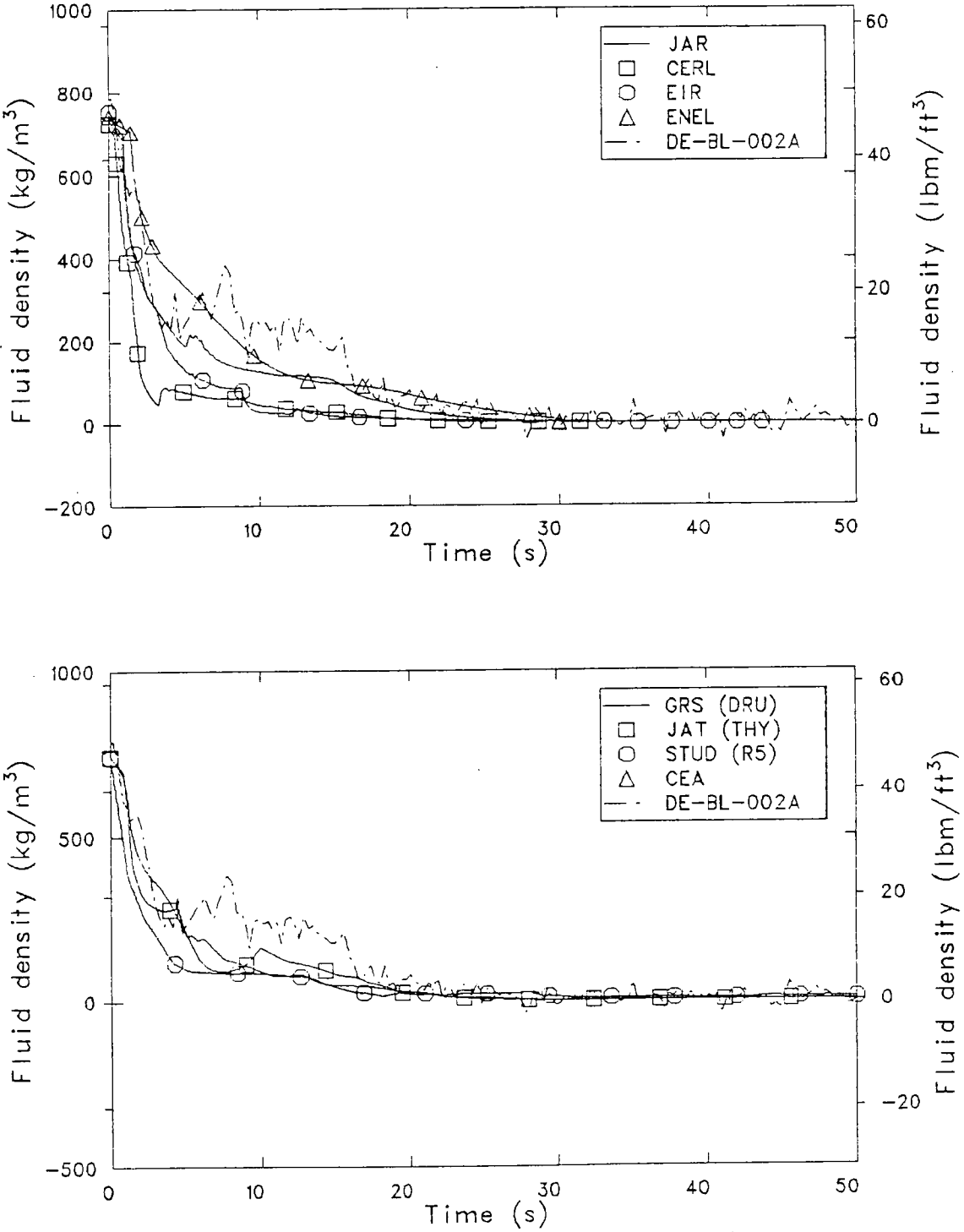

Figure 16. Comparison of measured and calculated broken loop hot leg density for the blind calculations.

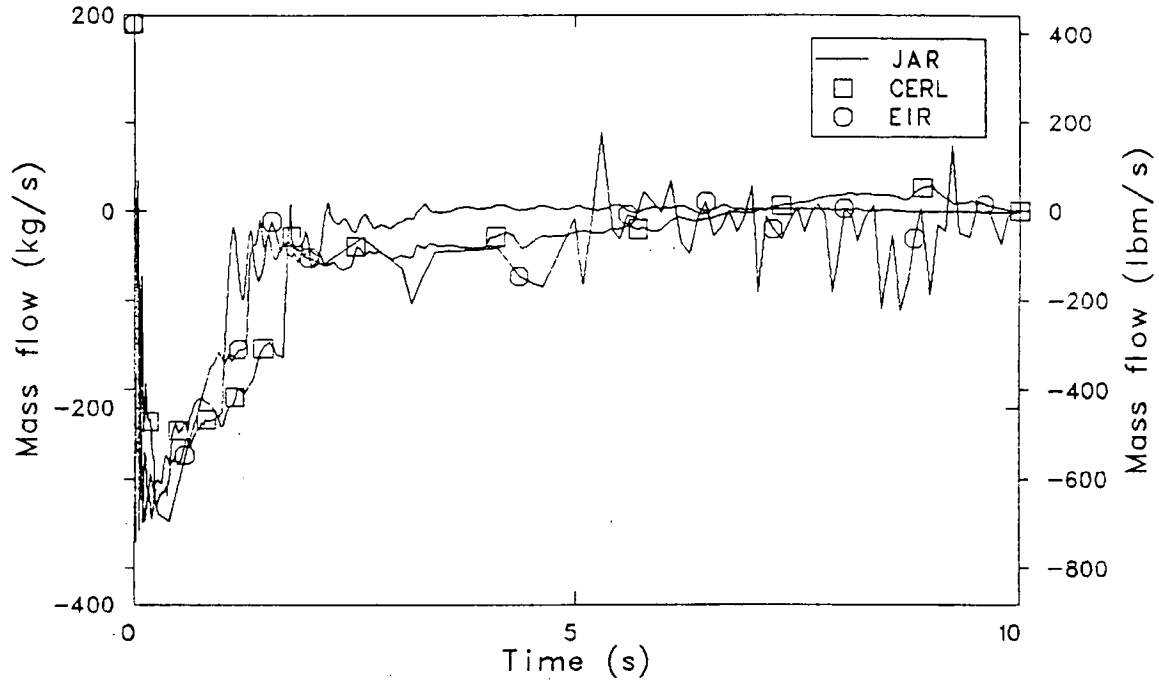

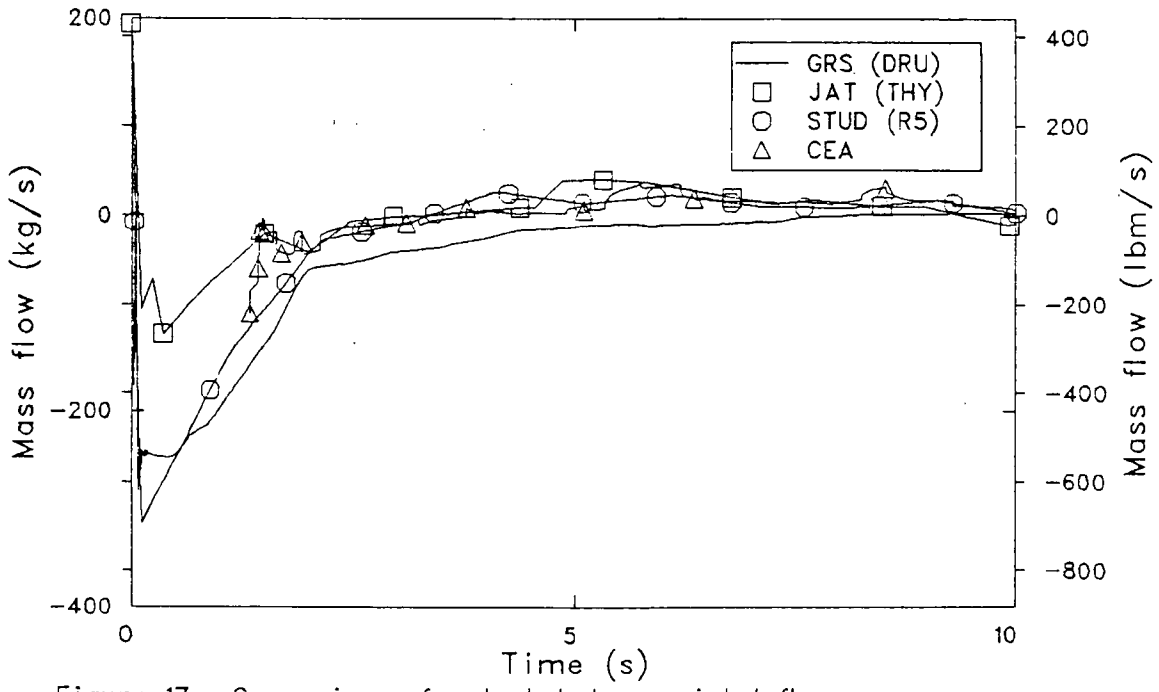

Figure 17. Comparison of calculated core inlet flows for the blind calculations.

same peak reverse flowrate. JAT's calculated peak flow was about 1/3 of that seen by the other calculations. By 10 s all calculated flows had essentially stopped.

For the calculation of a large pipe rupture, the break flow models were critical. As discussed in Section 3, virtually all participants used different models or multipliers for their break flow studies. Figure 18 and 19 present the results of these studies in comparison with data. In general the agreement between calculations and data is quite good. Peak cold leg flows calculated by CERL and CEA exceeded data significantly, while JAT underpredicted the cold leg flow substantially. In the hot leg only EIR underpredicted the break flow while most of the participants, including JAT, overpredicted the hot leg break flow. The discrepancies in break flow are better seen in Figure 20 which shows the integrated mass lost to the system through the breaks. EIR's calculated mass lost came the closest to matching data. JAT first underpredicted the mass lost during the first 9 s, then overpredicted. All other participants overpredicted the mass lost with STUD's mass lost being some 50% higher than data by 30 s.

Figure 21 shows the calculated mass inventory in the reactor vessel. While discrepancies in the initial mass make exact comparisons difficult, a qualitative review showed some explanable differences as well. EIR did not experience a refill in inventory, while STUD calculated an insurge between 15 s and 23 s, which emptied out by 30 s. GRS, JAT and JAR calculated refills starting between 25 s and 40 s.

Emergency core coolant injection is shown in Figures 22 and 23. All participants underpredictd the initial HPI peak flow. High pressure injection flow was overpredicted by STUD and JAT after the initial peak flow. Low pressure injection was calculated reasonably well by all participants, except JAR, which showed high flow as well as what appears to be some possible modeling problems.

4.6 Pump Speed

Pump coastdown, simulating the loss of offsite power in L2-5, is compared with data in Figure 24. Most participants followed the coastdown

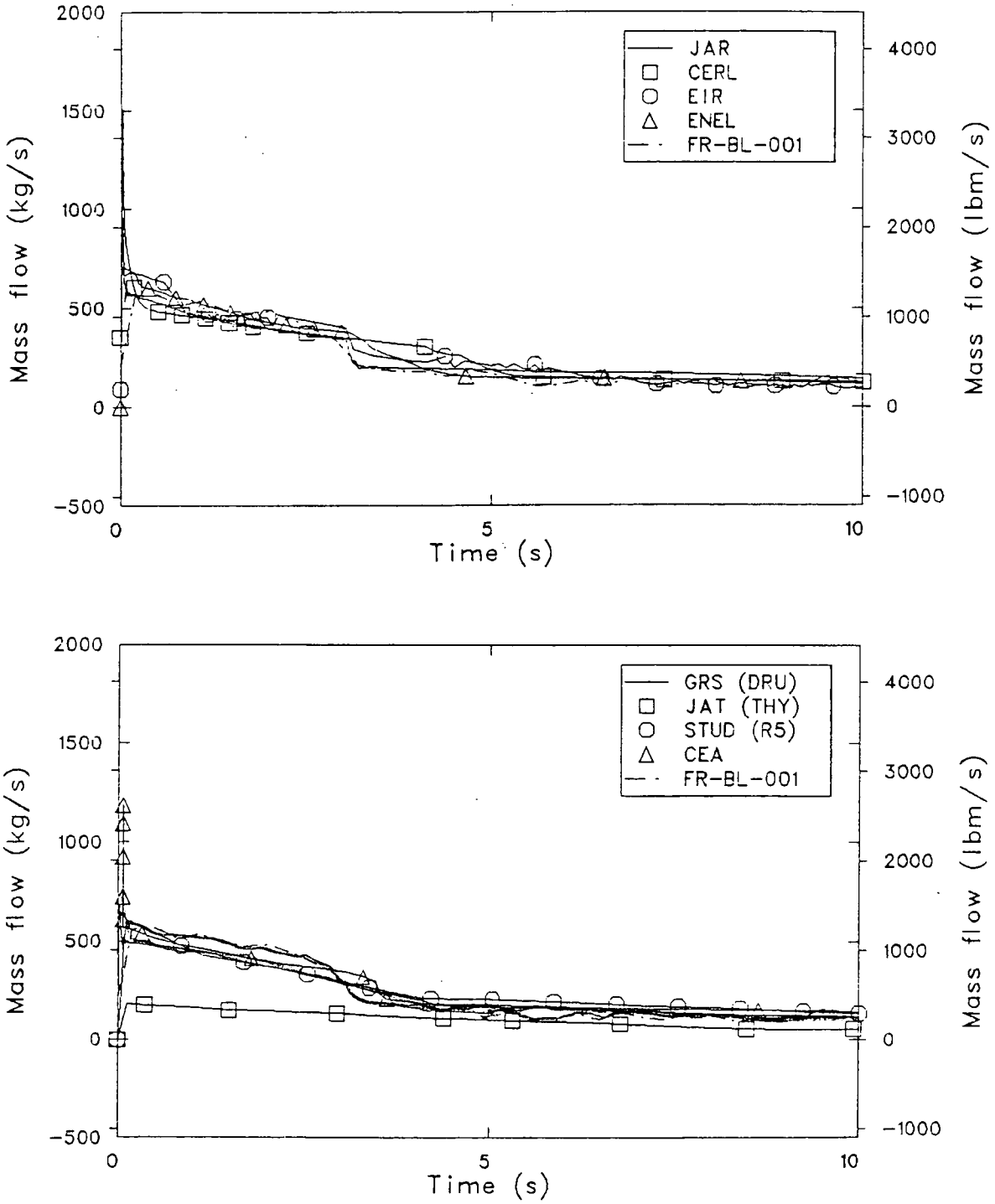

Figure 18. Comparison of measured and calculated broken loop cold leg break mass flow rate for the blind calculations.

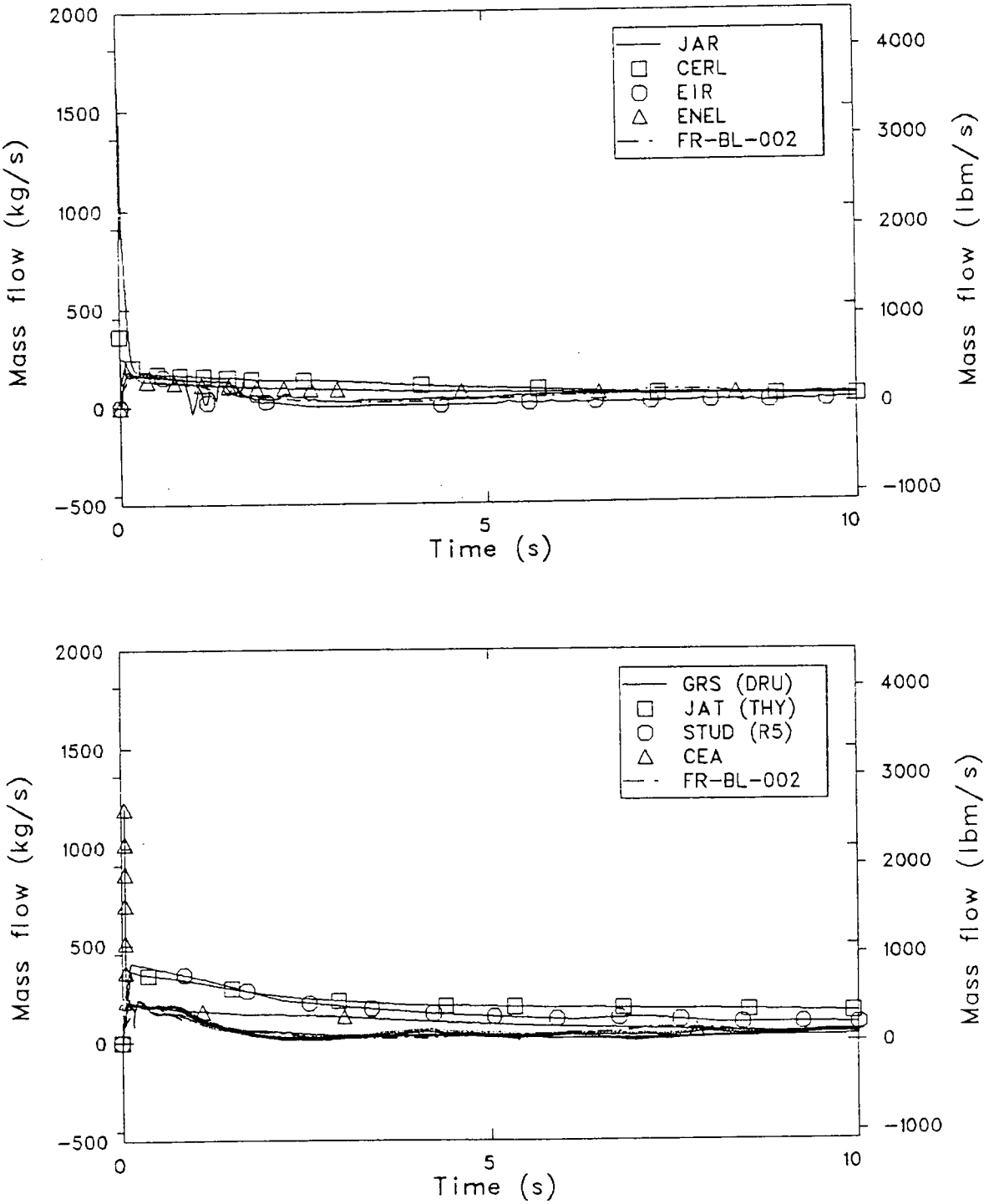

Figure 19. Comparison of measured and calculated broken loop hot leg break mass flow rate for the blind calculations.

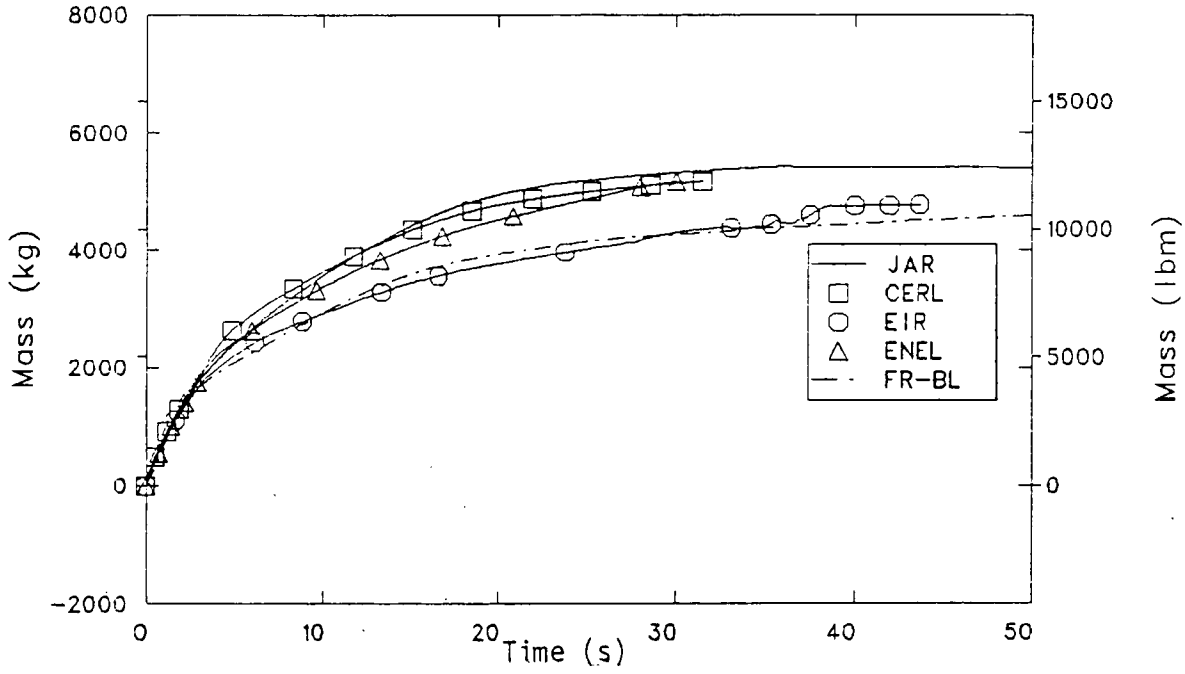

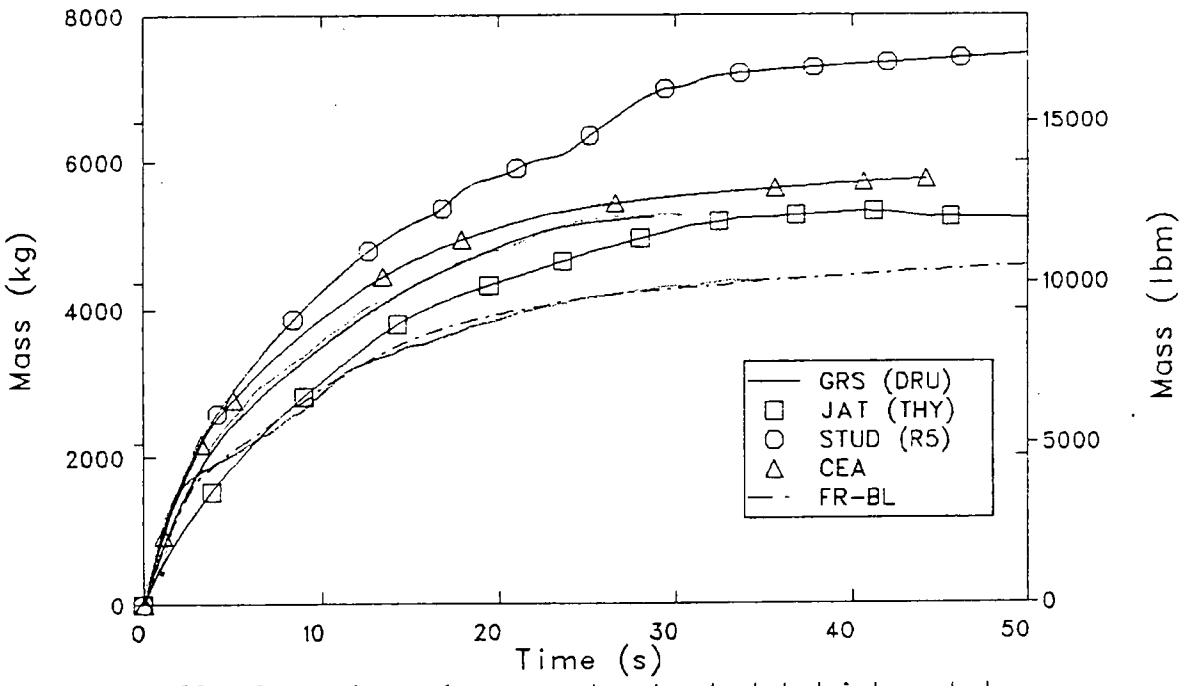

Figure 20. Comparison of measured and calculated integrated break flow for the blind calculations.

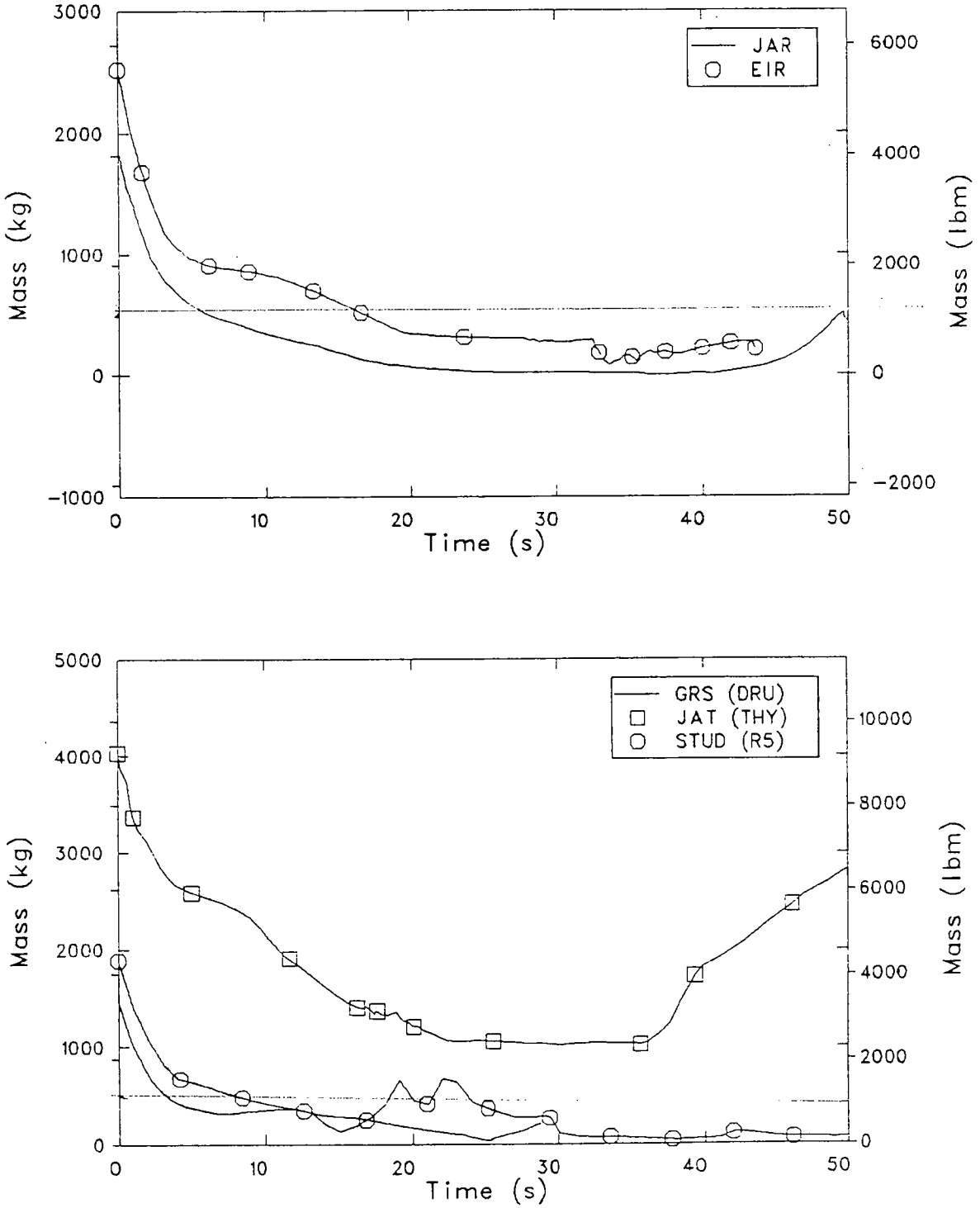

Figure 21. Comparison of calculated reactor vessel mass inventory for the blind calculations.

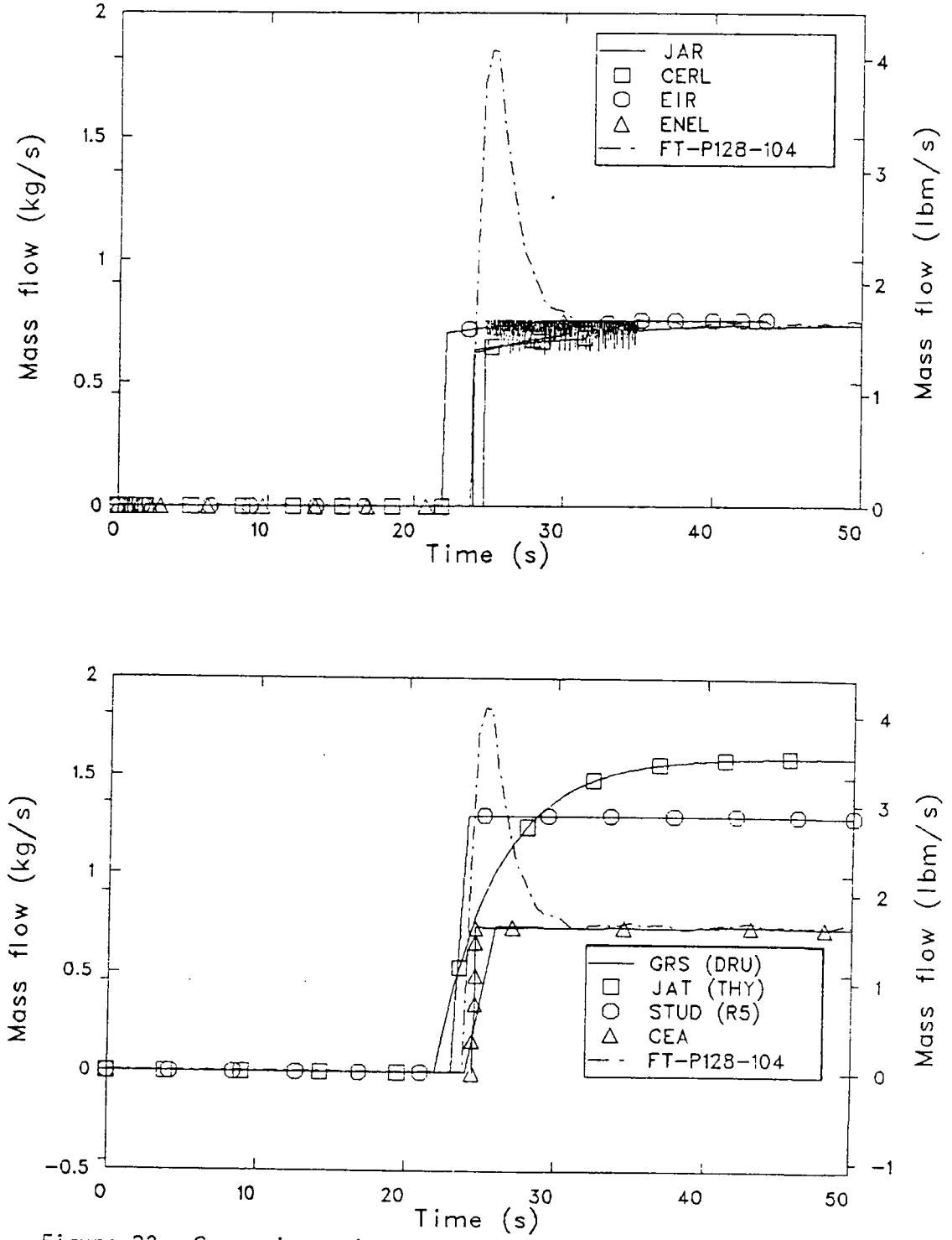

Figure 22. Comparison of measured and calculated HPIS flow for the blind calculations.

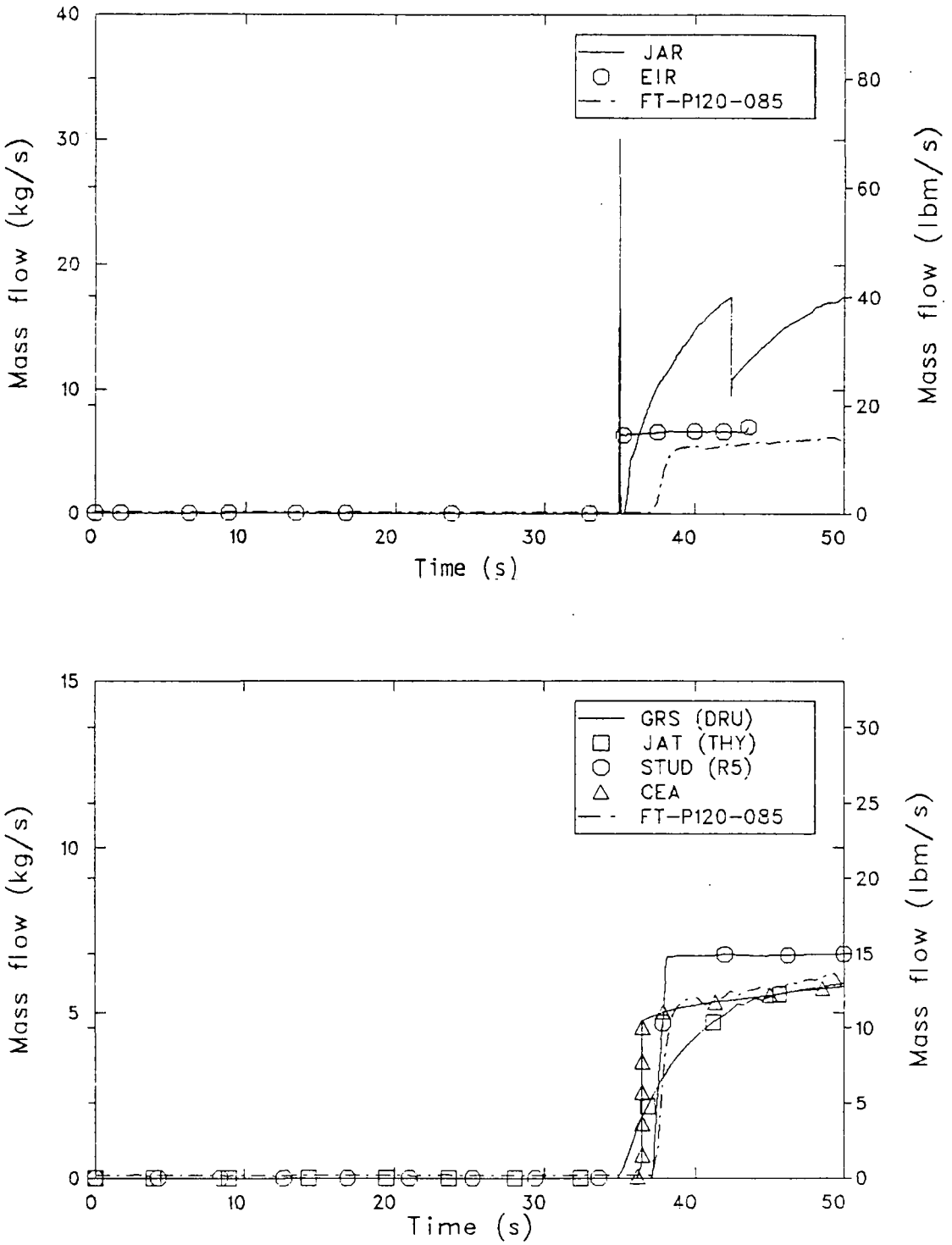

Figure 23. Comparison of measured and calculated LPIS flow for the blind calculations.

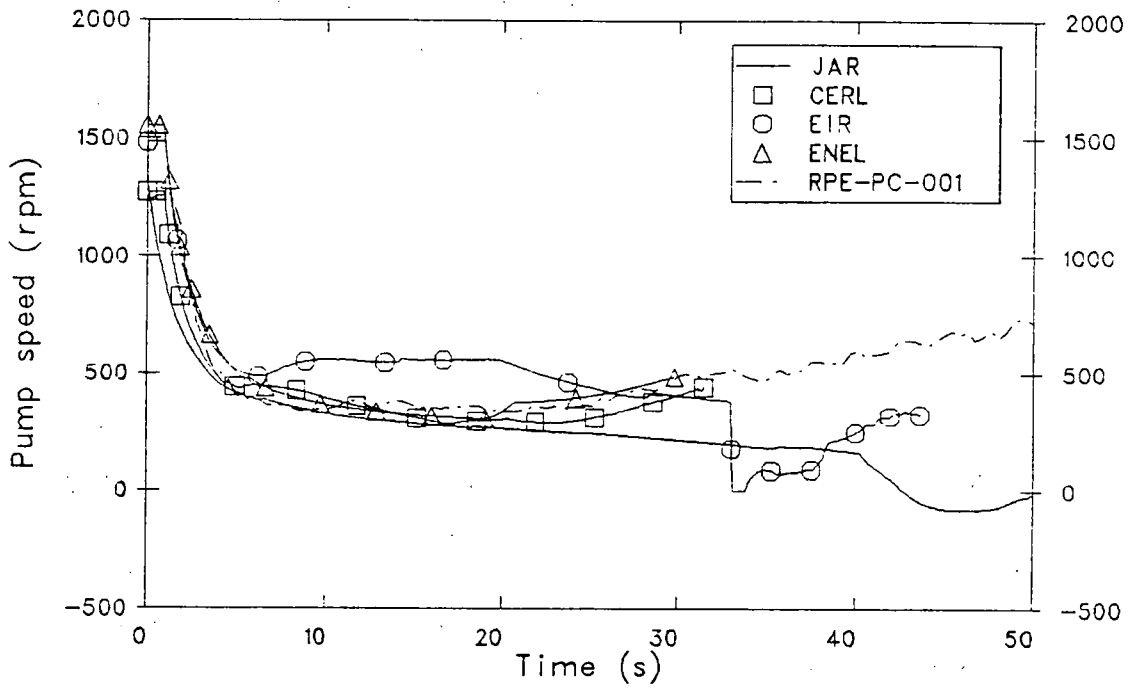

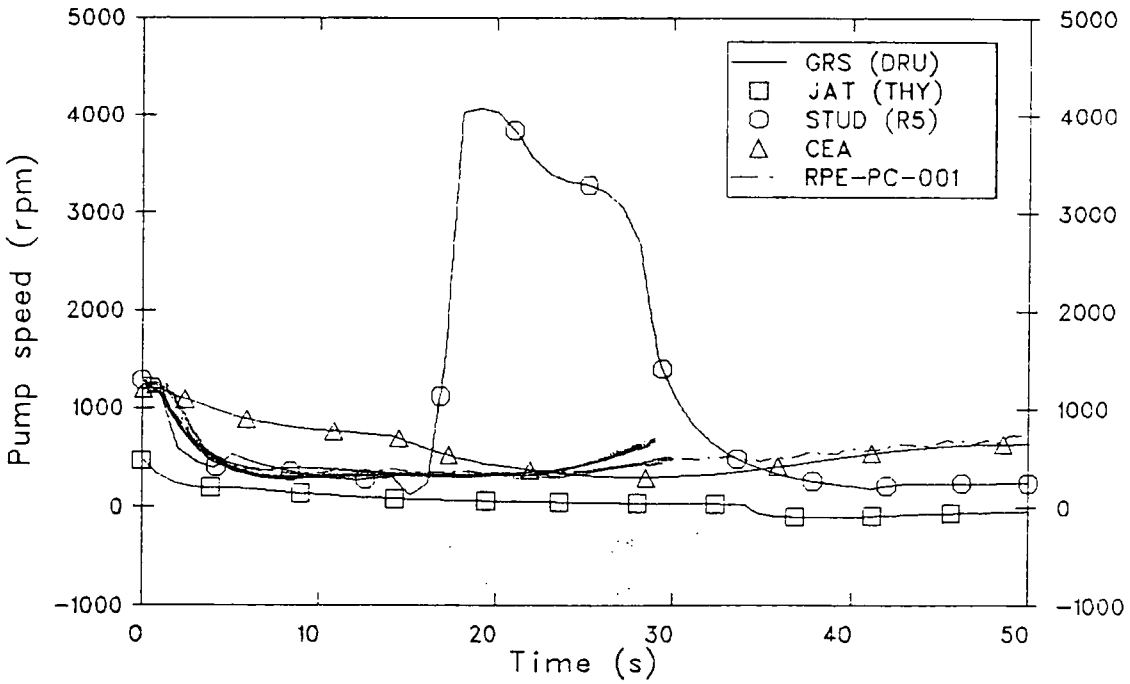

Figure 24. Comparison of measured and calculated reactor coolant pump speed for the blind calculations.

well, taking the various initial speeds into account. EIR calculated a much higher speed for the first 20 s, then degraded to an abrupt shut off at 34 s. Only the two Japanese submittals did not calculate a pump speed turnaround. STUD calculated a tremendous increase in pump speed, to nearly 400% of initial speed between 16 s and 31 s. This peak is similar to the pump speed increase experienced in L2-5 between 25 and 59 s, but the data never exceeded the pump's initial speed.

4.7 Rod Temperature

The comparison of cladding temperatures with data is difficult due to the variety of modeling techniques used by the participants to model the heat slabs in the core. With this in mind, Figures 25 and 26 present the comparisons with data for the 0.76 m (30 in.) elevation and 0.99 m (39 in.) elevation. For the first 30 s, GRS comes very close to matching the temperature profile at the 0.76 m level, with a peak slightly higher than data. JAR, ENEL, JAT and CEA all underpredict the temperatures but show the stable high temperature plateau seen in data. CERL overpredicts the temperature plateau, while STUD reaches the same peak as CERL but shows a definite quench. The quench seen in the STUD RELAP5 calculation starts at the same time as the increases in loop densities and the pump speed.

At the 0.99 m level, the data from L2-5 is characterized by two quenches at 15 s and 47 s. None of the participants, except EIR, calculated these quenches at the presented elevations. Initial increases in temperature were well predicted by all except EIR, which used an average core model for this elevation. Only JAR overpredicted the temperature prior to the 15 s data quench.

4.8 Summary

In summary, the eight blind calculations performed satisfactorily when calculating hydraulic behavior except when modeling problems, such as EIR's pressurizer, STUD's pump and JAR's LPIS, interfered. The predicted pressure-temperature histories were generally lower than data. Subcooling and superheat within the primary were not well predicted. Except in the intact loop cold leg, densities were adequately predicted. In the cold

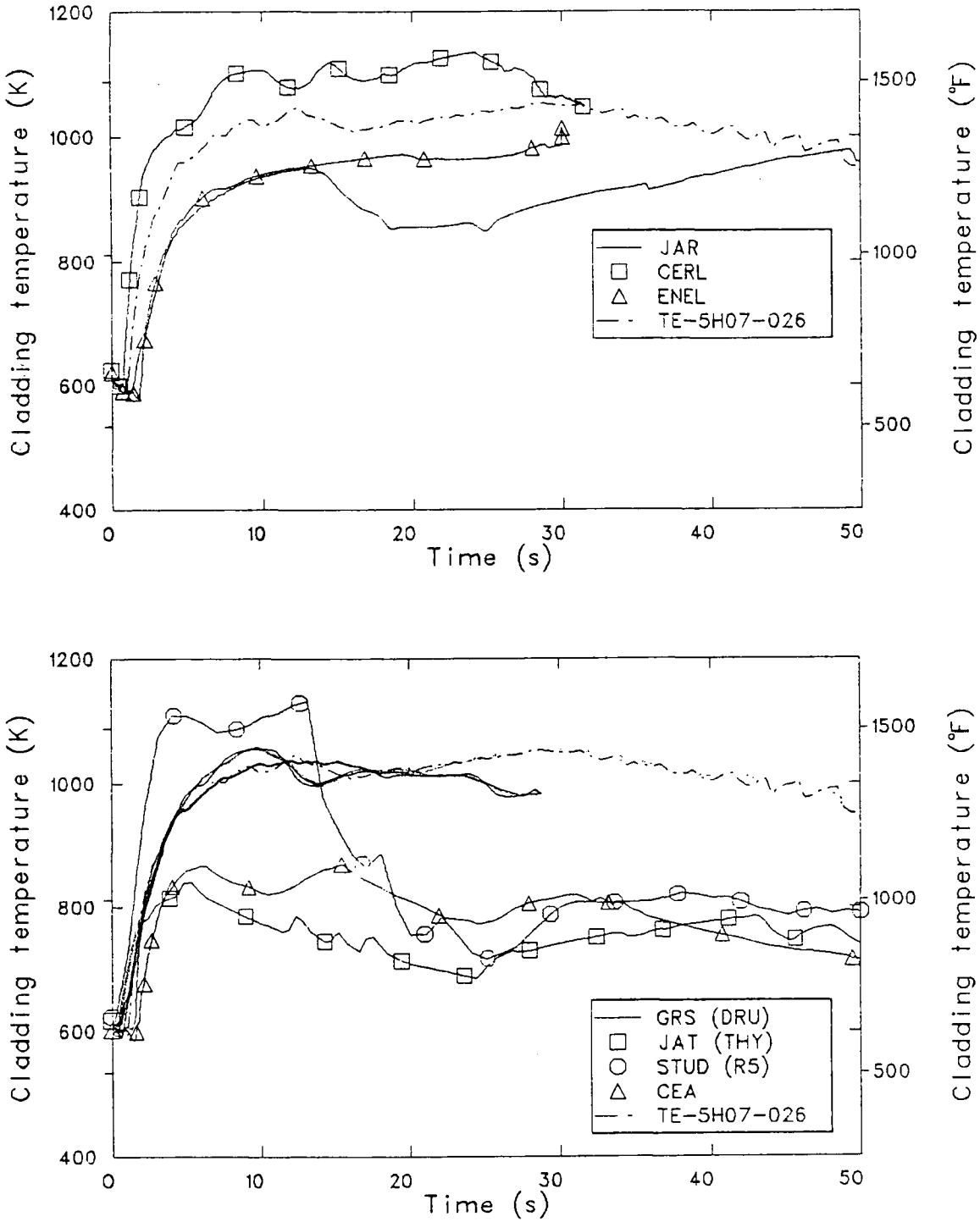

Figure 25. Comparison of measured and calculated rod cladding temperature at the 0.76m elevation for the blind calculations.

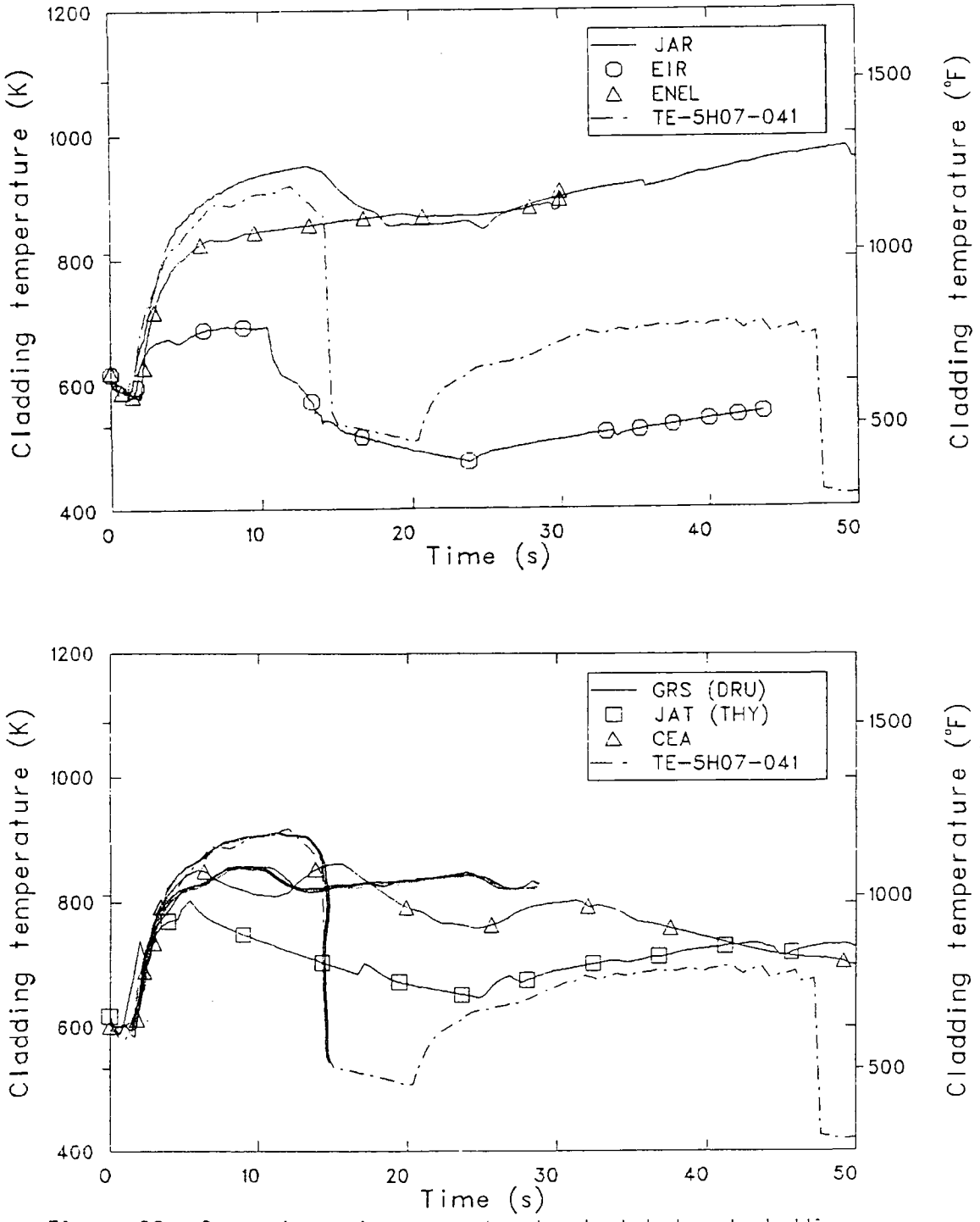

Figure 26. Comparison of measured and calculated rod cladding temperature at the .99m elevation for the blind calculations.

leg, however, the predictions ranged from liquid full to vapor full without the slug flow behavior seen in the data. Break flow and mass lost to the primary was overpredicted by all participants, except EIR. Calculations of ECC injection and pump speed were adequate except for the above mentioned modeling problems. Rod temperature profiles were very model dependant. Heatup rates were calculated well, while quenches of the clad were not predicted.

5. SUMMARY OF OPEN RESULTS

The calculations submitted by LANL, DCMN, VTT and the second EIR submittal were designated open calculations because the models used in these analyses were not submitted prior to the L2-5 experiment. These participants were alowed to make code or model changes to improve their predictions. Comparisons of experiment L2-5 data with the code predictions are provided in the following sections.

5.1 Sequence of Events

The measured and calculated sequence of events for the open calculation were included in Table 3. For the most part all open submittals calculated the experiment's sequence of events well. EIR and VTT scrammed the reactor earlier than the 0.24 s experiment scram. VTT predicted an early deviation from saturation temperatures while EIR predicted a later one. LANL tripped the pumps early at 0.24 s rather than 0.94 s. The participants calculated pressurizer voiding between 8 s (EIR) and 28 s (LANL). ECC initiation was well calculated. The time of peak clad temperatures, however, ranged from 5.2 s (VTT) to 50 s (LANL).

5.2 Pressure

The calculated pressure in the pressurizer, intact loop cold leg, broken loop hot leg, broken loop cold leg, and upper plenum are compared with data in Figures 27 to 31, respectively. EIR and VTT underpredicted the pressure in the pressurizer, while LANL and DCMN calculated the drop extremely well for the first 15 s, then overcalculated the pressure from 15 s to 40 s. In the loops and upper plenum, the same basic pattern was seen with EIR and VTT generally under the data and LANL and DCMN generally over. But all participants calculated the loop pressure history well.

Figure 32 shows the comparison between calculated secondary pressure and data. The EIR calculation showed the best comparison with data, following the pressure history quite well. The LANL calculation showed a slow oscillation in secondary pressure, while the VTT depressurized substantially.

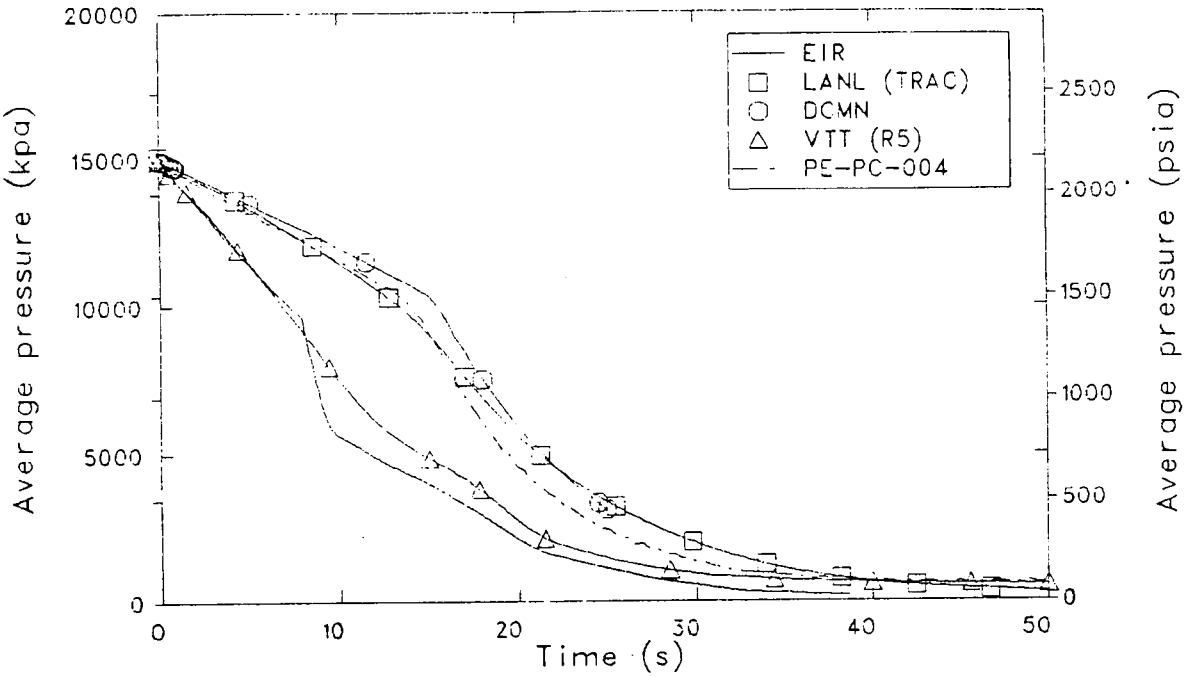

Figure 27. Comparison of measured and calculated pressurizer pressure for the open calculations.

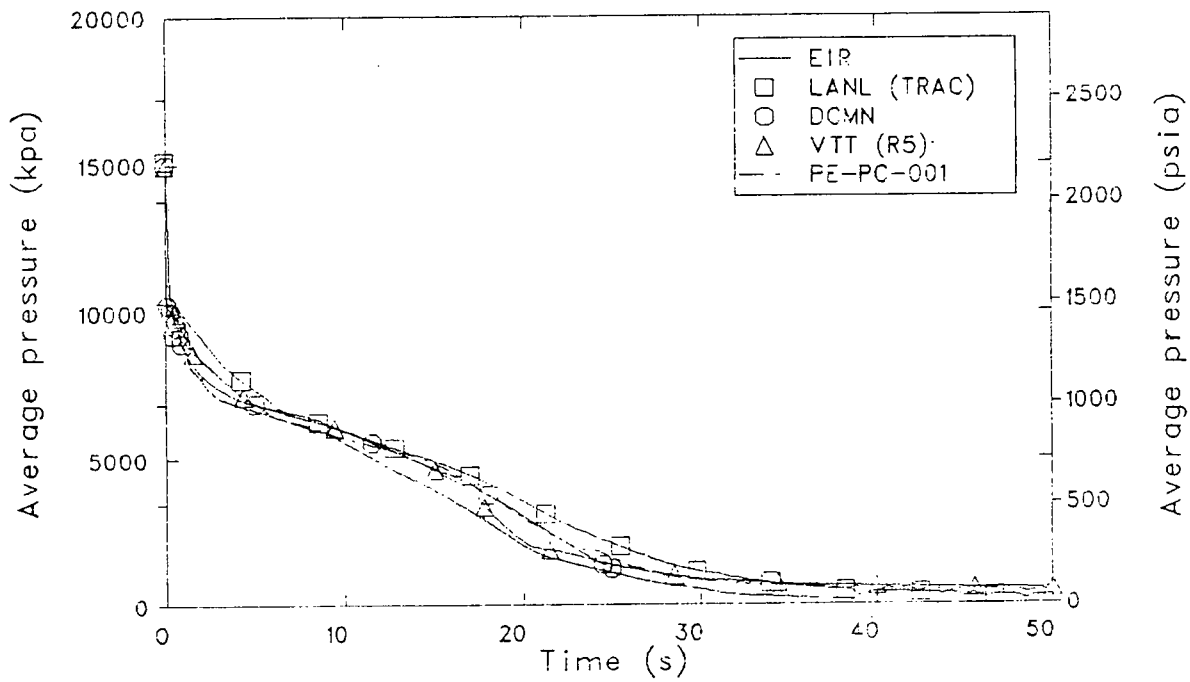

Figure 28. Comparison of measured and calculated intact loop cold leg pressure for the open calculations.

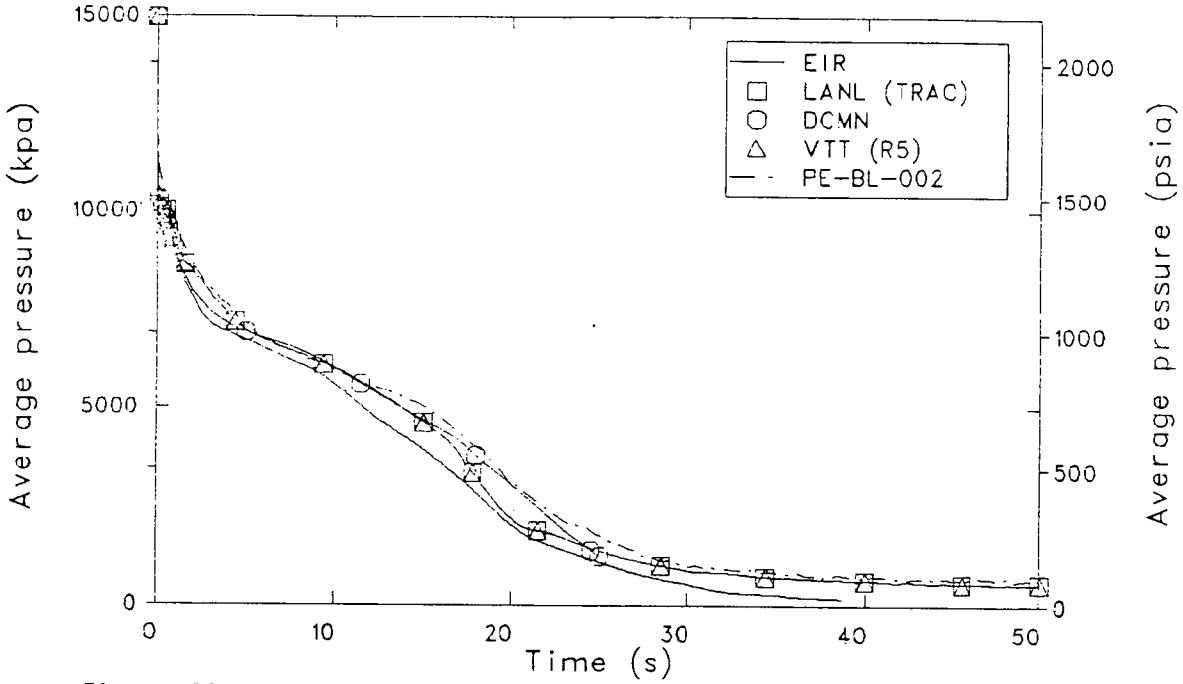

Figure 29. Comparison of measured and calculated broken loop hot leg pressure for the open calculations.

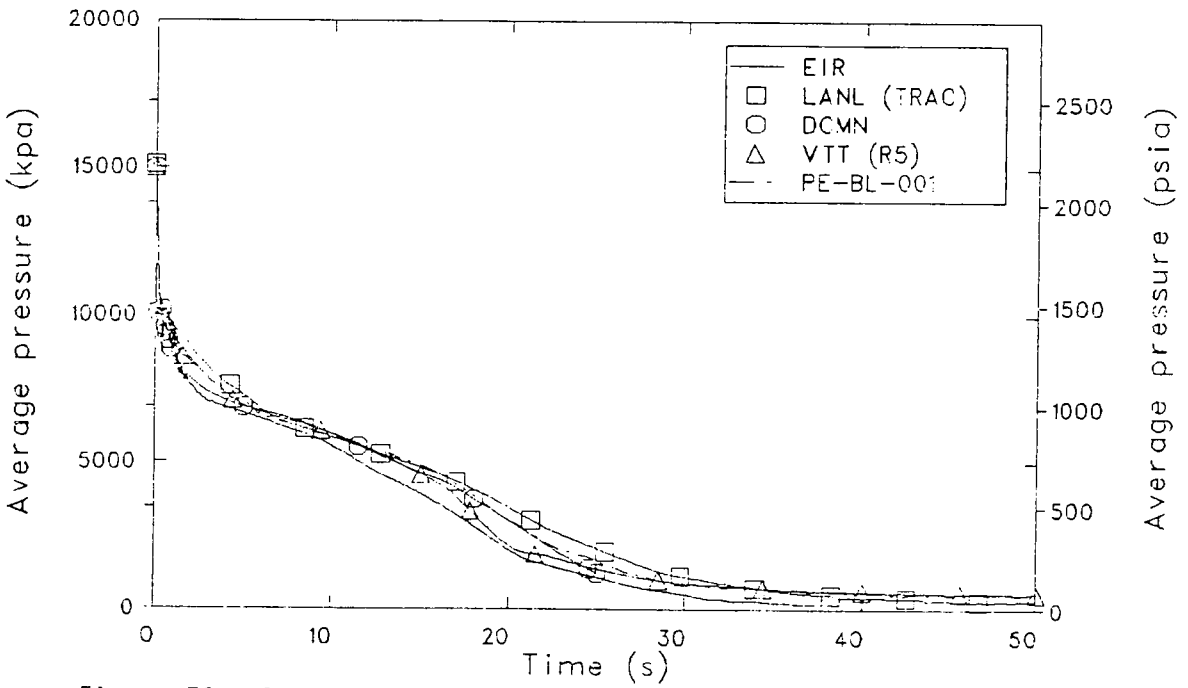

Figure 30. Comparison of measured and calculated broken loop cold leg pressure for the open calculations.

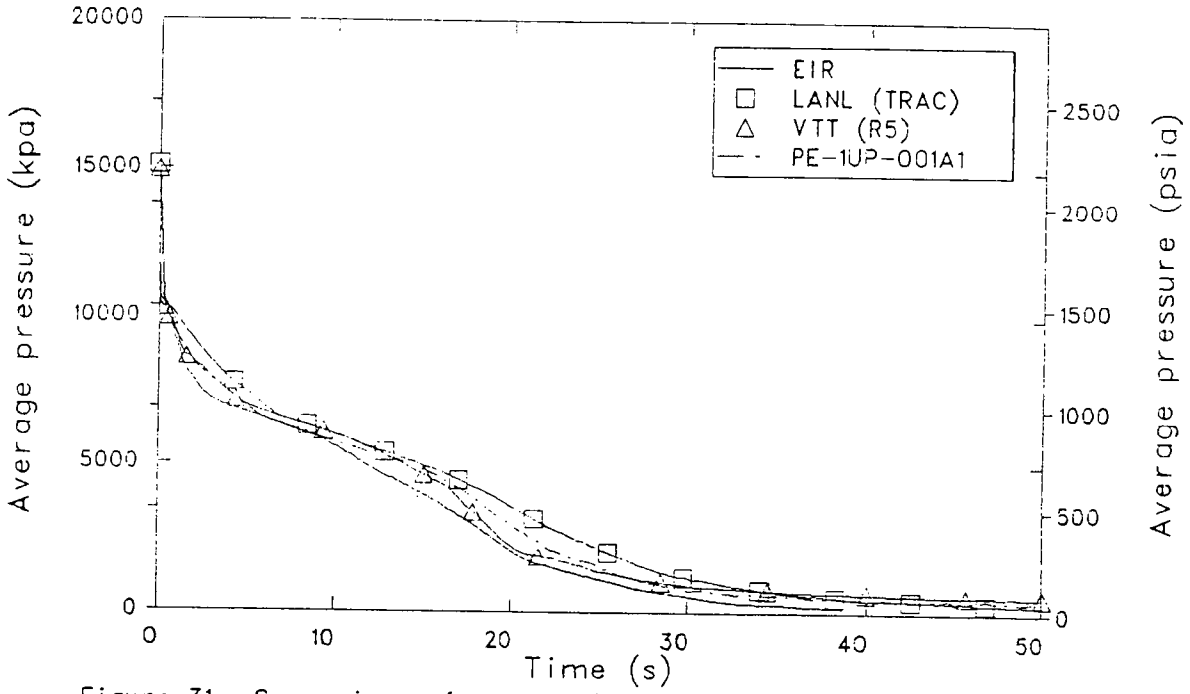

Figure 31. Comparison of measured and calculated upper plenum pressure for the open calculations.

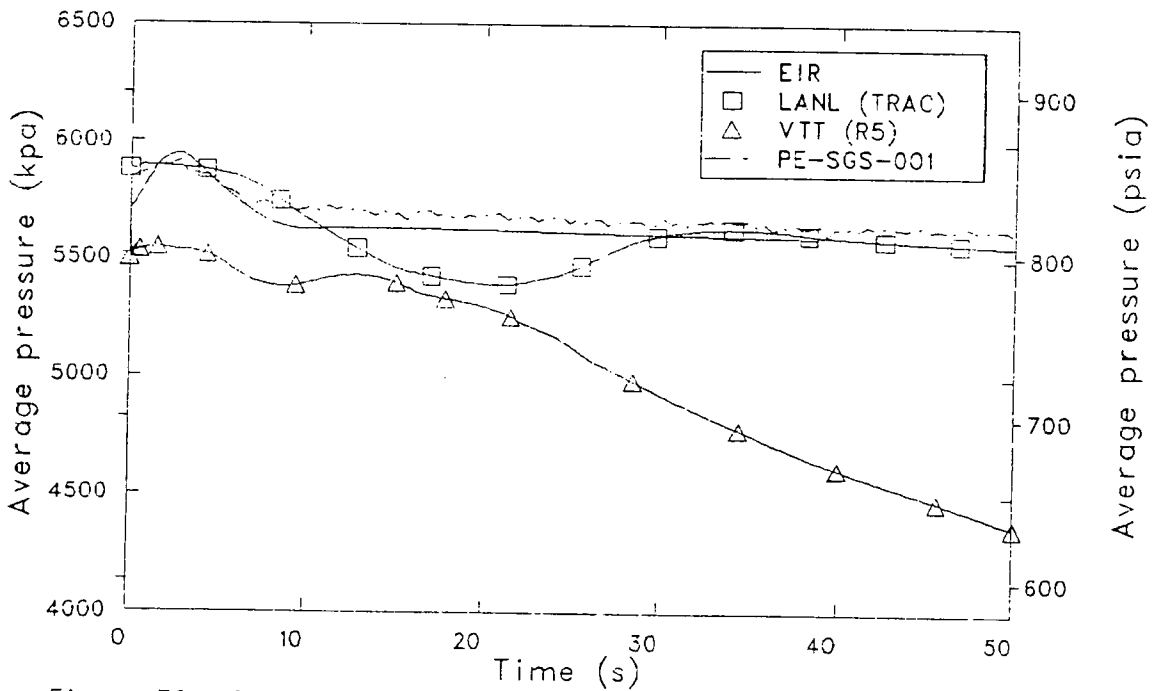

Figure 32. Comparison of measured and calculated steam generator secondary pressure for the open calculations.

5.3 Fluid Temperatures

Upper plenum temperatures are compared to data in Figure 33. For the first 28 s, the submittals showed the same relation to data as did the pressure histories, with EIR and VTT below data, and LANL and DCMN above. In this period, DCMN's RELAP4/MOD6 calculation followed data extremely well. At 28 s both the L2-5 data and EIR's calculation began to register some superheating. Magnitude of this superheat was higher in the calculation than in the data but the shape and trend of the curve was nearly identical.

Comparison of lower plenum and intact loop cold leg temperatures, shown in Figures 34 and 35, again show the same relationship as the pressure histories. EIR and VTT were generally lower than data until 28 s when the cooldown calculated by VTT slowed enough to reverse the trend. LANL's temperatures were higher than data until the 35 to 40 s range when the comparison reversed. DCMN's lower plenum temperature comparison was excellent.

Hot leg temperatures (Figure 36) again showed some superheating in the data. As in the upper plenum, only EIR calculated the superheat but at much higher levels. Both LANL and VTT calculated a cooldown which followed their depressurization histories.

All the open calculations underpredicted the average coolant temperature in the pressurizer shown in Figure 37. Secondary temperatures compared in Figure 38 show better results. The VTT calculation's secondary cooldown followed the depressurization previously mentioned in Section 5.2. The remaining two calculations stabilized by 15 s and remained constant, with LANL calculating an average temperature nearly identical to data.

5.4 Fluid Densities

The measured density and the calculated average density in the intact loop cold leg is shown in Figure 39. The calculations all showed the cold leg voiding with subsequent slug behavior later in the transient. The time

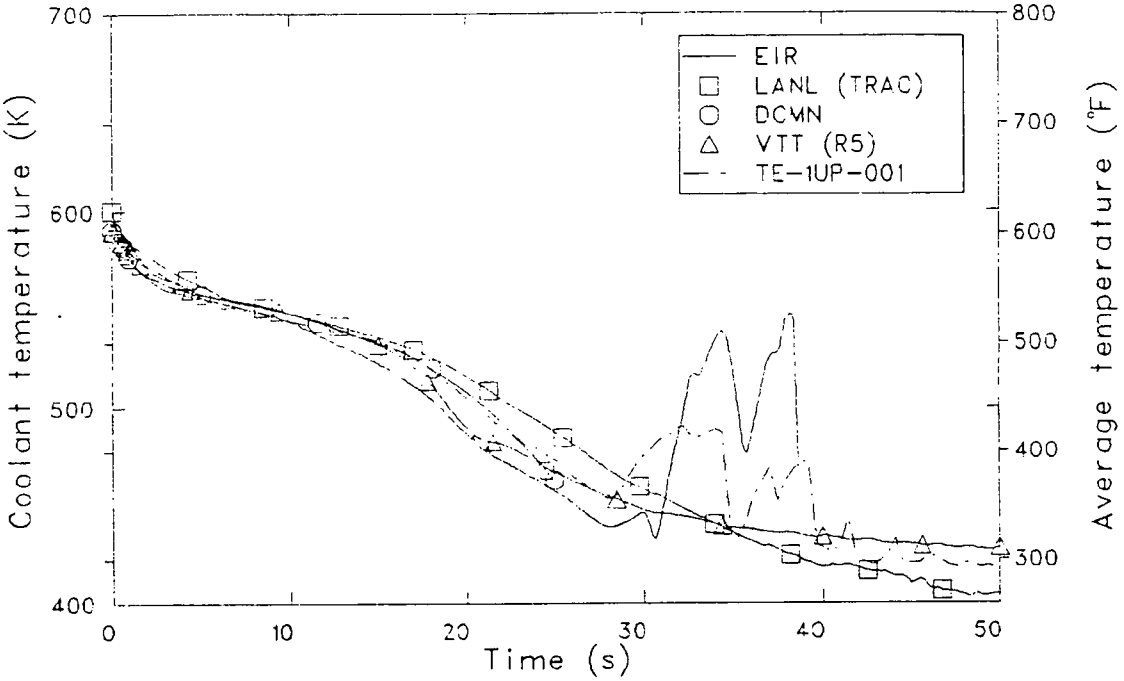

Figure 33. Comparison of measured and calculated upper plenum fluid temperature for the open calculations.

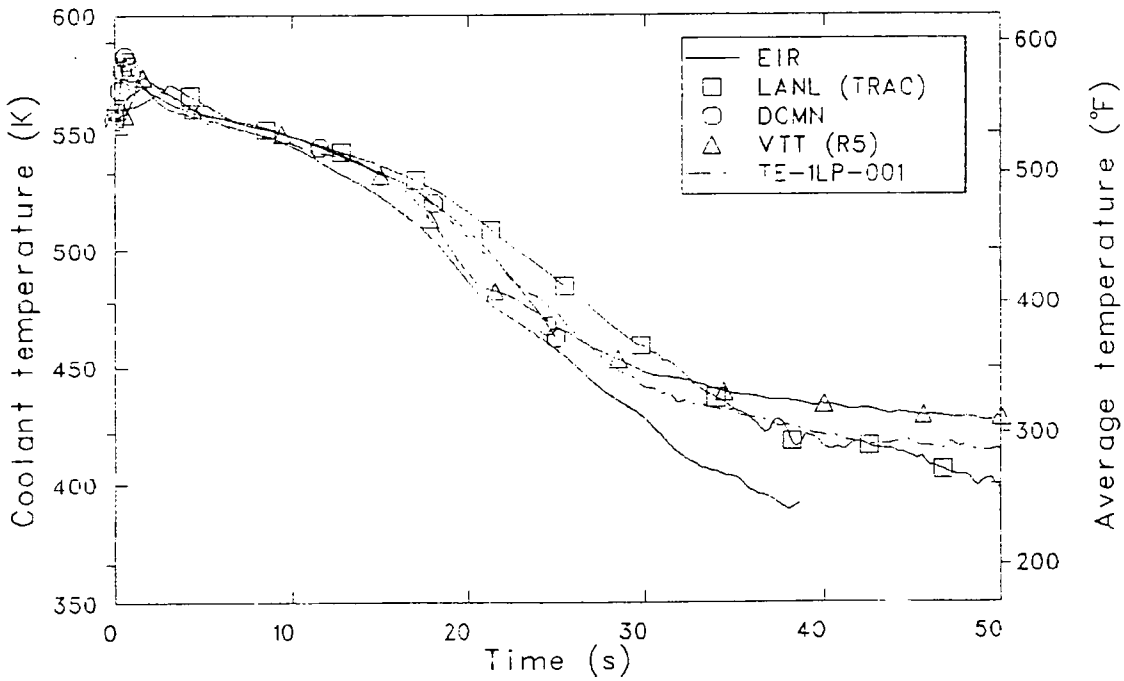

Figure 34. Comparison of measured and calculated lower plenum fluid temperature for the open calculations.

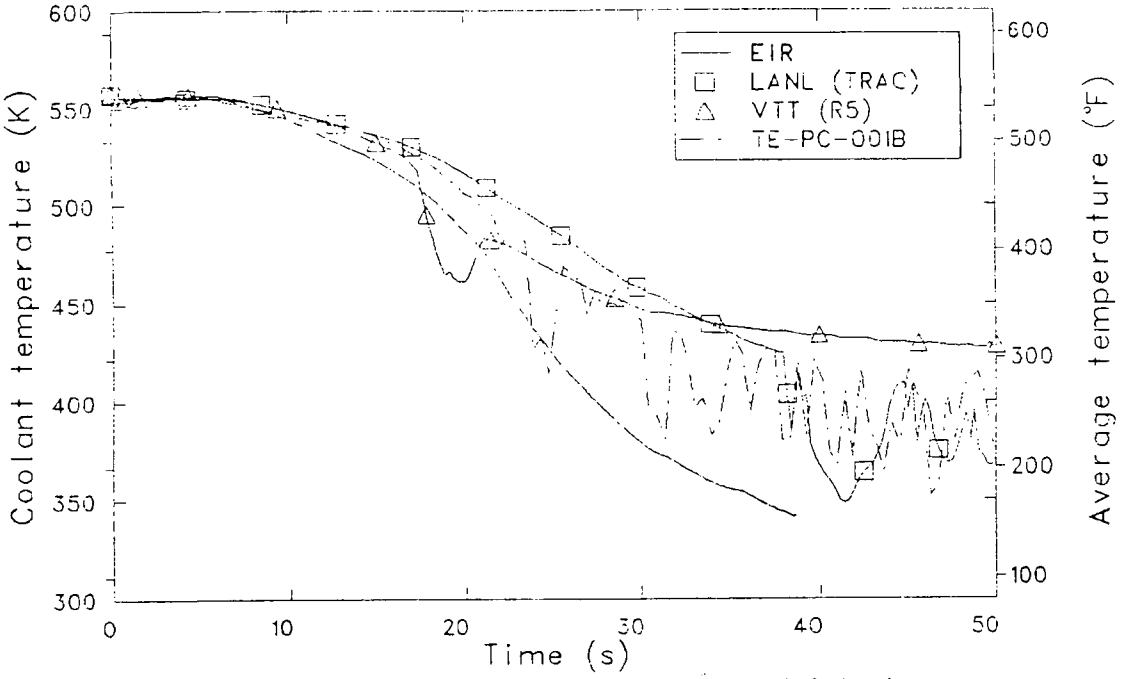

Figure 35. Comparison of measured and calculated intact loop cold leg temperature for the open calculations.

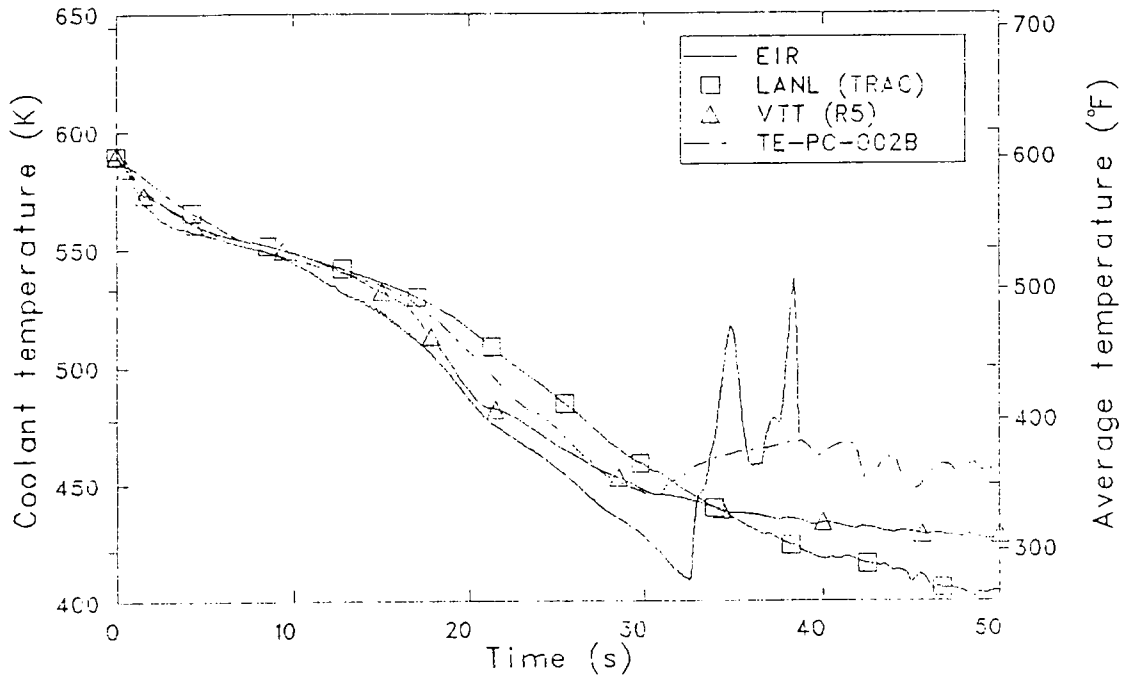

Figure 36. Comparison of measured and calculated intact loop hot leg temperaure for the open calculations.

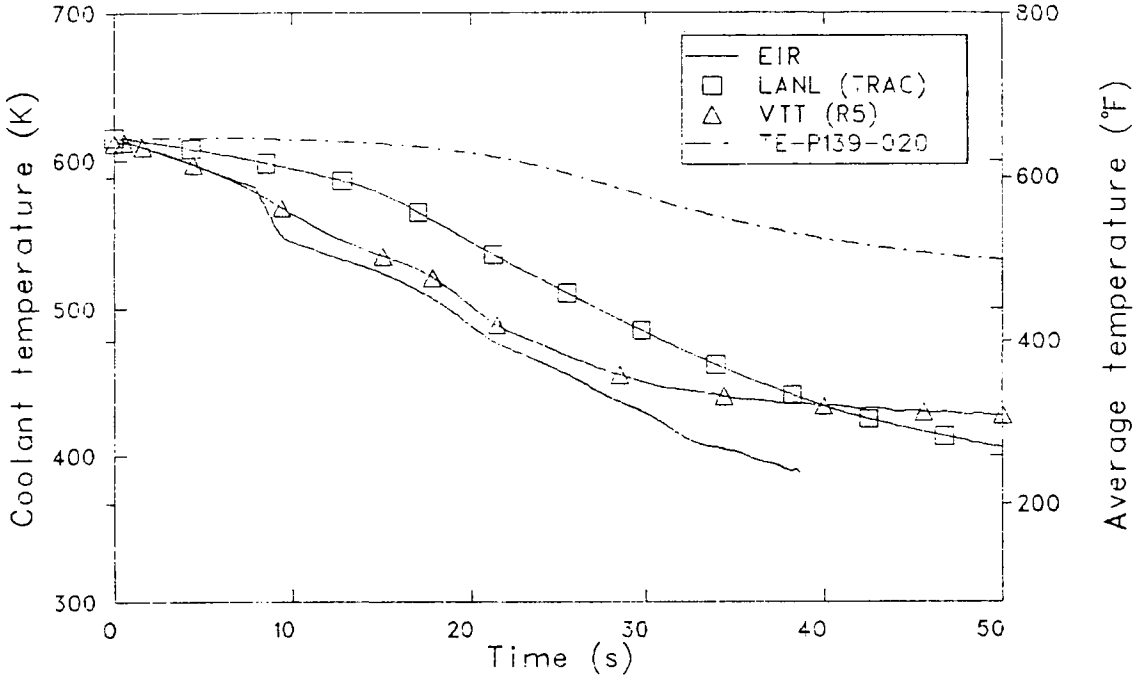

Figure 37. Comparison of measured and calculated pressurizer temperature for the open calculations.

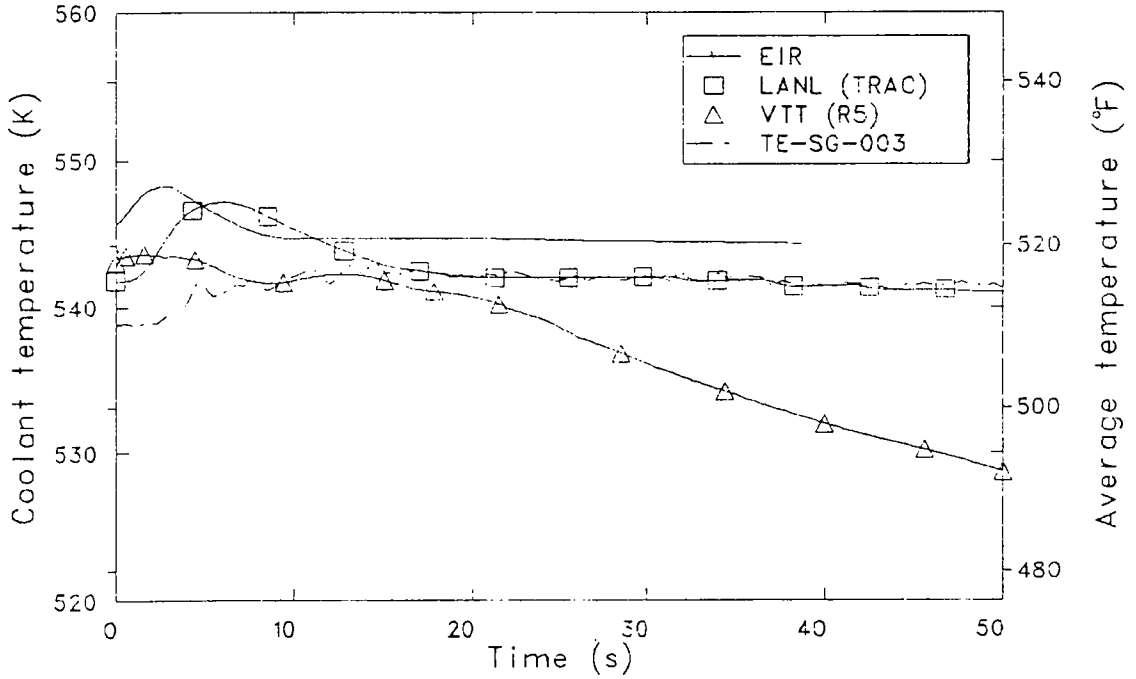

Figure 38. Comparison of measured and calculated steam generator secondary temperature for the open calculations.

the slug flow began varied from 16 s (VTT) to 39 s (LANL). The oscillations calculated by VTT were much less severe than those seen in the experiment and those calculated by other open participants.

Figure 40 compares the calculated average density in the intact loop hot leg with the density seen in the data. All calculations showed similar results with the hot legs simply voiding during the transient. The agreement with data was good for all the calculations.

The comparisons of calculated and measured densities in the broken loop are shown in Figures 41 and 42. All open calculations showed a slower voiding in the cold leg than data for the first 20 s. Both EIR and LANL calculated major slug flow through the cold leg at different times in the transient, but this phenomenon was not observed in the data. In the broken loop hot leg, the calculations showed a faster voiding than was observed in the test for the first 20 s. After this point, all submittals remained voided with the exception of the VTT calculation which experienced slug flow after 44 s.

5.5 Mass Flow

A comparison of calculated core inlet flows is shown in Figure 43. The reverse flow peak, characteristic of a cold leg rupture, was calculated to be much more severe by EIR than either LANL or VTT. However, by 10 s, all calculated flow had essentially stagnated.

One of the most critical comparisons was that of calculated break flow with data and is shown in Figures 44 and 45. These results reflected the various break flow models used by the participants. After 3 s, all of the participants overpredicted cold leg break flow. LANL underpredicted the peak flow in the first 0.5 s, while DCMN and EIR overpredicted the peak by 50 to 70%. VTT nearly matched the initial peak, earlier than data, then underpredicts the flow until 3 s. In the hot leg, VTT overpredicted the flow significantly, as did DCMN. EIR underpredicted the flow, while LANL followed the hot leg flow history reasonably well. However, the bottom

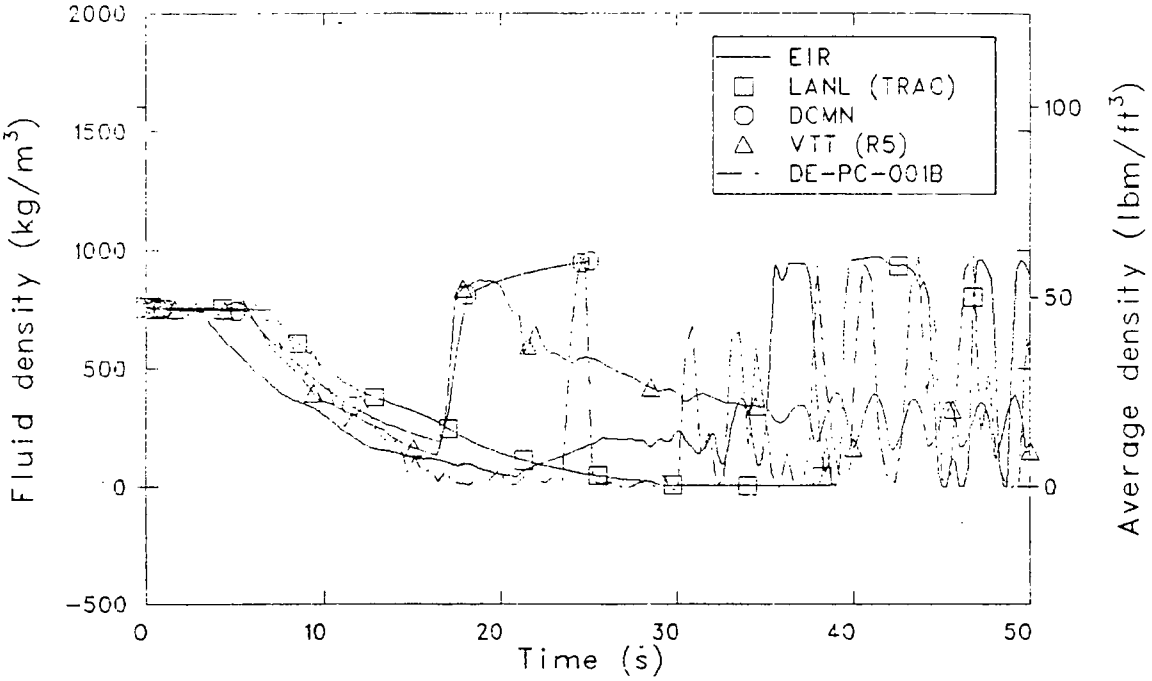

Figure 39. Comparison of measured and calculated intact loop cold leg density for the open calculations.

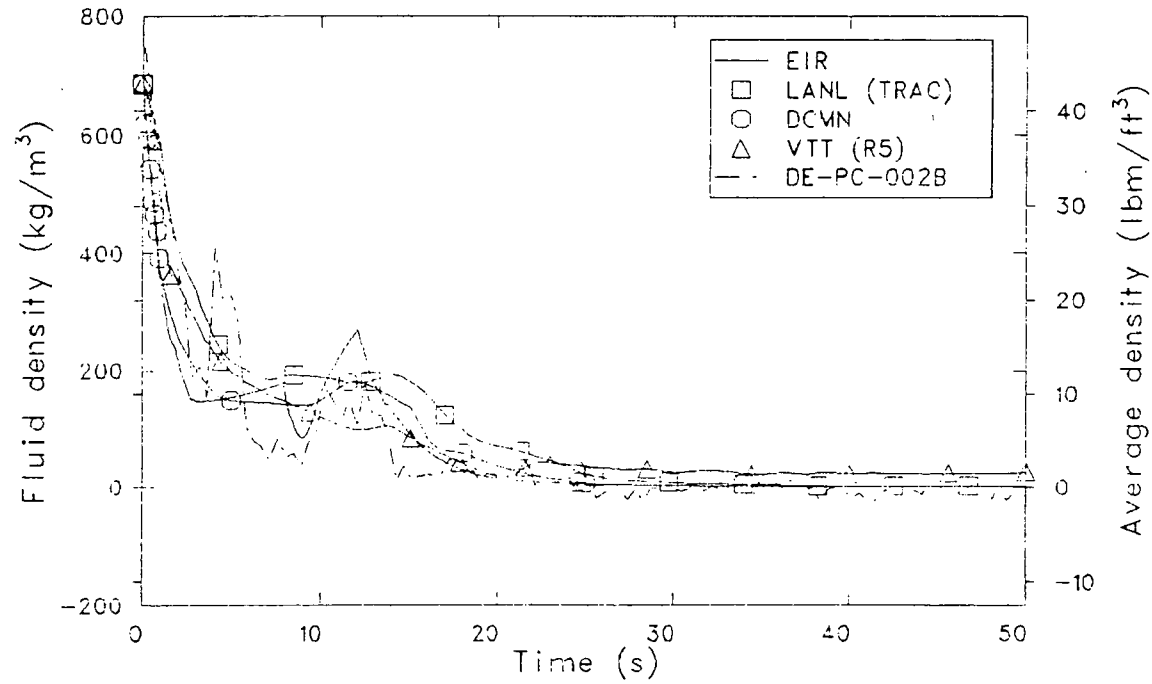

Figure 40. Comparison of measured and calculated intact loop hot leg density for the open calculations.

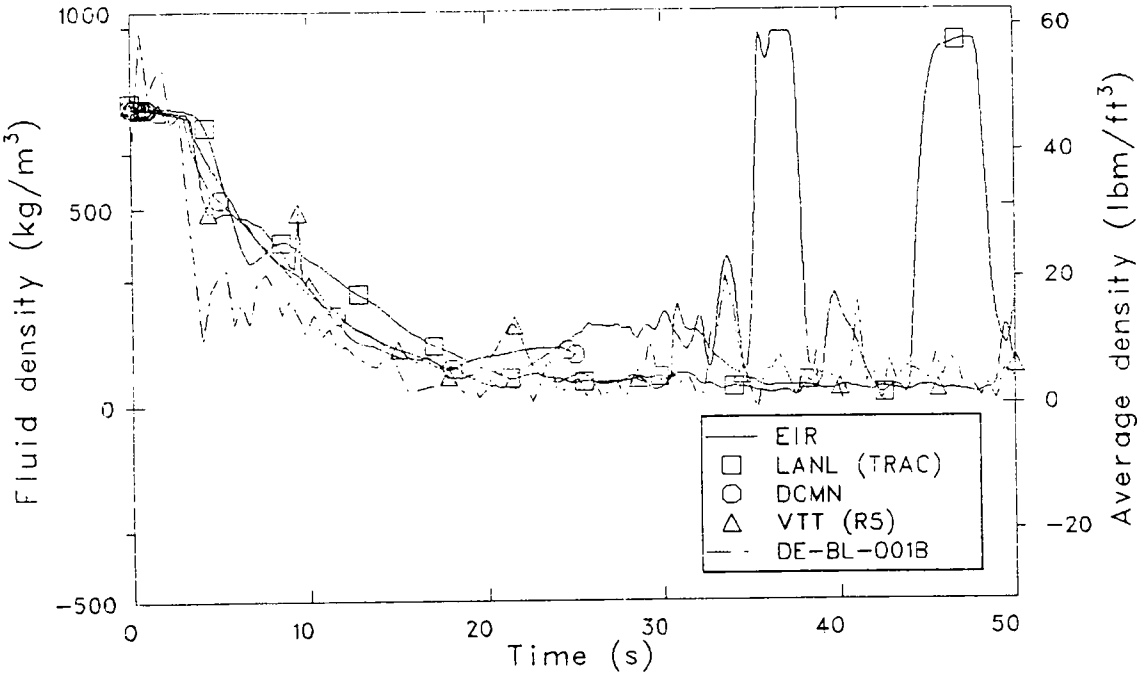

Figure 41. Comparison of measured and calculated broken loop cold leg density for the open calculations.

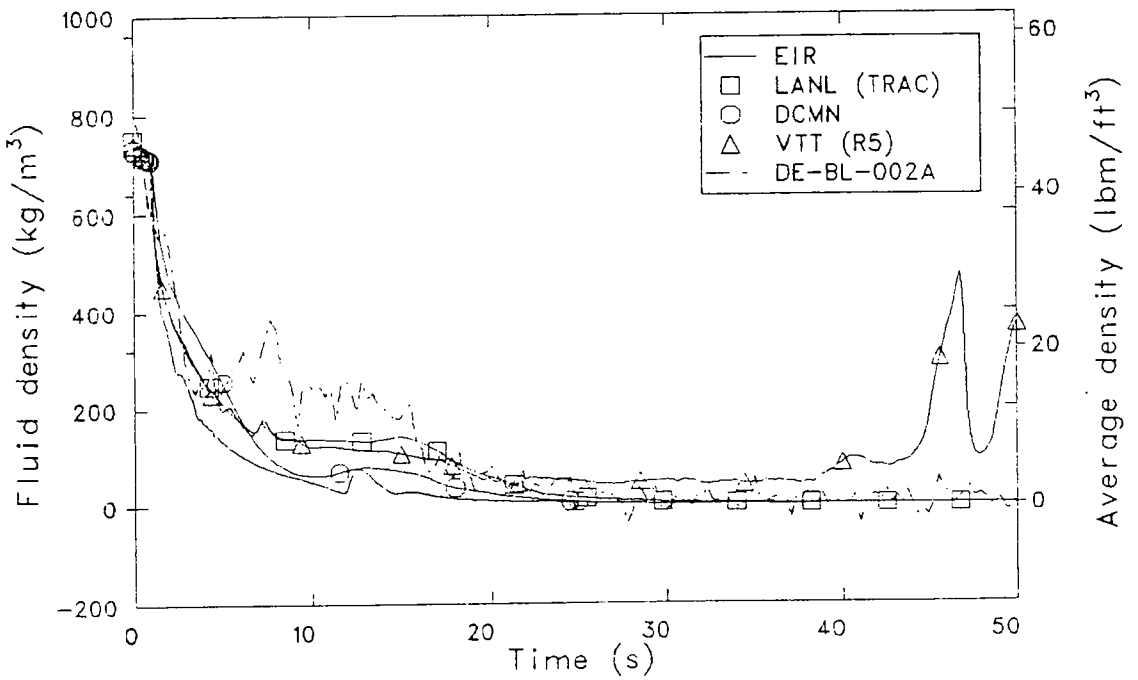

Figure 42. Comparison of measured and calculated broken loop hot leg density for the open calculations.

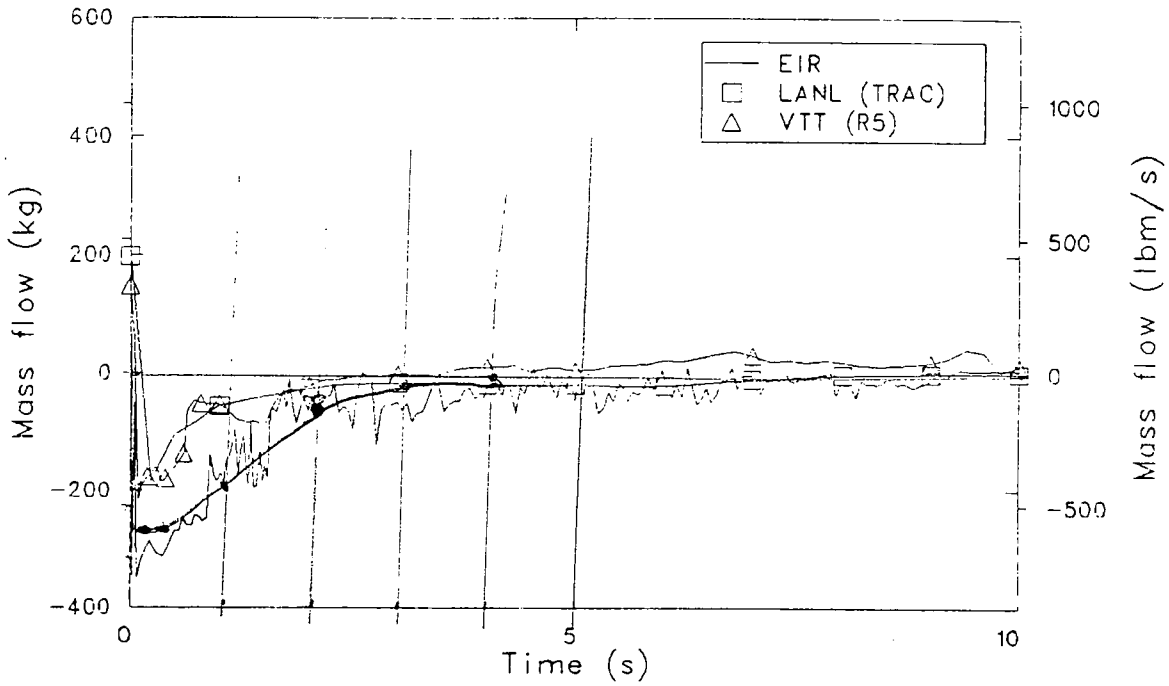

Figure 43. Comparison of calculated core inlet flows for the open calculations.

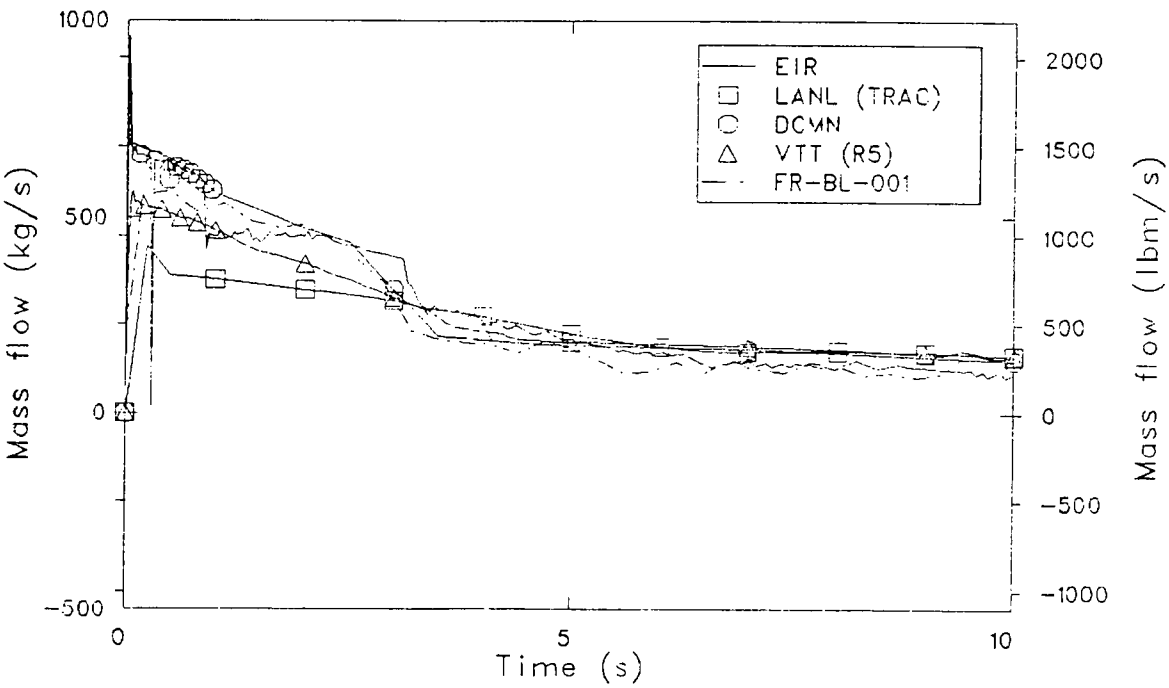

Figure 44. Comparison of measured and calculated broken loop cold leg break mass flow rate for the open calculations.

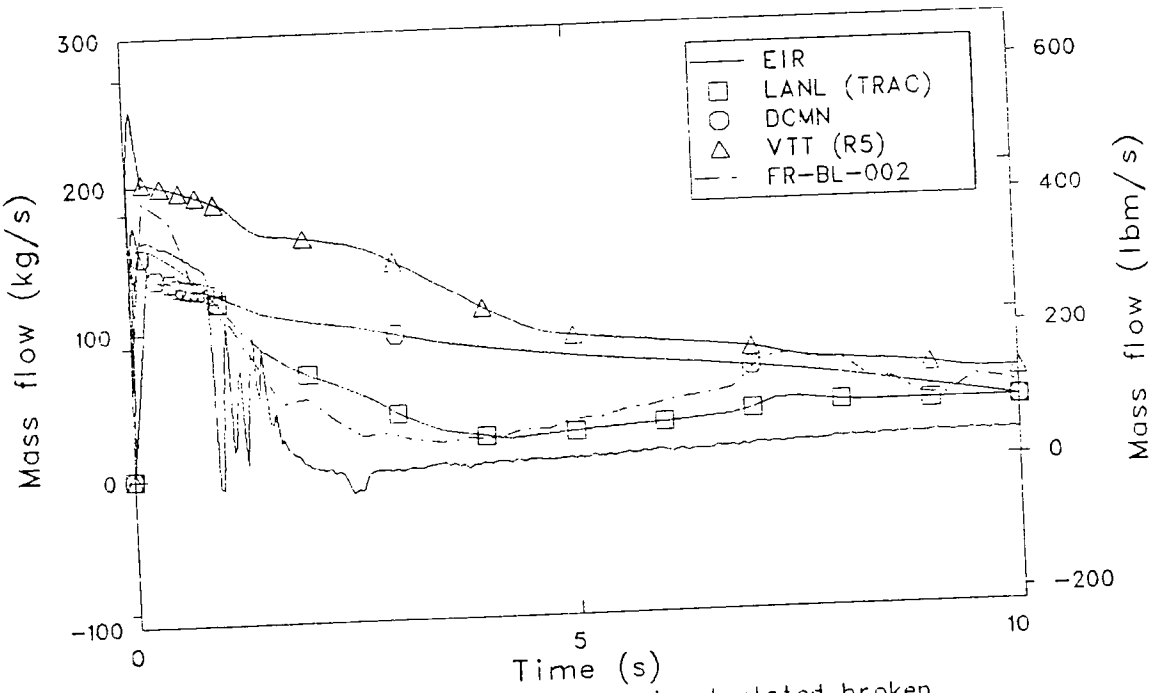

Figure 45. Comparison of measured and calculated broken loop hot leg break mass flow rate for the open calculations.

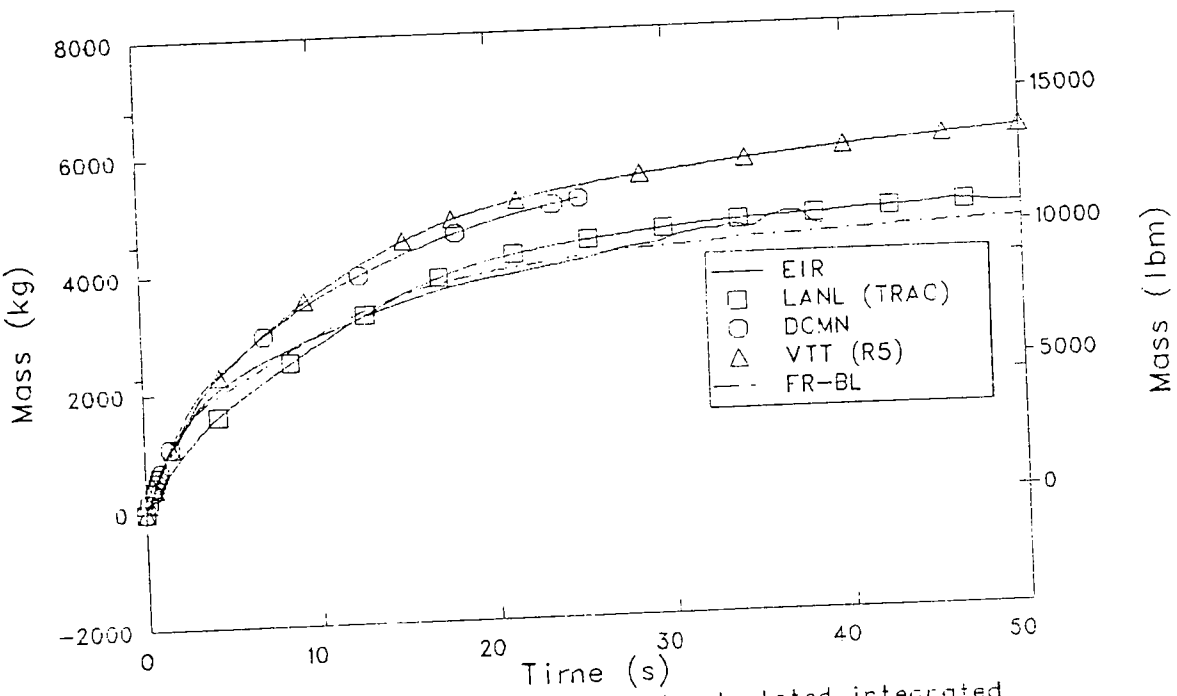

Figure 46. Comparison of measured and calculated integrated break flow for the open calculations.

line, mass lost from the system in Figure 46, showed that EIR came closest to correctly calculating the total mass lost while LANL, DCMN, and VTT overpredicted the event.

A comparison of calculated reactor vessel mass inventories is shown in Figure 47. EIR's initial mass inventory, was significantly lower than LANL or VTT, and all calculations showed differences in final mass inventories. Neither EIR or VTT showed an inventory turnaround or refill while the LANL TRAC calculation began to increase at 20 s.

Emergency core coolant flows are compared to data in Figures 48 and 49. EIR calculated an earlier HPI initiation than the other participants, but the significant difference was LANL's flow rate, approximately two times higher than the data or the other calculations. This high flow was probably a factor in the fast turnaround of LANL's vessel inventory previously mentioned. LPI flow comparisons showed EIR again preceding all calculations, as well as data.

5.6 Pump Speed

Measured and calculated pump speed is presented in Figure 50. Apart from the initial value discrepancy, there were no major problems with any of the submittals.

5.7 Rod Temperatures

Rod cladding temperatures are shown in Figures 51 and 52, at 0.76 m (30 in.) and 0.99 m (39 in.) respectively. As with the blind calculations, the significance of these curves was questionable due to the various modeling approaches to core cladding heat slabs. At the 0.76 m level, VTT's peak temperature at 5.2 s was close to the peak reached in the actual test but the cladding cooled off significantly from that point. Neither EIR or LANL reached the data peak, although the relatively stable high temperature history seen by LANL is more characteristic of data. At the 0.99 m elevation, data showed two major quenches, at 15 s and 46 s. VTT's calculation showed a earlier downturn from 5 to 10 s, then stayed relatively low. LANL, EIR, and DCMN did not display the characteristic quench behavior at all.

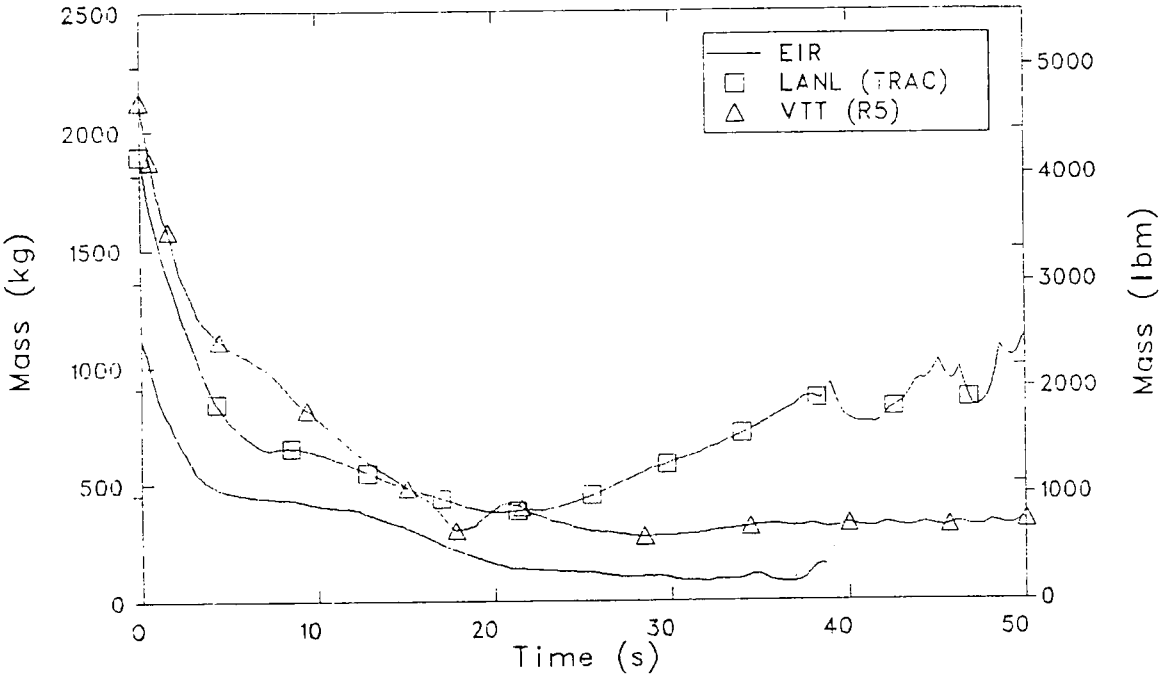

Figure 47. Comparison of calculated reactor vessel mass inventory for the open calculations.

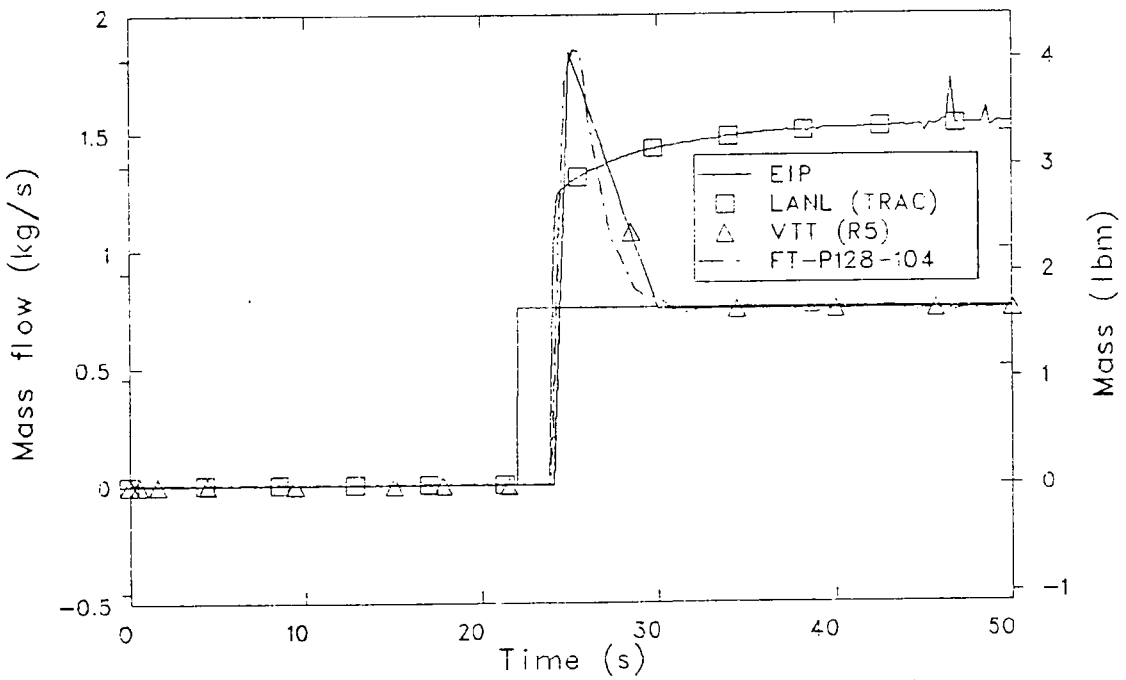

Figure 48. Comparison of measured and calculated HPIS flow for the open calculations.

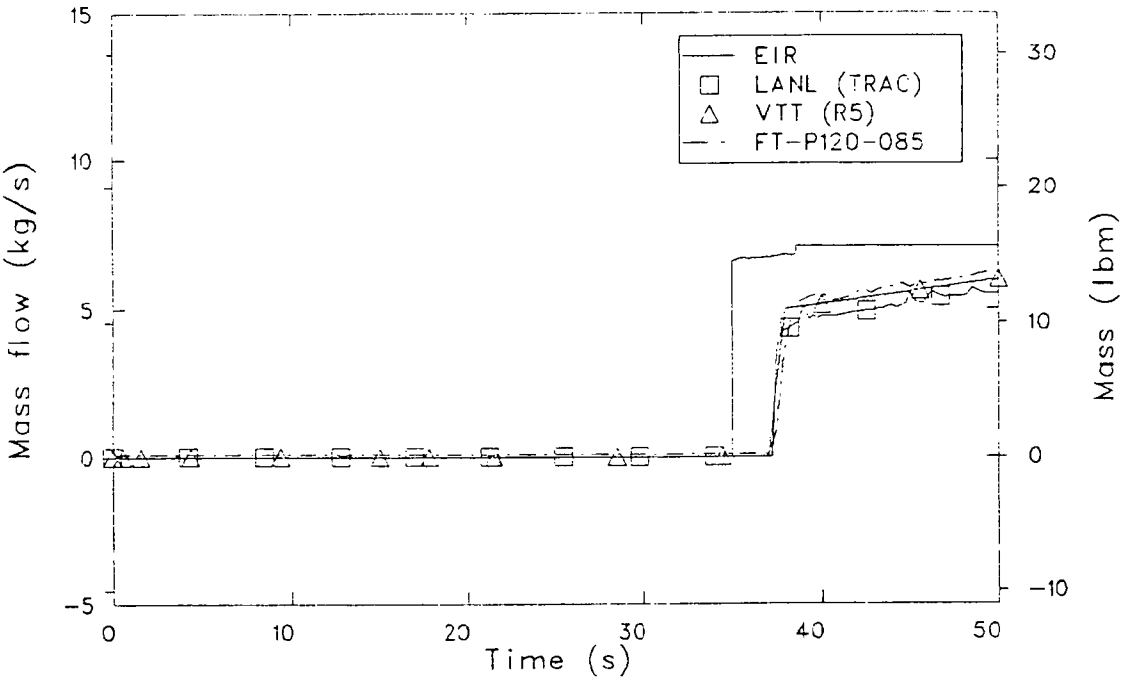

Figure 49. Comparison of measured and calculated LPIS flow for the open calculations.

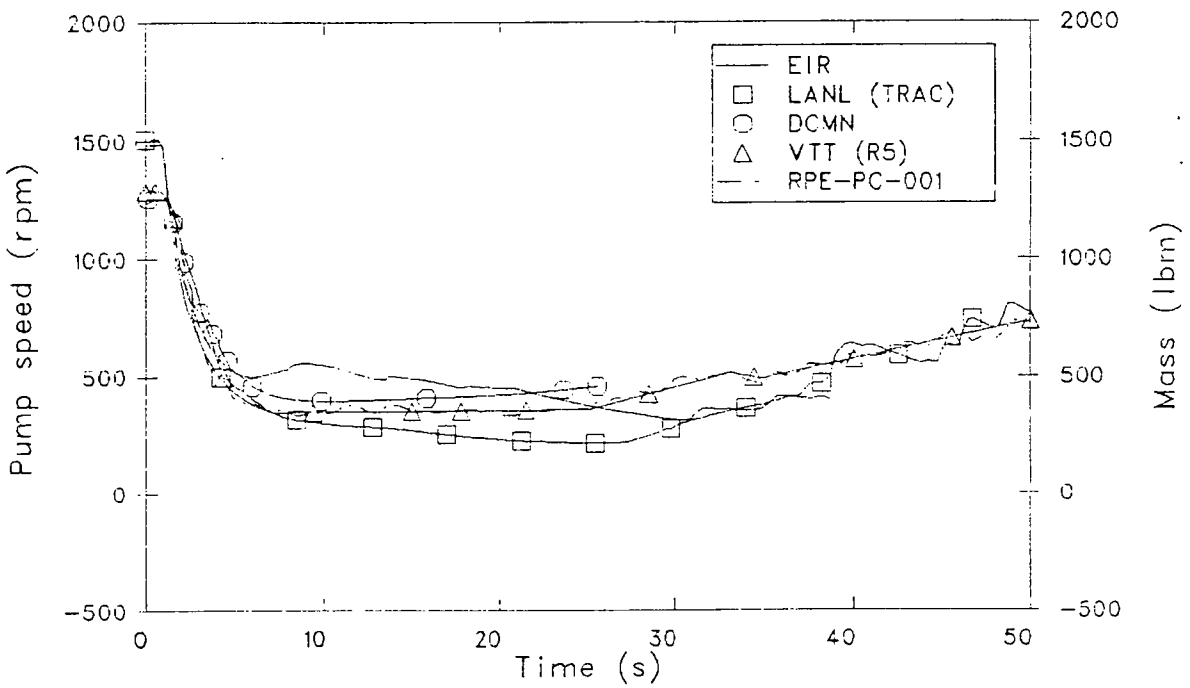

Figure 50. Comparison of measured and calculated reactor coolant pump speed for the open calculations.

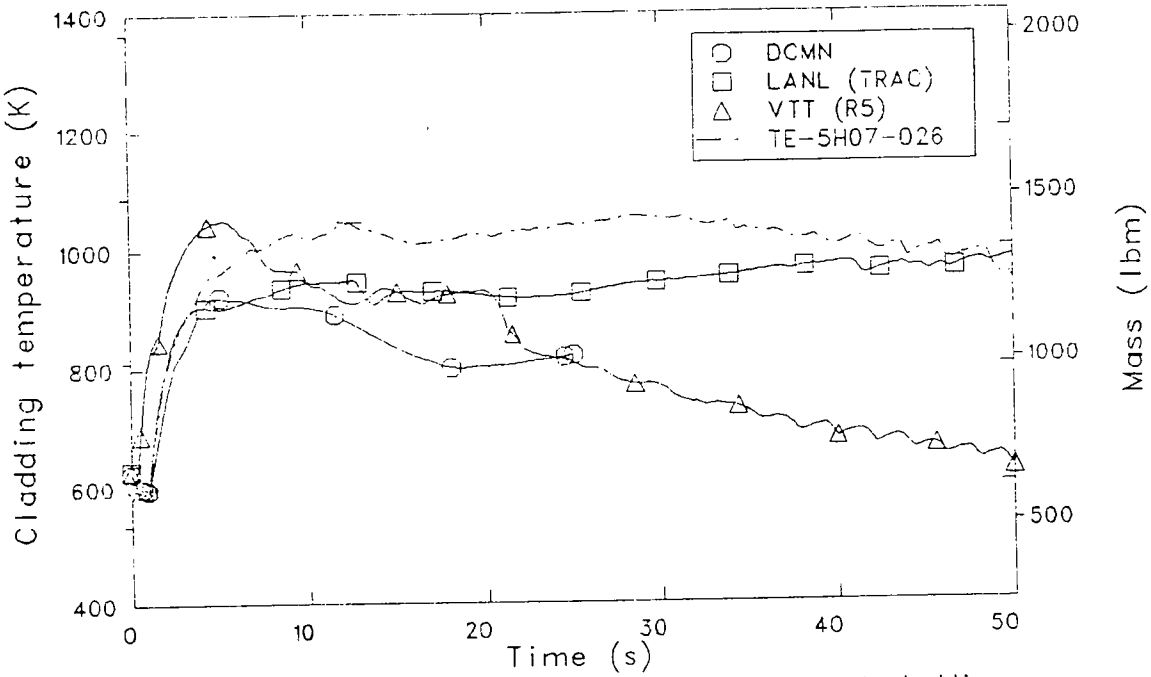

Figure 51. Comparison of measured and calculated rod cladding temperature at the 0.76m elevation for the open calculations.

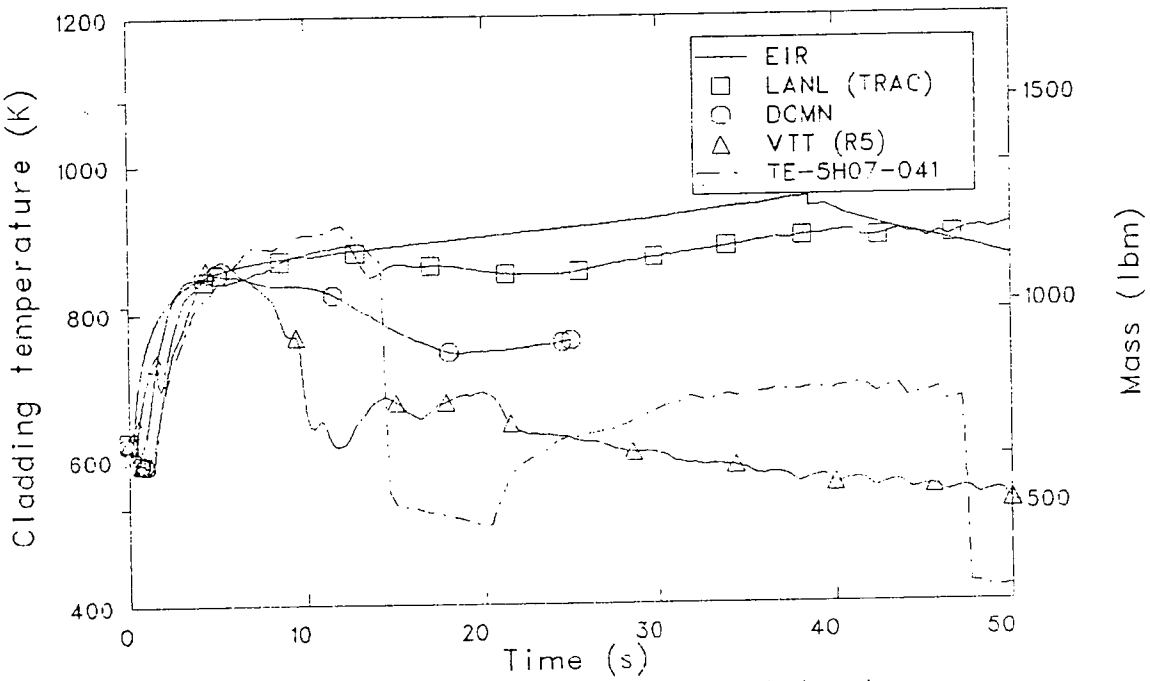

Figure 52. Comparison of measured and calculated rod cladding temperature at the .99m elevation for the open calculations.

5.8 Summary

In summary, as with the blind calculations the open submittals performed well in calculating the hydraulic responce of the LOFT system. Pressure-temperature histories were somewhat closer to data than the majority of the blind calculations. As before, subcooling and superheat accounted for the main discrepancies. Slug flow behavior in the intact loop cold leg was handled better in the open calculations than the blind submittals, however, this slug flow appeared in the broken loop differing from data. Break flow was overpredicted by everyone except EIR. ECC flow was calculated adequately except by LANL. Rod temperatures was again quite model dependant and, while heatups were calculated adequately quenches were less adequately predicted.

6. CONCLUSIONS AND RECOMMENDATIONS

Comparison of the calculated results with L2-5 data have led to the following conclusions.

Hydraulic parameters, such as depressurization rate and fluid temperatures were calculated well by most participants. Comparisons began to experience difficulties when voiding and superheating occurred. (Sections 4.2, 4.3, 5.2, 5.3)

Densities in the hot legs of the facility were calculated correctly, but the densities in the cold leg, which experienced cold ECC flow, were less well predicted. (Sections 4.4, 5.4)

Break flow was overpredicted by nearly all participants with particular problems encountered in flow from the broken loop hot leg. (Sections 4.5, 5.5)

Good comparison of clad temperatures with data was hampered by the variety of core heat slab models used. In general, participants calculated the heat up of clad surfaces adequately and predicted the clad quenches less well. (Sections 4.7, 5.7)

It is recommended that all participants review the comparisons and provide comments on their particular calculations. This will provide a better understanding of the models and codes used for the benefit of all ISP-13 participants. These comments may be mailed to the author of this report or provided at the meeting, tentatively scheduled for July 1983.

7. REFERENCES

1. P. D. Bayless and J. M. Divine, Experiment Data Report for LOFT Large Break Loss-of-Coolant Experiment L2-5, NUREG/CR-2826, EGG-2210, August 1982.

2. D. L. Reeder, LOFT System and Test Description (5.5 ft Nuclear Core 1 LOCEs), NUREG/CR-0247, TREE-1208, July 1978.

APPENDIX A
PARTICIPANT NODALIZATION DIAGRAMS

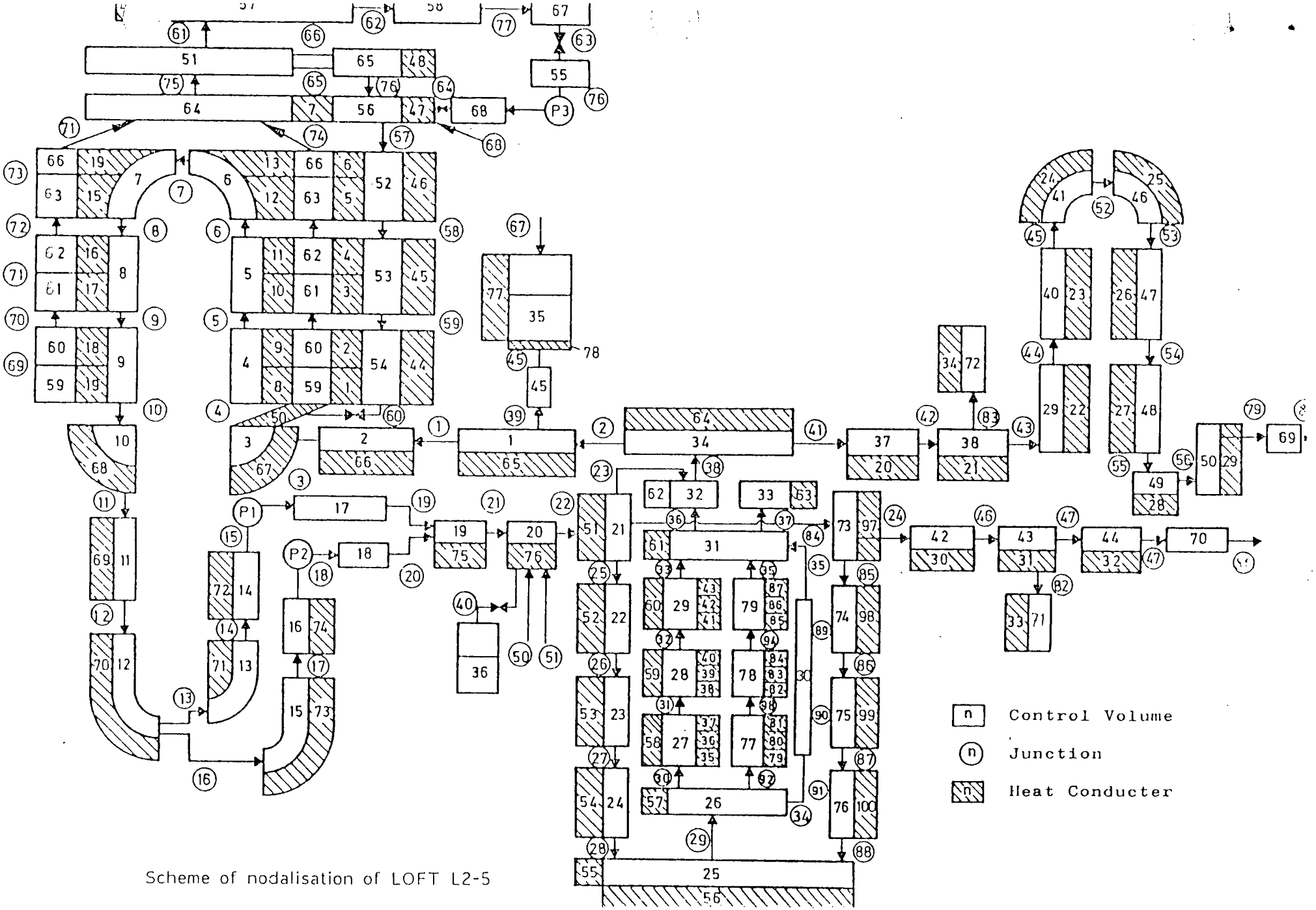

Scheme of nodalisation of LOFT L2-5

Figure A-1. ISP-13 DRUFAN nodalization for the GRS blind calculation.

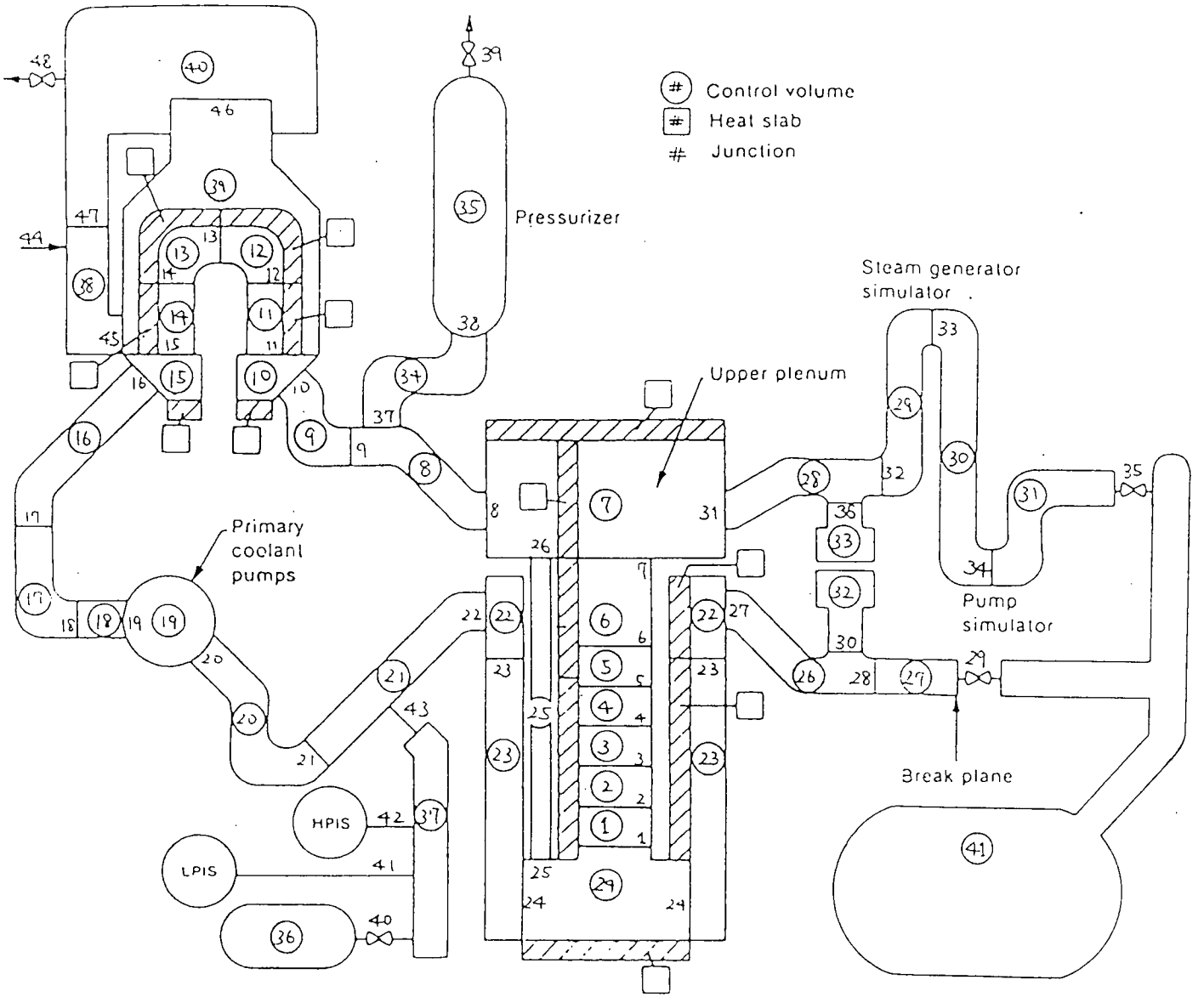

Figure A-2. ISP-13 ISP-13 RELAP4/MOD6 nodalization for the JAR blind calculation.

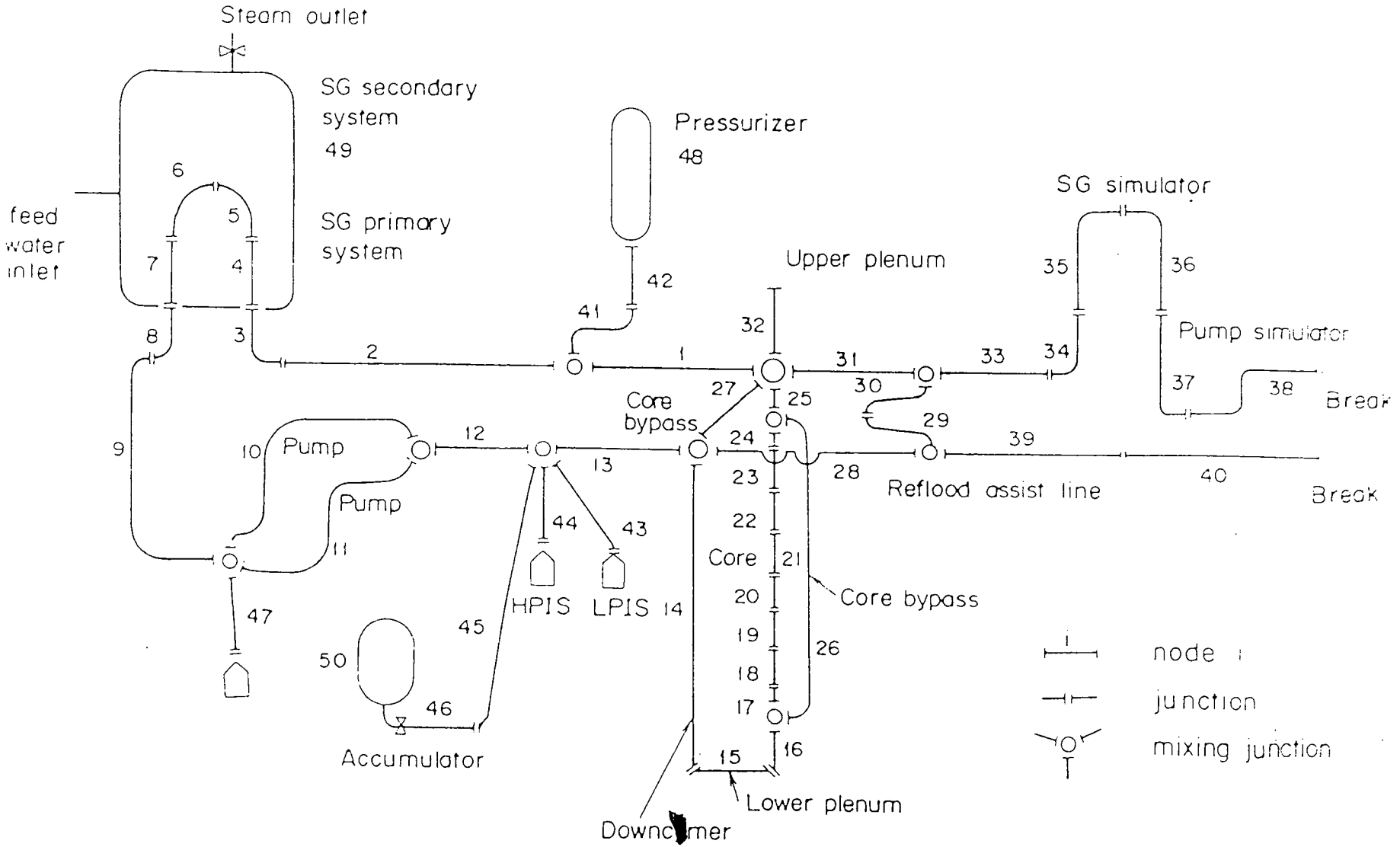

Figure A-3. ISP-13 THYDE-P1 nodalization for the JAT blind calculation.

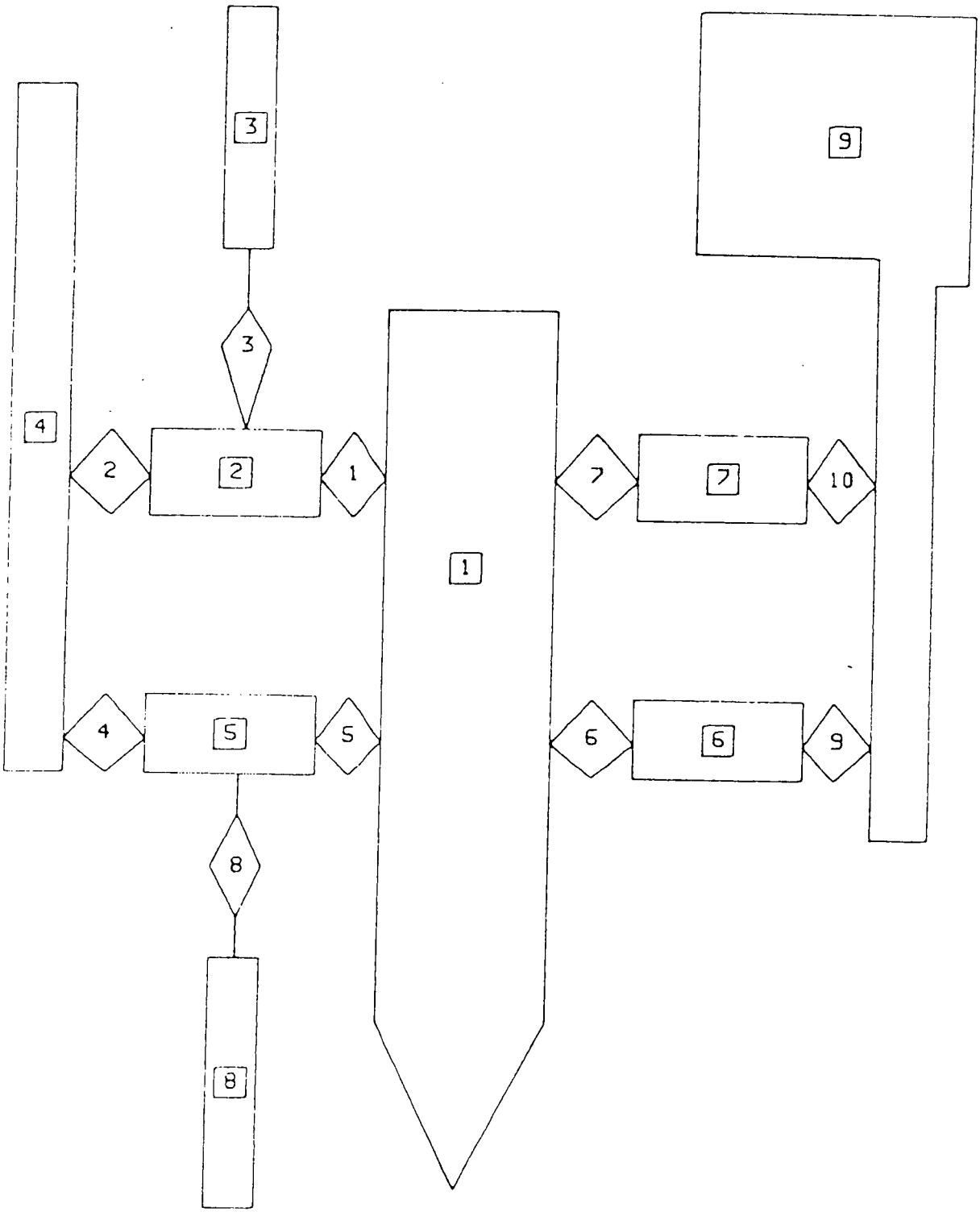

Figure A-4a. ISP-13 RELAP4/MOD6 nodalization for the CERL blind calculation - system components.

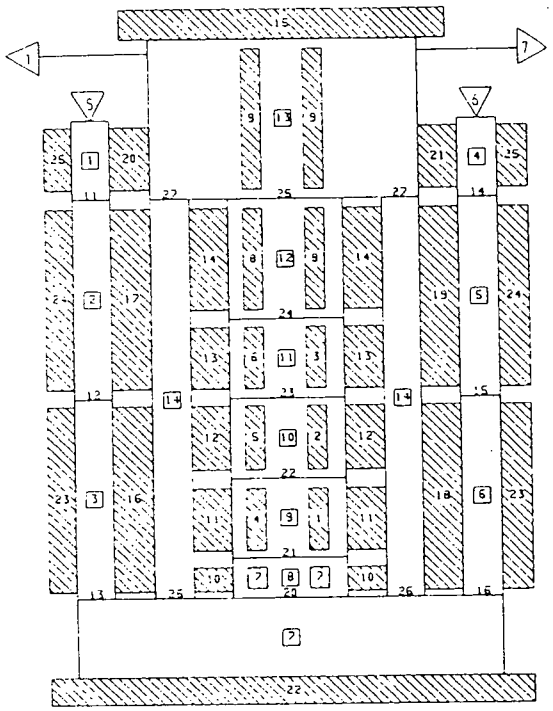

Component 1. Reactor Pressure Vessel.

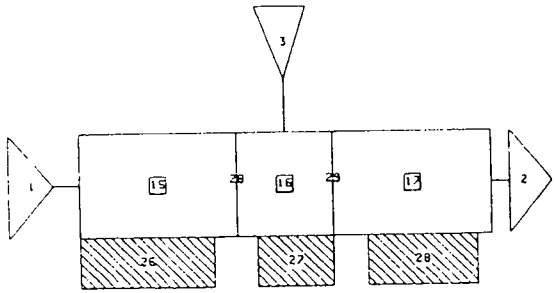

Component 2. Intact Loop Hot Leg.

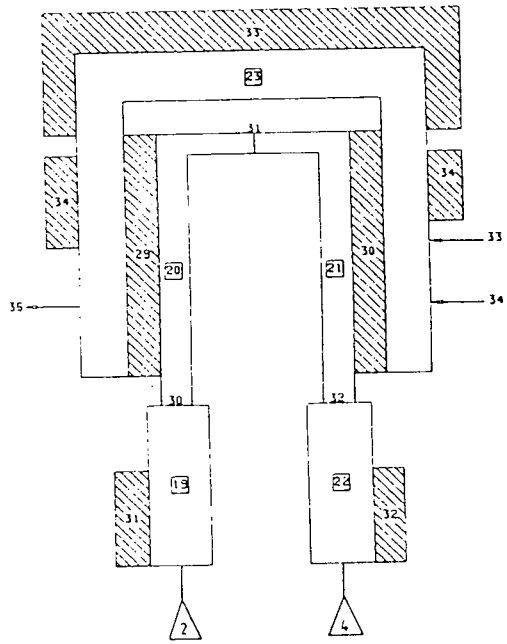

Component 4. Steam Generator.

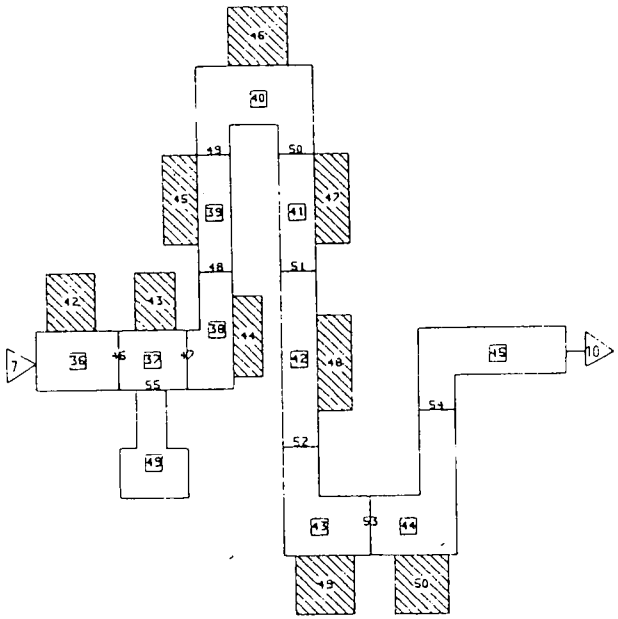

Component 7. Broken Loop Hot Leg.

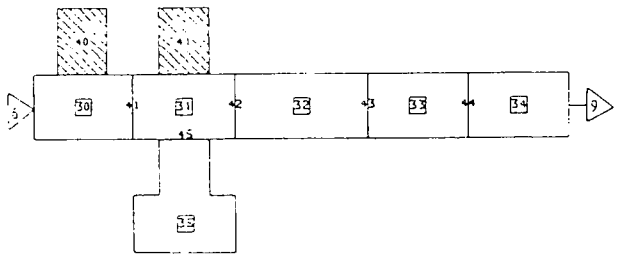

Component 6. Broken Loop Cold Leg.

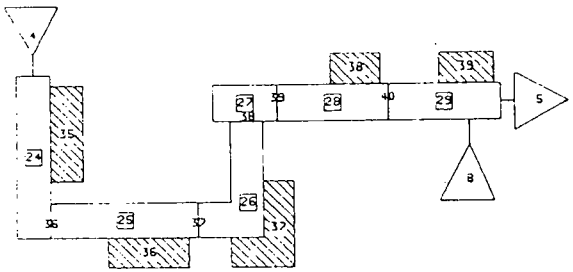

Component 5. Intact Loop Cold Leg.

Figure A-4b. ISP-13 RELAP4/MOD6 nodalization for the CERL blind calculation - component detail.

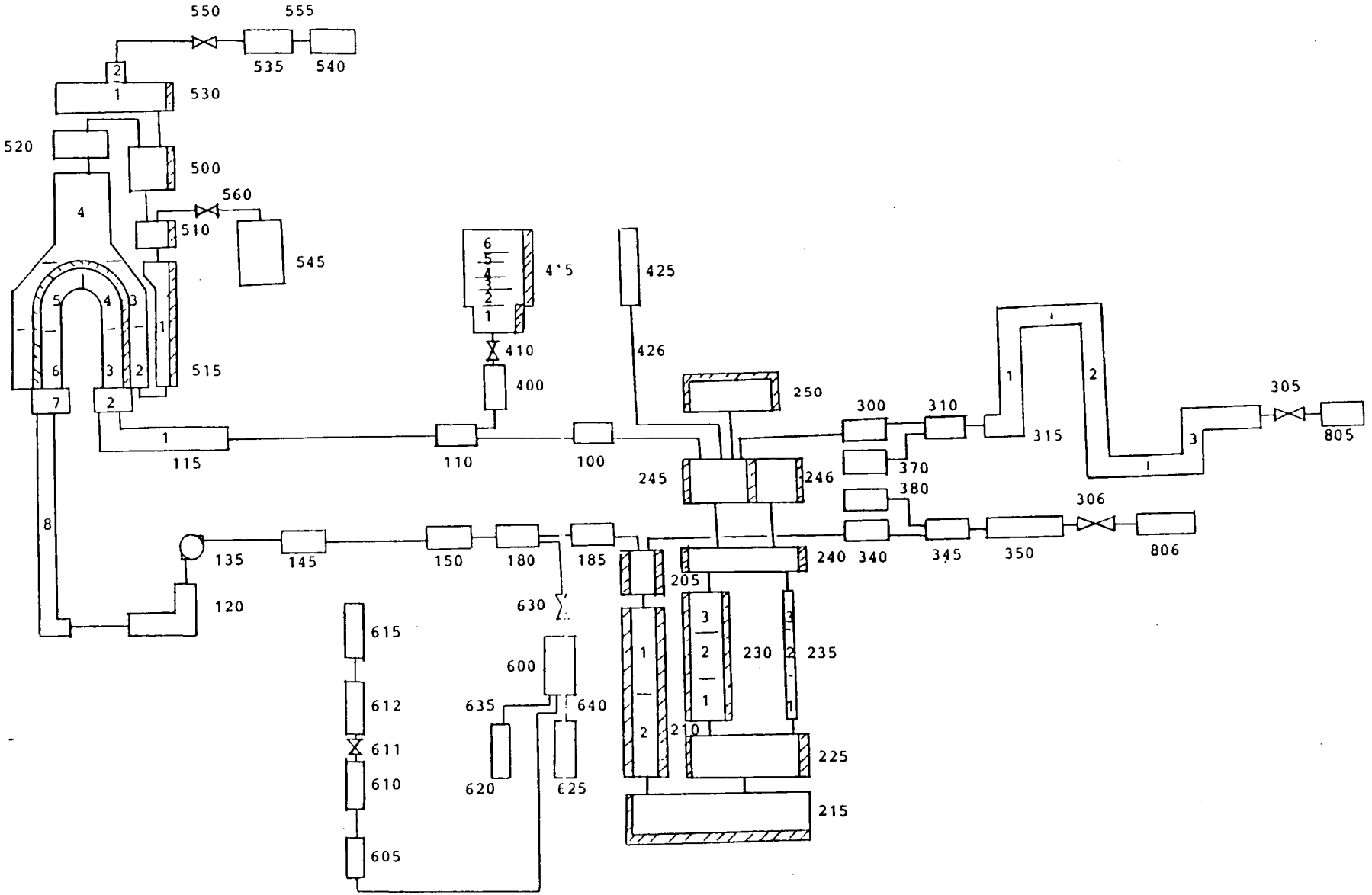

Figure A-5. ISP-13 RELAP5/MOD1 nodalization for the STUD blind calculation.

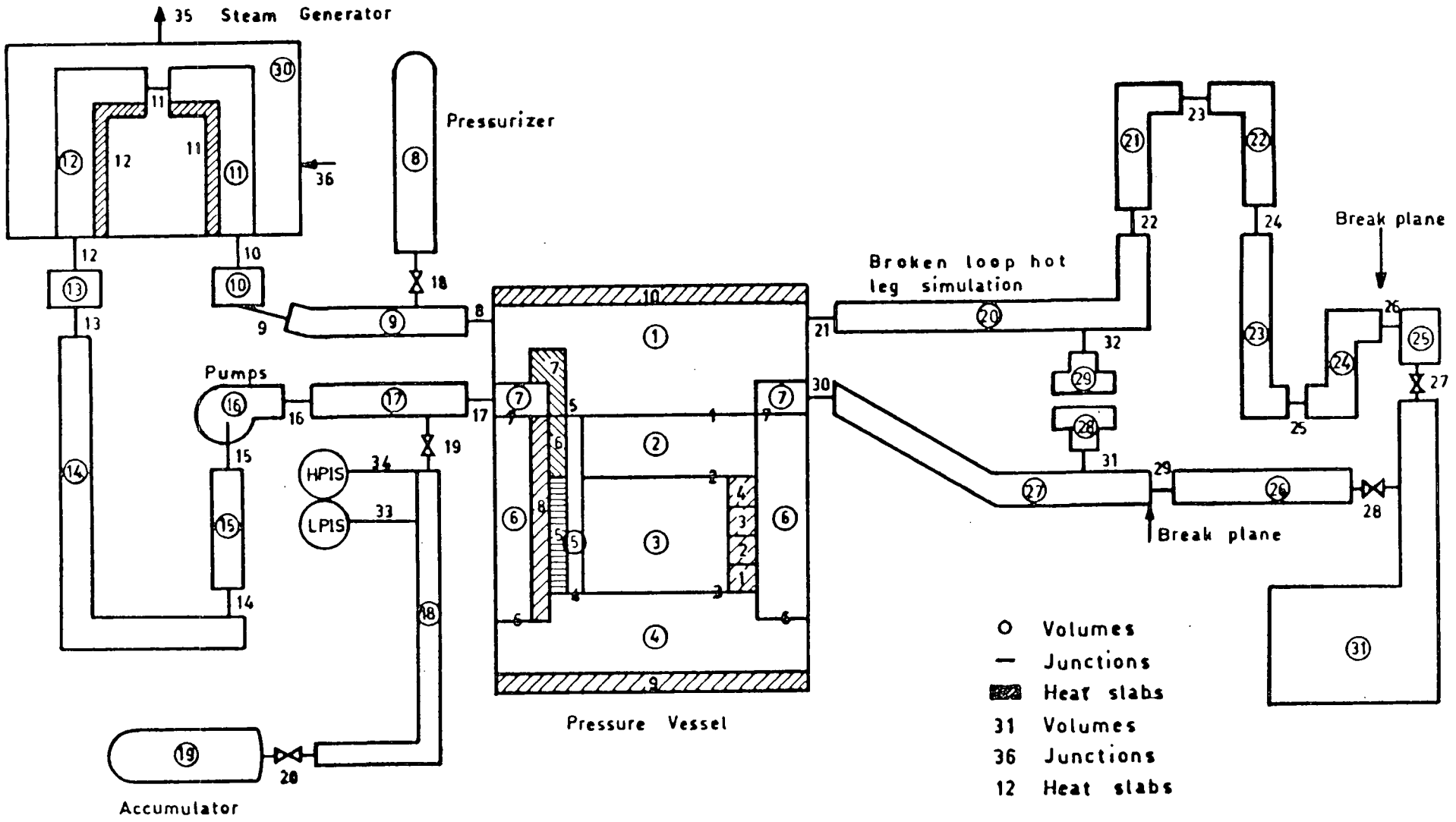

Figure A-6. ISP-13 RELAP4/MOD6 nodalization for the EIR blind calculation.

ATTACHMENT 1

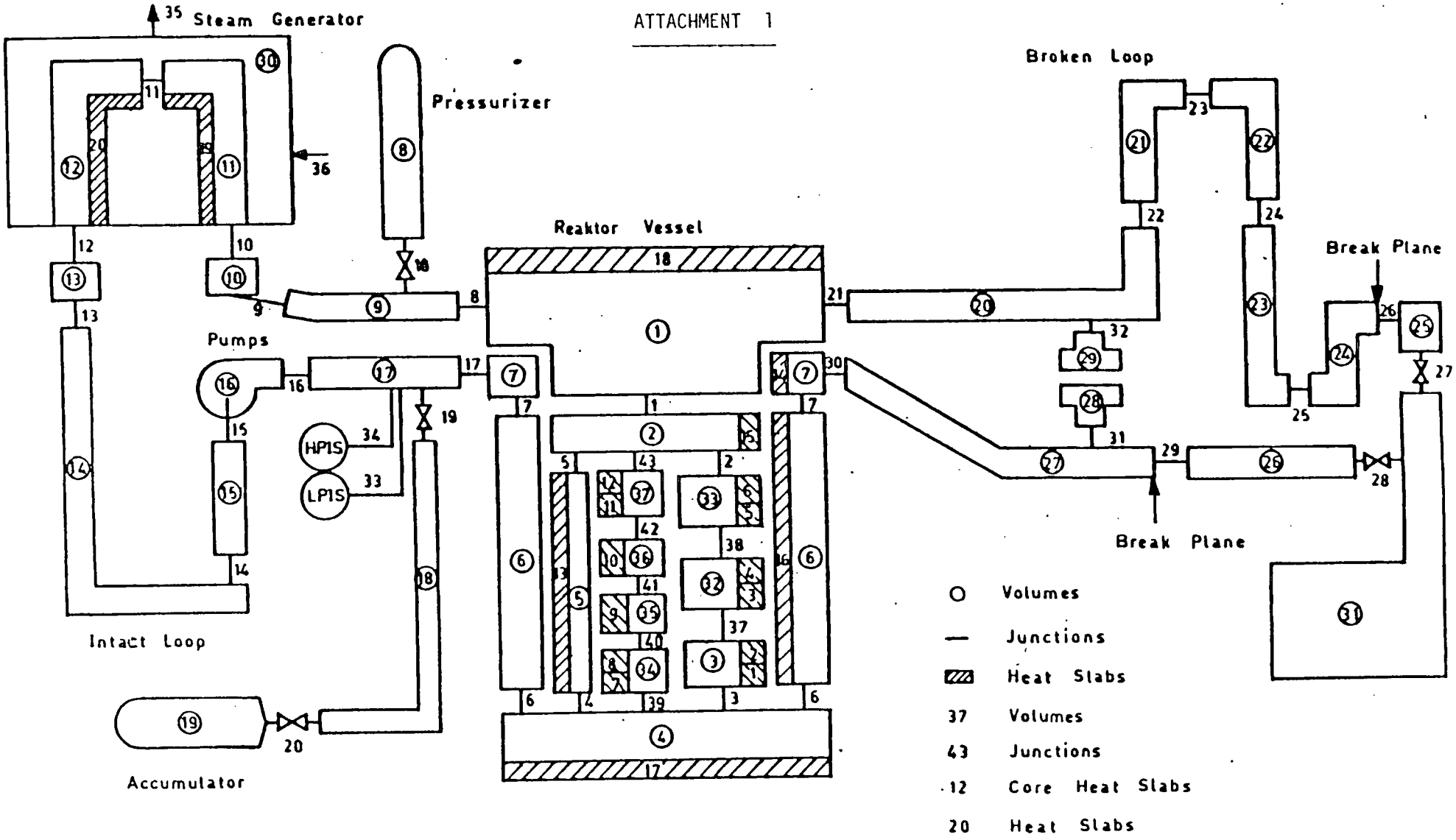

Figure A-7. ISP-13 RELAP4/MOD6 nodalization for the EIR open calculation.

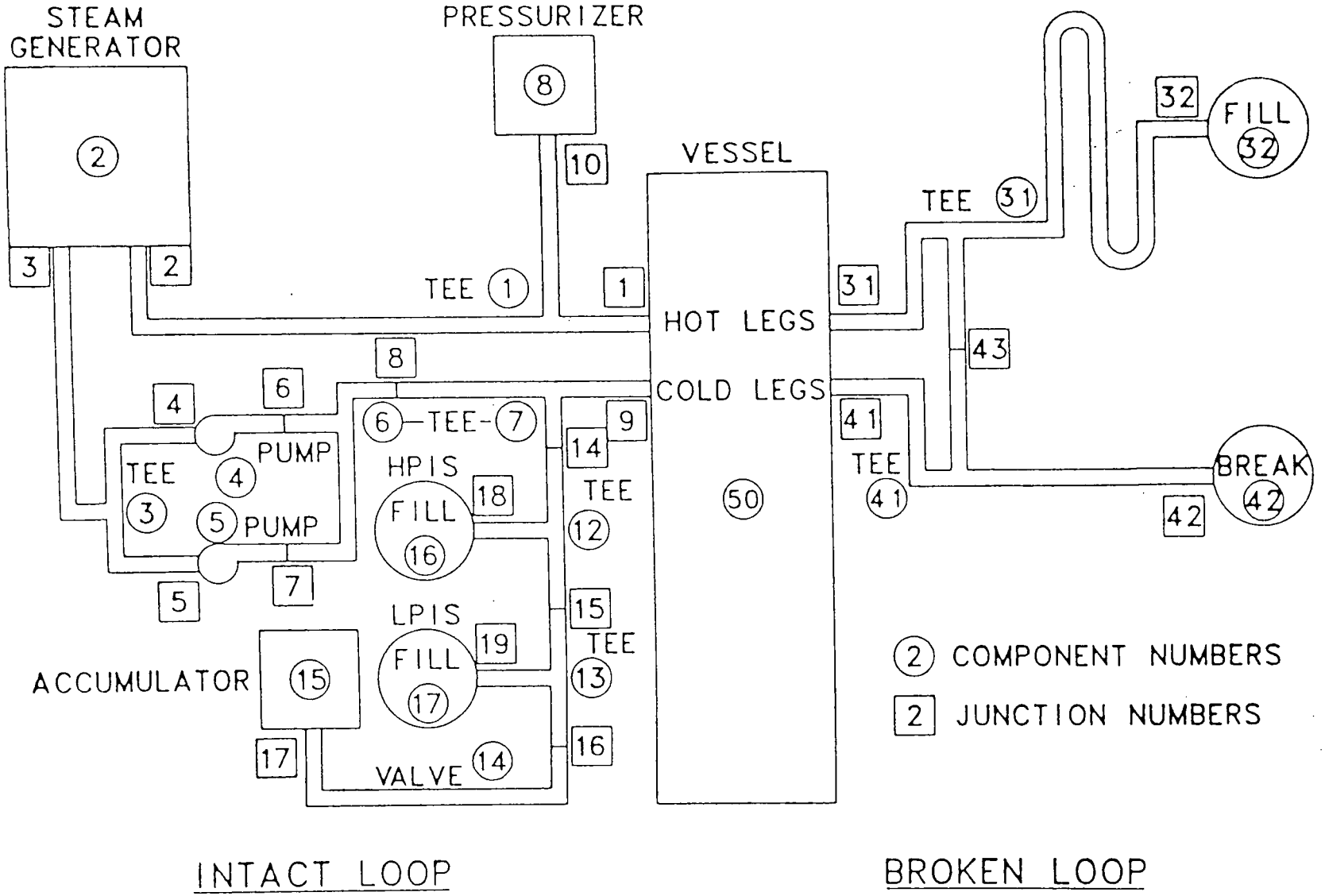

Figure A-8. ISP-13 TRAC-PD2 nodalization for the LANL open calculation.

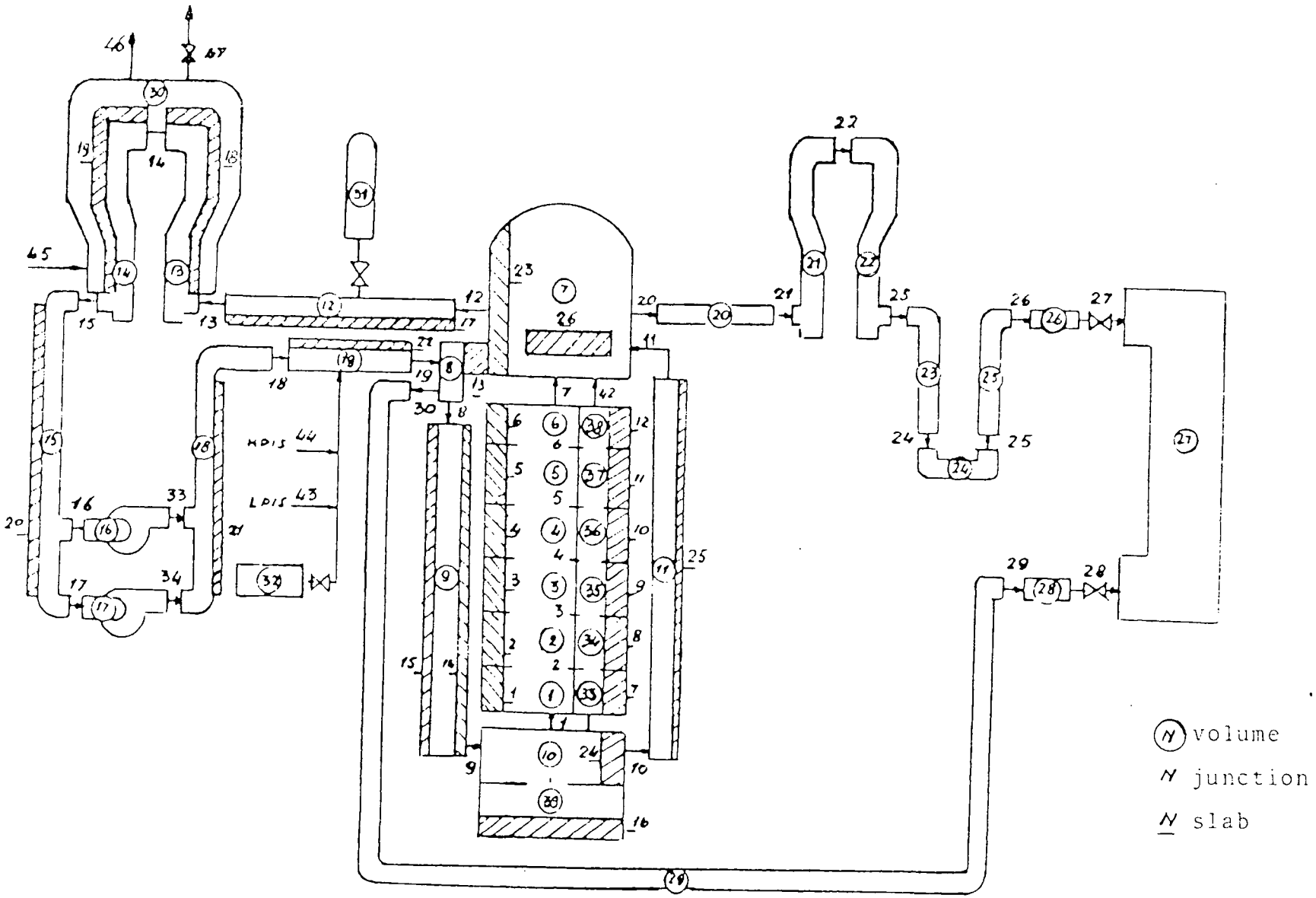

Figure A-9. ISP-13 RELAP4/MOD6 nodalization for the ENEL blind calculation.

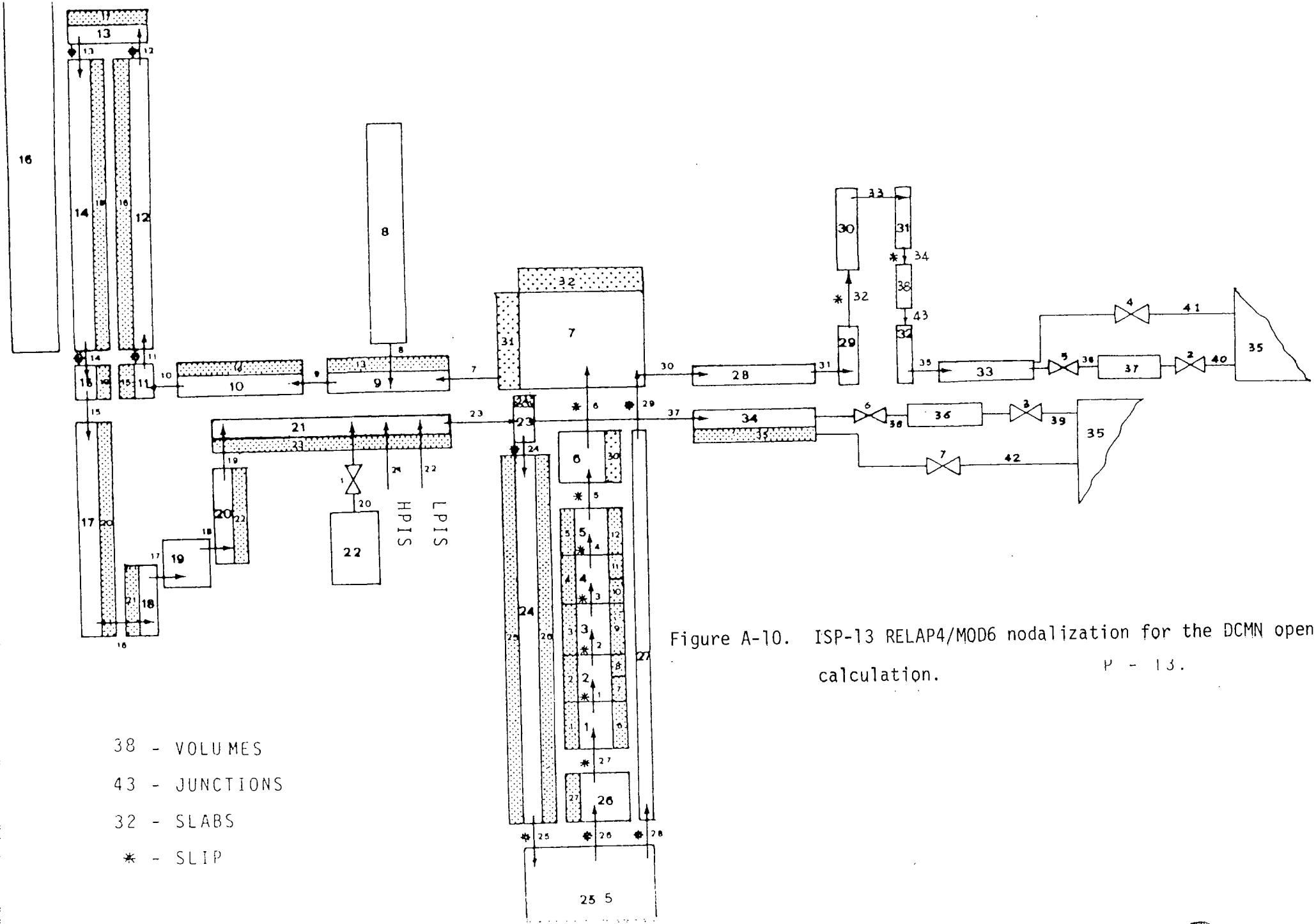

Figure A-10. ISP-13 RELAP4/MOD6 nodalization for the DCMN open calculation.

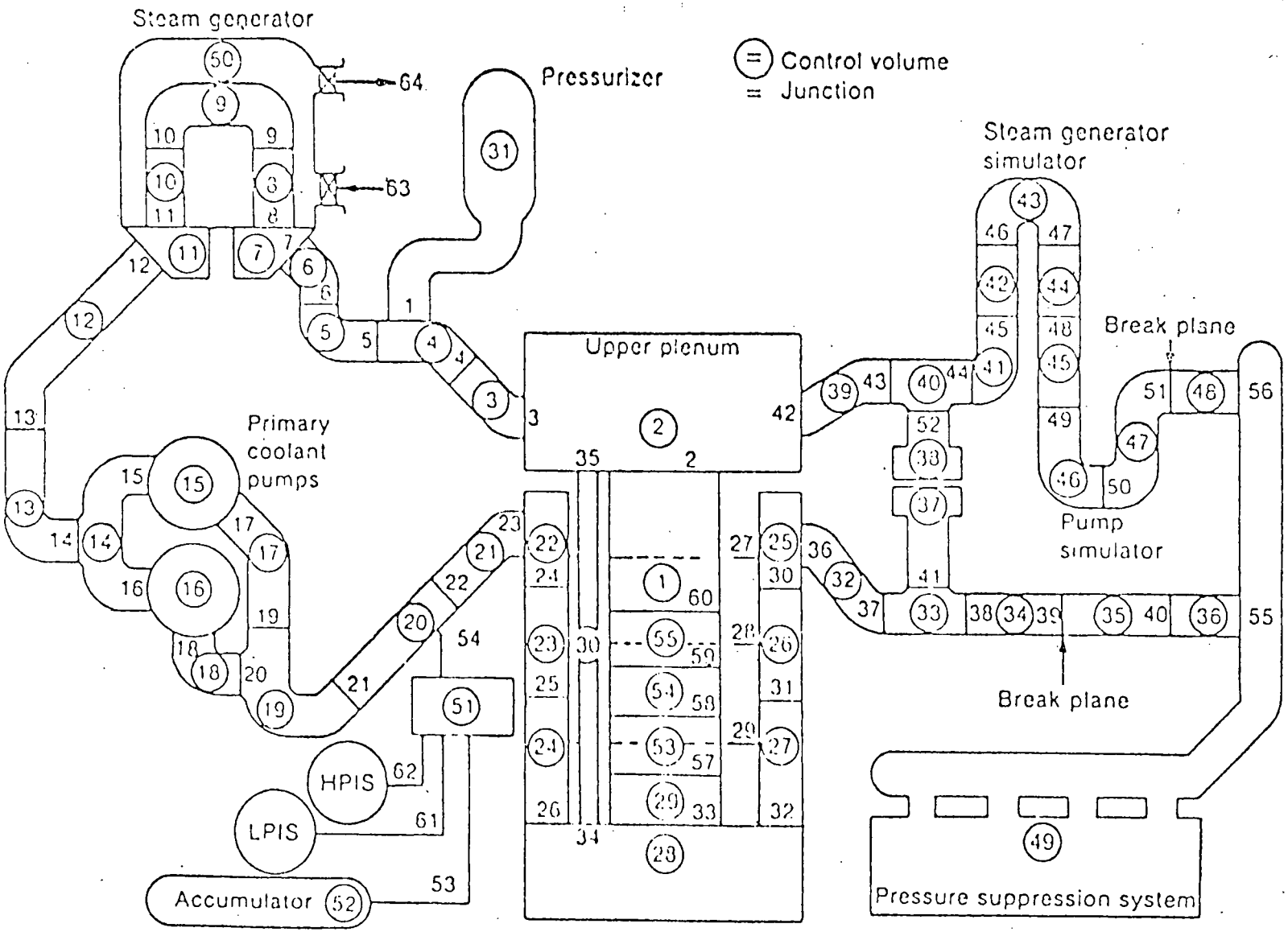

Figure A-11. ISP-13 RELAP4/MOD6 nodalization for the CEA blind calculation.

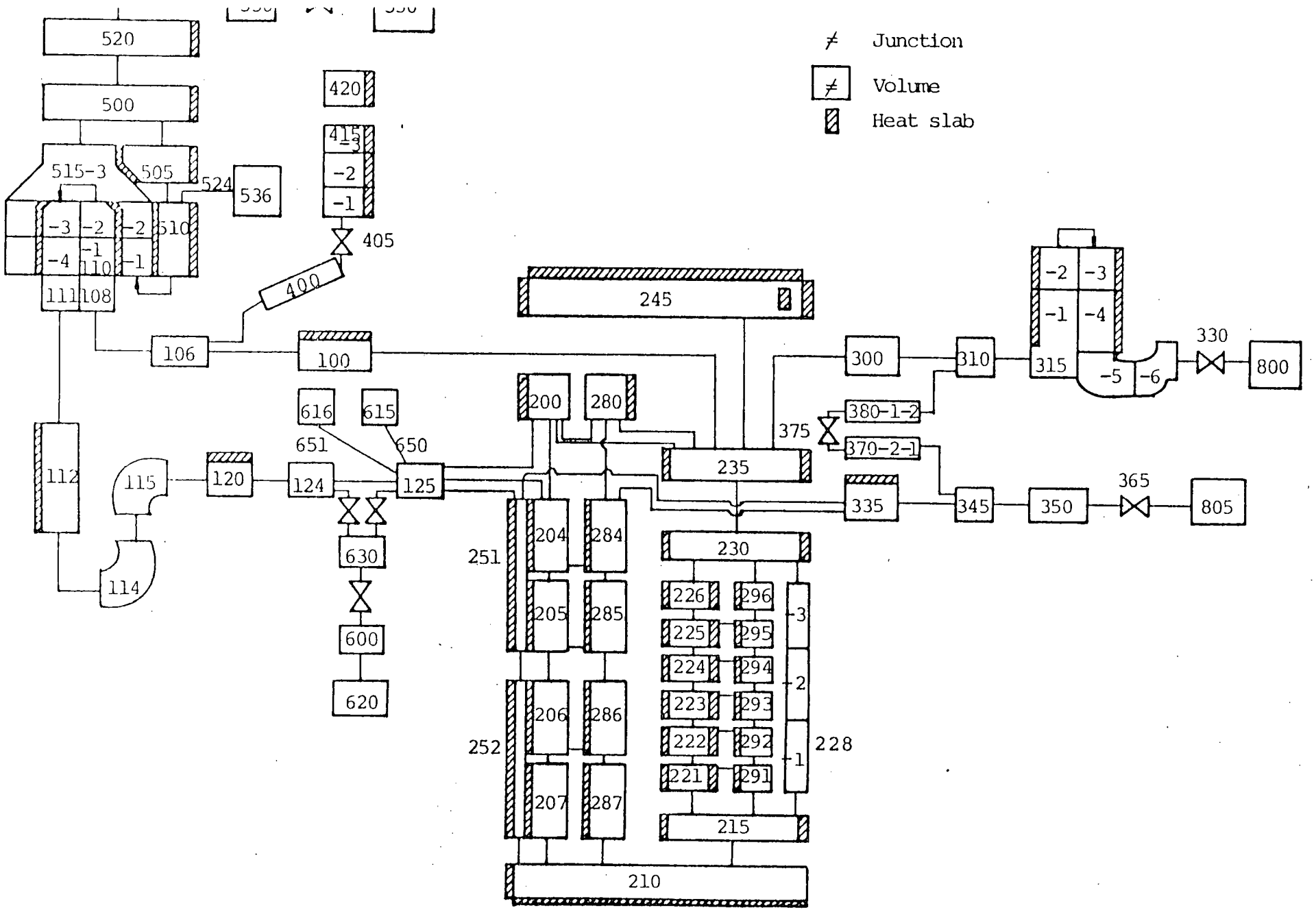

Figure A-12. ISP-13 RELAP5/MOD1 nodalization for the VTT open calculation.

NRC FORM 335 (11-81)

U.S. NUCLEAR REGULATORY COMMISSION

BIBLIOGRAPHIC DATA SHEET

1. REPORT NUMBER *(Assigned by DDC)*: EGG-NTAP-6276

TITLE AND SUBTITLE

International Standard Problem 13
(LOFT Experiment L2-5)
Preliminary Comparison Report

2. *(Leave blank)*

3. RECIPIENT'S ACCESSION NO.

7. AUTHOR(S)

J. D. Burtt, S. A. Crowton

5. DATE REPORT COMPLETED
MONTH: April | YEAR: 1983

9. PERFORMING ORGANIZATION NAME AND MAILING ADDRESS *(Include Zip Code)*

EG&G Idaho, Inc.
Idaho Falls, ID 83415

DATE REPORT ISSUED
MONTH: April | YEAR: 1983

6. *(Leave blank)*

8. *(Leave blank)*

12. SPONSORING ORGANIZATION NAME AND MAILING ADDRESS *(Include Zip Code)*

Division of Accident Evaluation
Office of Nuclear Regulatory Research
U.S. Nuclear Regulatory Commission
Washington, DC 20555

10. PROJECT/TASK/WORK UNIT NO.

11. FIN NO.
A6047

13. TYPE OF REPORT
Technical Report

PERIOD COVERED *(Inclusive dates)*

15. SUPPLEMENTARY NOTES

14. *(Leave blank)*

16. ABSTRACT *(200 words or less)*

LOFT Experiment L2-5 was designated International Standard Problem 13 by the Organization for Economic Cooperation and Development. Comparisons between measurements from Experiment L2-5 were made with calculations from 11 International participants using five different computer codes. LOFT Experiment L2-5 simulated a double ended guillotine cold leg rupture of a primary coolant loop of a large pressurized water reactor, coupled with a loss of offsite power.

17. KEY WORDS AND DOCUMENT ANALYSIS

17a. DESCRIPTORS

17b. IDENTIFIERS/OPEN-ENDED TERMS

18. AVAILABILITY STATEMENT
Unlimited

19. SECURITY CLASS *(This report)*: Unclassified

21. NO OF PAGES

20. SECURITY CLASS *(This page)*: Unclassified

22. PRICE
S